

**GENETIC DETERMINANTS OF FINAL NEPHRON NUMBER DURING
KIDNEY DEVELOPMENT**

by

Jacklyn Quinlan

A thesis submitted to the Graduate and Postdoctoral Studies Office of McGill University
in partial fulfillment of the requirements of the Degree of Masters of Science

February 2007

Department of Human Genetics
McGill University
Montreal, Quebec
Canada

© Copyright by Jacklyn Quinlan, 2006



Library and
Archives Canada

Bibliothèque et
Archives Canada

Published Heritage
Branch

Direction du
Patrimoine de l'édition

395 Wellington Street
Ottawa ON K1A 0N4
Canada

395, rue Wellington
Ottawa ON K1A 0N4
Canada

Your file *Votre référence*
ISBN: 978-0-494-32854-5
Our file *Notre référence*
ISBN: 978-0-494-32854-5

NOTICE:

The author has granted a non-exclusive license allowing Library and Archives Canada to reproduce, publish, archive, preserve, conserve, communicate to the public by telecommunication or on the Internet, loan, distribute and sell theses worldwide, for commercial or non-commercial purposes, in microform, paper, electronic and/or any other formats.

The author retains copyright ownership and moral rights in this thesis. Neither the thesis nor substantial extracts from it may be printed or otherwise reproduced without the author's permission.

AVIS:

L'auteur a accordé une licence non exclusive permettant à la Bibliothèque et Archives Canada de reproduire, publier, archiver, sauvegarder, conserver, transmettre au public par télécommunication ou par l'Internet, prêter, distribuer et vendre des thèses partout dans le monde, à des fins commerciales ou autres, sur support microforme, papier, électronique et/ou autres formats.

L'auteur conserve la propriété du droit d'auteur et des droits moraux qui protègent cette thèse. Ni la thèse ni des extraits substantiels de celle-ci ne doivent être imprimés ou autrement reproduits sans son autorisation.

In compliance with the Canadian Privacy Act some supporting forms may have been removed from this thesis.

Conformément à la loi canadienne sur la protection de la vie privée, quelques formulaires secondaires ont été enlevés de cette thèse.

While these forms may be included in the document page count, their removal does not represent any loss of content from the thesis.

Bien que ces formulaires aient inclus dans la pagination, il n'y aura aucun contenu manquant.


Canada

Our greatest glory is not in never failing, but in rising up every time we fail.

- Ralph Waldo Emerson

ABSTRACT

Fetal branching determines final nephron number. Mild nephron deficit causes hypertension in “normal” adults. Thus, mechanisms that control branching are important. *PAX2* and retinoic acid (RA) have profound effects on final nephron number, although the mechanism remains unknown.

We hypothesised that common variations in *PAX2* cause subtle reduction in nephrons. We associated haplotype tagging single nucleotide polymorphisms (htSNPs) in *PAX2* with a reduction in kidney mass in “normal” newborns and identified a haplotype on which an ancestral polymorphism is presumed to lie. We identified a SNP in linkage disequilibrium with this haplotype that caused alterations in *PAX2* expression, linking reduction in expression with reduced nephrons.

We hypothesized that *Lgll*, a pulmonary branching morphogen, is stimulated by RA to affect renal branching. We characterized *Lgll* expression in the kidney and its response to RA. Finally, we showed that *Lgll*^{+/-} embryos have reduction in kidney branching, implicating *Lgll* in nephron formation.

RÉSUMÉ

Le nombre final de néphrons est déterminé durant le développement embryonnaire des reins. Un déficit minime de ramifications pouvant causer un risque accru de développement de l'hypertension artérielle à l'âge adulte. Donc, les mécanismes qui contrôlent ces événements sont importants. *PAX2* et l'acide rétinoïque (AR) influencent la quantité de néphrons formés. Cependant, le mécanisme par lequel ces molécules agissent reste inconnu.

Nous avons postulé que des variations fréquentes de *PAX2* causent une réduction du nombre de néphrons dans la population générale. Nous avons associé des polymorphismes d'un seul nucléotide (PSN) qui identifient des haplotypes de *PAX2* avec une réduction dans la taille des reins d'un nouveau-né normal. Par suite, nous avons identifié l'haplotype qui contient supposément le polymorphisme ancestral causal. Nous avons identifié un PSN lié avec cet haplotype qui cause une altération de l'expression de *PAX2*, ce qui entraîne une réduction simultanée d'ARN et de néphrons.

Nous avons émis l'hypothèse que *Lgll*, un gène impliqué dans les ramifications des alvéoles pulmonaires, est stimulé par AR pour affecter les ramifications des néphrons rénaux. Nous avons caractérisé l'expression de *Lgll* dans le rein et sa stimulation par l'AR. Finalement, nous avons montré une réduction de ramifications rénales dans les souris transgéniques *Lgll*^{+/-}, ce qui implique *Lgll* dans la formation des néphrons.

TABLE OF CONTENTS

ABSTRACT	ii
RÉSUMÉ	iii
TABLE OF CONTENTS	iv
LIST OF FIGURES	viii
LIST OF TABLES	x
ABBREVIATIONS	xi
ACKNOWLEDGEMENTS	xiii
CHAPTER 1 - INTRODUCTION	1
1.1 BACKGROUND.....	2
1.2 RENAL HYPOPLASIA – CLINICAL CONSEQUENCES.....	2
1.3 MAMMALIAN KIDNEY DEVELOPMENT	6
1.4 RENAL BRANCHING MORPHOGENESIS	6
1.5 <i>PAX2</i>	13
1.5.1 <i>Pax2 and branching morphogenesis</i>	13
1.5.1.1 Pax2 and its expression pattern	13
1.5.1.2 Pax2 regulates multiple developmental pathways.....	16
1.5.1.3 Human PAX2 mutations and disease	19
1.5.1.4 Pax2 Mouse Models	20
1.5.2 <i>Are common variants in the human PAX2 gene associated with subtle renal hypoplasia in the normal population?</i>	20
1.5.2.1 The genetics of common complex diseases.....	20
1.5.2.2 Study of common complex diseases – the Hap Map project.....	22
1.5.2.3 What is known about the PAX2 gene and its variants?.....	26
1.6 Retinoic Acid.....	28
1.6.1 <i>Retinoic acid and branching morphogenesis</i>	28
1.6.1.1 Retinoid metabolism and mode of action in the kidney	30

1.6.1.2 Retinoic acid maintains c-ret expression in the UB via an indirect pathway	34
1.6.2 <i>How does the effect of RA on nephrogenic mesenchyme induce branching of the ureteric bud? Lessons from other organs.</i>	36
1.6.2.1 Pulmonary mesenchymal cells stimulate branching morphogenesis of the epithelial lung bud.	36
1.6.2.3 LGL1 was identified as a branching morphogen in lung mesenchyme	40
1.6.2.4 LGL1, a candidate RA-induced branching morphogen in kidney?	40
CHAPTER 2 – THESIS PROPOSAL	41
2.1 Thesis Proposal	42
CHAPTER 3 – COMMON htSNPs IN PAX2 ASSOCIATE A HAPLOTYPE WITH SUBTLE RENAL HYPOPLASIA.....	44
3.1 INTRODUCTION.....	45
3.2 MATERIALS AND METHODS	46
3.2.1 <i>Study subjects</i>	46
3.2.2 <i>Renal Volume</i>	47
3.2.3 <i>Serum cystatin C measurement</i>	47
3.2.4 <i>Genomic DNA isolation</i>	47
3.2.5 <i>Choice of htSNPs in the PAX2 gene region</i>	47
3.2.6 <i>PAX2 htSNP genotypes</i>	48
3.2.7 <i>PAX2 Haplotypes</i>	48
3.2.8 <i>Statistical Analysis</i>	49
3.2.9 <i>PAX2 allele expression assay</i>	51
3.3 RESULTS.....	52
3.3.1 <i>Linkage disequilibrium in the PAX2 gene +/- 10kb region of the CEPH population</i>	52
3.3.2 <i>Characteristics of study subjects</i>	52
3.3.3 <i>Frequencies of PAX2 variants in study subjects and level of LD between htSNPs</i>	58
3.3.3 <i>Genetic association analyses</i>	58
3.3.4 <i>PAX2 haplotypes</i>	58

3.3.5 Allelic Imbalance.....	59
3.4 DISCUSSION	66
CONNECTING TEXT FOR CHAPTERS 3 AND 4.....	74
CHAPTER 4 - LGL-1, A NOVEL RA INDUCIBLE RENAL BRANCHING MORPHOGEN	75
4.1 INTRODUCTION.....	76
4.2 MATERIALS AND METHODS	77
4.2.1 Reverse Transcriptase-Polymerase Chain Reaction Analysis.....	77
4.2.2 Cell Culture.....	78
4.2.3 In Situ Hybridization	78
4.2.4 HEK 293 transient transfections	79
4.2.5 Electrophoresis and Western blot immunanalysis.....	79
4.2.6 Immunohistochemistry.....	80
4.2.7 Lgl1 Promoter Region: Putative binding site detection	80
4.2.8 Lgl1 Transfection and Reporter Gene Assays with RA and GC.....	81
4.2.9 RA and GC stimulation of Lgl1 mRNA measured by real-time RT-PCR....	81
4.2.10 Fetal Kidney Explant Cultures	82
4.2.11 Counting UB tips of Lgl ^{+/-} /Hoxb7/Gfp embryos	83
4.2.12 Cystatin C measurements in aged Lgl1 heterozygotes	84
4.2.13 Data presentation and Statistical Analysis.....	84
4.3 RESULTS.....	86
4.3.1 Lgl1 mRNA is expressed in the kidney	86
4.3.2 LGL1 protein is present in the developing mouse kidney.....	89
4.3.3 Lgl1 promoter analysis.....	89
4.3.4 Regulation of Lgl1 promoter activity	89
4.3.5 Lgl1 mRNA expression is increased by retinoids and/or glucocorticoids...	93
4.3.6 atRA increases UB branching and Lgl1 mRNA in kidney explants, while GC decreases UB branching	97
4.3.7 Lgl1 ^{+/-} / Hoxb7/Gfp E12.5- E13 embryonic mouse kidneys have fewer UB branch tips than wildtype littermates	98

4.3.8 <i>Eight-month-old Lgl1^{+/-} mice do not have significantly increased levels of cystatin C</i>	98
4.4 DISCUSSION	104
CHAPTER 5 - CONCLUSIONS	110
5.1 CONCLUSIONS AND FUTURE DIRECTIONS	111
5.2 SUMMARY	113
REFERENCES	115
APPENDIX I	126
APPENDIX II	127

LIST OF FIGURES

Figure 1.1 Distribution of Nephron Endowment.....	5
Figure 1.2 Early kidney development in <i>Hoxb7/Gfp</i> mouse kidney	9
Figure 1.3 Nephrogenesis from mesenchymal condensates.....	10
Figure 1.4 Types of renal branching morphogenesis	12
Figure 1.5 <i>Pax2</i> expression in development	15
Figure 1.6 Model of anti-apoptotic function of <i>Pax2</i>	18
Figure 1.7 DNA sequence variations	25
Figure 1.8 Number of nephrons (glomeruli) as a function of fetal plasma vitamin A (retinol).....	29
Figure 1.9 Conversion of vitamin A to retinoic acid and its degradation.....	32
Figure 1.10 Retinoic acid action in cells	33
Figure 1.11 Model of indirect effects of RA on UB branching.....	35
Figure 1.12 Development of the human lung.....	39
Figure 3.1 Linkage disequilibrium between SNPs in the <i>PAX2</i> gene region of CEPH population.....	54
Figure 3.2 Distribution of study parameters.....	56
Figure 3.3 Correlation between study parameters.....	57
Figure 3.4 Linkage disequilibrium in <i>PAX2</i> htSNPs in Caucasian cohort.....	61
Figure 3.5 Schematic depiction of haplotypes in Caucasian cohort.....	63
Figure 3.6 Allele specific expression of <i>PAX2</i>	65
Figure 3.7 Normal distribution of nephron number	71
Figure 4.1 <i>Lgll</i> ^{+/-} genotyping PCR reactions	85
Figure 4.2 <i>Lgll</i> mRNA expression.....	87
Figure 4.3 <i>Lgll</i> mRNA expression pattern	88
Figure 4.4 LGL1 protein expression	91
Figure 4.5 LGL1 protein expression pattern	92
Figure 4.6 Potential binding sites in the 5' flanking sequences of <i>Lgll</i> and promoter studies.....	94

Figure 4.7 <i>Lgl1</i> mRNA expression in mK3 cells stimulated with retinoids and cortisol ..	95
Figure 4.8 <i>Lgl1</i> mRNA expression in mK4 cells after retinoid and cortisol treatment	96
Figure 4.9 E11.5 <i>Hoxb7/Gfp</i> explants treated +/- all trans retinoic acid (atRA, 10^{-6} M) , +/- cortisol (GC, 10^{-7} M) for 96 h	99
Figure 4.10 E11.5 <i>Hoxb7/Gfp</i> Explant Growth.....	100
Figure 4.11 <i>Lgl1</i> mRNA expression in E11.5 <i>Hoxb7/Gfp</i> explants treated for 96h +/- atRA (10^{-6} uM).....	101
Figure 4.12 E12.5 <i>Lgl1/Hoxb7/Gfp</i> kidneys	102
Figure 4.13 <i>Lgl1</i> ^{+/-} aged mice do not have increased levels of serum cystatin C.....	103
Figure 4.14 Model of the dual function of <i>Lgl1</i> in development	108

LIST OF TABLES

Table 1.1 Nephrogenic time table	8
Table 1.2 Molecules in common between the kidney and other branching organs.....	38
Table 3.1 Choice of <i>PAX2</i> htSNPs.....	50
Table 3.2 Characteristics of study subjects	55
Table 3.3 Frequencies of htSNPs in <i>PAX2</i> in Caucasian cohort.....	60
Table 3.4 Association of individual htSNPs in <i>PAX2</i> with study parameters	62
Table 3.5 Association of haplotypes with study parameters	64
Table 3.6 List of primers and probes used in Sequenom.....	73

ABBREVIATIONS

9cisRA	9-cis retinoic acid
atRA	all-trans retinoic acid
B2M	β -2-microglobulin
C3H	inbred mouse strain
cDNA	complementary DNA
DNA	deoxyribonucleic acid
E	embryonic day
EGF	epidermal growth factor
EGFR	epidermal growth factor receptor
Emx2	Empty spiracles homologue 2 (drosophila)
Eya2	Eyes absent 2 homologue (drosophila)
FGF	fibroblast growth factor
GAPDH	glyceraldehydes-3-phosphate dehydrogenase
GC	glucocorticoid
gDNA	genomic deoxyribonucleic acid
GDNF	glial-cell derived neurotrophic factor
GFR	glomerular filtration rate
GFR1α1	glial-cell derived neurotrophic factor receptor alpha-1
GPC3	glypican 3
HEK 293	human embryonic kidney 293 cells
HGF	hepatocyte growth factor
HOX	homeo-box gene
IMCD	murine inner medulla collectind duct cell line
LGL1	late gestion lung protein 1
MET	mesechymal to epithelial transition
mK3	murine mesenchymal cell line
mK4	murine mesenchymal cell line in epithelial transition
MM	metanephric mesenchyme
mRNA	messenger ribonucleic acid

OMIM	online Mendelian inheritance in man
P	post-natal day
PAX	paired-box gene
PBS	phosphate buffered saline
PCR	polymerase chain reaction
PFA	paraformaldehyde
PKD	polycystic kidney disease
RARα	retinoic acid receptor alpha
RARβ2	retinoic acid receptor beta 2
RARγ	retinoic acid receptor gamma
RCS	renal-coloboma syndrome
RNA	ribonucleic acid
RT-PCR	reverse transcription polymerase chain reaction
RXR	retinoid X receptor
SD	standard deviation
SEM	standard error mean
UB	ureteric bud
VUR	vesico-ureteral reflux
WNT	homologue of the <i>Drosophila</i> wingless-type gene
WT1	Wilm's tumor gene 1

ACKNOWLEDGEMENTS

I have had a wonderful graduate training experience at McGill and the success I have achieved could not have been accomplished without the help of many people. I would like to thank you, Dr. Paul Goodyer for the continued support and encouragement throughout my training in your laboratory both as an undergraduate and as a graduate student. The experience of working with you has only increased my desire to learn even more. Your patience, optimism, and enthusiasm for science have been important factors in my growth.

To the renal group, both the Goodyer and the Gupta labs, at Place Toulon, I greatly appreciate the camaraderie we have shared throughout the years. Thank you to Dr. Diana Iglesias, Pierre-Alain Huber, Leelee Chu, Alison Dziarmaga, Elena Pascuet, Inga Murawski, Tristan Alie, Dave Myburgh, Anne-Marie Patenaude, Tiffany Cohen, and Zhao Zang. I appreciate enormously the help you extended through insightful suggestions, trouble shooting assistance and lengthy discussions. I am fortunate to have been included in your circles. I would like to extend a special thanks to two members of this group: Inga and Elena, you have been exceptionally supportive through your friendships.

I would like to thank the members of my committee: Dr. Feige Kaplan, Dr. Constantin Polichronakos, and Dr. Indra Gupta. I appreciate your feedback and the collaborations we have shared. Thank you, Dr. Feige Kaplan and your laboratory members, Katia Nadeau, Isabelle Monteau, Leslie Ribero, and Jack Lan, I appreciate all of your assistance in the *Lgll* project. Thank you to both Dr. Feige Kaplan and Dr. Neil Sweezey for use of the *Lgll* promoter vector, the *Lgll* cDNA vector for ISH experiments, the LGL1 antibody, and the *Lgll*^{+/+} mouse. From Dr. Polichronakos' laboratory, thank you Dr. Huiqi Qu, for help in the analysis of my genes project, Luc Marchand, for help in designing the allelic imbalance experiments, Luyong Qu and Suzanna Anjos, thank you for helping me understand the complexity of SNPs and allelic imbalance. Dr. Indra

Gupta, thank you for sharing with me some of your considerable knowledge of the kidney.

I would like to thank Dr. Frank Costantini for the *Hoxb7/Gfp* mouse. For the help I received at Place Toulon, a special thanks to Dr. He for sharing your expertise in histology, and to Jodie Middleton in the animal facilities, thank you for your dedicated service and assistance in serum collection for the cystatin C measurements.

Thank you to Dr. Thomas Hudson and the Genome Centre team: Alexandre Montpetit for your skills in genotyping, Mathieu Lemire for your help with statistics, Donna Sinnett, for the help with Peak Picker.

Thanks to Diane Laforte for my training in recruitment. Also, thank you to my recruitment team: Fiona Houghton, Chadhana Rajou, Meghan Goodyer, and Elena Pascuet, thanks for all of your hard work at the RVH. To the staff at the Royal Victoria Hospital, the nurses in the birthing centre, the pre-admission clinic, and the postpartum unit, I appreciate the extra time you took to collect the specimens. Thanks to Dr. Ann Roy and the radiology technicians, Rose Meusgarve, Richard Bolduc, Richard Blondeau, and Danica Horvat, for the newborn's ultrasounds.

I want to thank my family and friends for your unconditional love and support. Your continued interest in my projects and your sensible advice have kept me on the right track. Your belief in me and your confidence in my ability to improve the world are responsible for my continued perseverance.

PREFACE

This thesis is written in accordance with the guidelines of the Faculty of Graduate Studies at McGill University. This thesis is comprised of five chapters and two appendices. Chapter I, is an introduction explaining the rationale for the research as well as background information that is relevant to this thesis. Chapters 3 and 4 are data chapters and are in the form in which they will be submitted for publication. Connecting texts between Chapters 3 and 4 is provided in accordance with Section C of the Guidelines for Submitting a Doctoral or Master's Thesis in the manuscript-based format. Appendix I consists of publications that arose during the course of the candidate's graduate work, such as review, where the candidate is second author, as well as published abstracts and conferences attended. Appendix II consists of permissions and compliance forms. Gene and protein nomenclature was assigned following the guidelines summarized by the Society for the Study of Reproduction (www.ssr.org/NomenBullets.html). This summary is based on guidelines provided by HGNC (HUGO Gene Nomenclature Committee) (www.gene.ucl.ac.uk/nomenclature) for human genes and proteins and on guidelines from Mouse Genome Informatics – The Jackson Laboratory (www.informatics.jax.org/mgihome/nomen) for mouse genes and proteins.

CHAPTER 1

INTRODUCTION

1.1 BACKGROUND

The kidney is an essential organ that develops through interactions between the embryonic mesenchyme and a tree-like epithelial structure, the ureteric bud. The extent of ureteric bud branching during development determines final nephron number and functional capacity of the adult kidney (Hinchliffe, Sargent et al. 1991). Interestingly, the number of nephrons in “healthy” human populations varies dramatically. Recently, this variance was shown to be clinically important, with those in the lower percentiles having an increased risk of developing essential hypertension and end-stage renal disease (Cullen-McEwen, Kett et al. 2003; Keller, Zimmer et al. 2003)

Two developmental pathways have been implicated in determining final nephron number. The first involves the developmental transcription factor PAX2 which is critical for normal nephrogenesis. PAX2 haploinsufficiency causes renal hypoplasia (Renal Coloboma Syndrome (Sanyanusin, Schimmenti et al. 1995) and homozygous *Pax2* mutations cause renal agenesis (Porteous, Torban et al. 2000). The primary objective of this part of my research project was to determine whether common variations in the human *PAX2* gene are associated with subtle renal hypoplasia in normal term newborns.

A second developmental pathway controlling final nephron number involves retinoic acid. In fetal kidney, maternal retinol is converted to retinoic acid in mesenchymal cells. Observations in retinoic acid receptor knockout mice suggest that retinoic acid stimulates mesenchymal cells to release an unknown secreted factor which drives branching of the ureteric bud (Batourina, Gim et al. 2001). In the developing lung, mesenchymal cells secrete a novel branching morphogen, LGL1 (Kaplan, Ledoux et al. 1999; Oyewumi, Kaplan et al. 2003). The second part of my project was to determine whether LGL1 functions as a retinoic acid-responsive branching morphogen in fetal kidney, participating in regulation of final nephron number.

1.2 RENAL HYPOPLASIA – CLINICAL CONSEQUENCES

The most frequent (40-60%) cause of end-stage renal disease in children involves disturbances of renal development, resulting in renal hypoplasia with or without dysplasia (Tejani, Sullivan et al. 1997; Ardissino, Dacco et al. 2003). Renal hypoplasia refers to a kidney with significantly fewer nephrons than normal; the kidneys are small but, on

biopsy, do not contain undifferentiated tissues (The Kidney, Vize, PD, Woolf, AS, Bard, JBL, Elsevier Science, 2003). Dysplasia refers to a kidney with suboptimal nephron number and disorganization of renal tissue and structure. Renal hypoplasia may be bilateral or, more frequently, unilateral. In patients with renal hypoplasia, the risk of functional deterioration and end-stage renal disease is thought to arise from the diminished renal reserve (The Kidney, p767).

Surprisingly, even “healthy, normal” individuals have great variability in the number of nephrons per kidney. This appears to have implications for long-term renal function. A rigorous study by Nyengarrd and Bensen first reported this variability in which it was shown that the number of nephrons in 37 normal human kidneys ranged from ~300,000 to more than 1 million, a greater than threefold spread (Nyengaard and Bendtsen 1992). Using a multiethnic cohort, the nephron range was found to be even larger (210,332 – just over 1.8 million) (Hoy, Hughson et al. 2006). These studies clearly show that some humans are born with substantially fewer nephrons than others; however, it was not initially believed that this variation had any clinical significance.

It is known that environmental factors influence kidney development in utero. Severe vitamin A deficiency (VAD) causes renal agenesis, with even mild VAD causing 24% decrease in kidney weight and a 20% reduction in nephron number (Lelievre-Pegorier, Vilar et al. 1998). Low birth weight is also associated with subtle renal hypoplasia (Tulassay and Vasarhelyi 2002). Although these factors may be important in developing countries where malnutrition and maternal VAD are common, in Europe and North America, where maternal malnutrition is not normally a problem, nephron number nevertheless varies widely in term newborns (Clark and Bertram 1999). Presumably, this diversity is attributable to a genetic contribution.

A direct link between decreased nephron number and hypertension is suggested by observations made from studying the glial derived neurotrophic factor (*Gdnf*) knockout mouse (Cullen-McEwen, Drago et al. 2001). The *Gdnf* gene is critical for nephrogenesis; homozygous knockouts fail to form kidneys (Sanchez, Silos-Santiago et al. 1996). Surprisingly, the heterozygotes were initially believed to be normal. However, in a follow-up study, the 1 month old *Gdnf* +/- mice were found to have a subtle phenotype, in which kidney size was decreased by 25%, and total nephron number

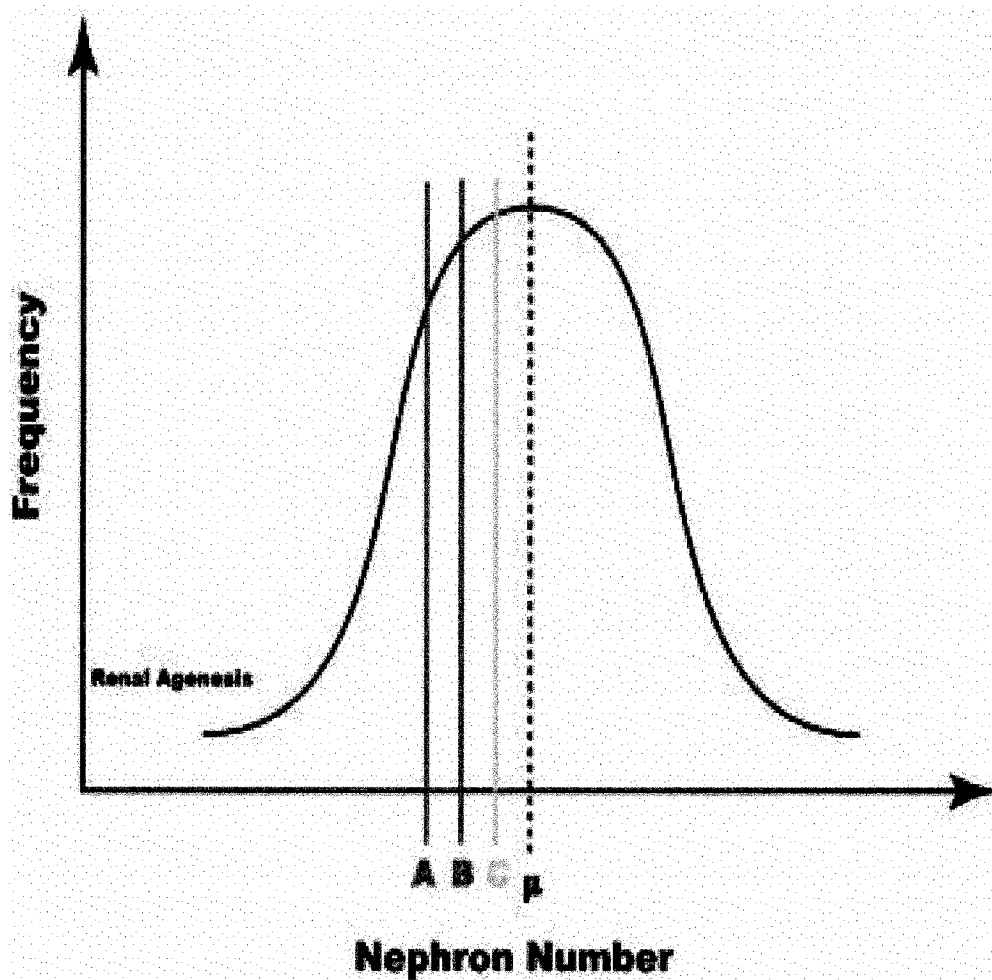
decreased by 30% (Simons, Provoost et al. 1994); (Fassi, Sangalli et al. 1998); (Vehaskari, Aviles et al. 2001). Although certain rat strains with lower birth weight have been shown to have a reduction in nephron number, increased blood pressure and increased susceptibility to renal injury (Simons, Provoost et al. 1994; Fassi, Sangalli et al. 1998; Vehaskari, Aviles et al. 2001), the *Gdnf* heterozygotes had no difference in body size compared to their wildtype littermates (Cullen-McEwen, Drago et al. 2001; Cullen-McEwen, Kett et al. 2003). At one month of age, no glomerular hypertrophy or abnormalities in renal function were found (Cullen-McEwen, Drago et al. 2001). However, by 14 months of age, hypertension and compensatory glomerular hypertrophy were noted, even though glomerular filtration rates were no different from control animals (Cullen-McEwen, Kett et al. 2003).

In keeping with these experimental data, Keller et al. performed autopsy studies in humans, linking a reduction in nephron number with essential hypertension (Keller, Zimmer et al. 2003). In this report, 10 middle-aged patients with documented hypertension were carefully matched to 10 controls. It was observed that patients with hypertension had roughly 50% fewer nephrons compared to their normotensive controls (Keller, Zimmer et al. 2003). As with the *Gdnf* mutant mice, each glomerulus was about twice the size of those of the controls and there was an increased prevalence of glomerulosclerosis (Keller, Zimmer et al. 2003).

These studies clearly associate congenital nephron deficit with an increased susceptibility for developing hypertension. As of yet, the molecular mechanisms that determine how many nephrons will form remain unknown.

Figure 1.1 Distribution of Nephron Endowment

Among humans, nephron number varies widely from 300,000 to 1.1 million per kidney (Nyengaard and Bendtsen 1992). In this schematic diagram depicting the normal distribution of nephrons, the mean nephron number in normal humans is shown (μ). In children with heterozygous PAX2 mutations, reduced mean (20–50% of normal) kidney sizes is shown (A). Among patients with essential hypertension reported by Keller, Zimmer et al. 2003 the nephron deficit (53% of age-matched controls) was less pronounced, but was associated with hypertension and glomerulosclerosis (B). *Line C* represents the mean number of nephrons (70% of normal) in mice bearing heterozygous GDNF mutations compared with wild-type controls (Cullen-McEwen, Drago et al. 2001). These mice also develop hypertension and glomerular hypertrophy (Cullen-McEwen, Drago et al. 2001). Renal agenesis is indicated at the *far left* of the normal range. (Dziarmaga, Quinlan et al. 2006)



1.3 MAMMALIAN KIDNEY DEVELOPMENT

In mammals, the kidney develops in three distinctive stages. The first two kidney-like structures, the pronephros and mesonephros, arise from the Wolffian duct. However, these two primordial kidneys degenerate in early embryonic development (The Kidney, 2003, Chapter 21, page 378) (see Table 1.1). It is the third, the metanephros, which becomes the permanent kidney. The metanephric kidney is formed when the ureteric bud (UB) branches from the Wolffian duct to invade the mass of undifferentiated metanephric mesenchyme (MM) (Saxen 1987). This process begins in the first month of fetal life in humans and at embryonic day (E) 10.5 in the mouse. Thereafter, reciprocal signalling allows the MM to induce the UB to grow and branch, forming the collecting duct system, while the UB induces the MM to condense at the tips of the UB and form epithelial structures that will become nephrons, the filtering units of the kidney. This process is known as renal branching morphogenesis.

1.4 RENAL BRANCHING MORPHOGENESIS

Nephrogenesis, the formation of nephrons, is dependent on the extent of fetal UB branching (Hinchliffe, Sargent et al. 1991). The end result of nephrogenesis is an arborized (tree-like) system of collecting ducts, connected to nephrons that develop concurrently from the mesenchymal condensates adjacent to the ampullary tips.

Arborization of the UB is considered to take place most often by iterative terminal bifurcation events. This form of branching results in the first bifurcation of the UB, to the T-bud stage at the 6th week gestation in humans and at E11.5 in rodents (Figure 1.2 A). Subsequently, expansion of the tip precedes the next round of dichotomous terminal bifurcation (Figure 1.2 B). With each round of dichotomous branching, the number of UB tips doubles. Thus, in the dichotomous branching model, the number of branching events (n) gives rise to 2n branch tips. Signals from each ureteric bud tip induce adjacent MM cells to condense and form aggregates. These aggregates undergo a mesenchymal to epithelial transition (MET), whereby the mesenchyme cell phenotype is converted to a polarized epithelium with its apical surface lining a central lumen. The rapidly growing renal vesicle goes through a number of shape changes, described as "comma-shaped",

and then "S-shaped" bodies that will form individual nephrons which fuse with the ureteric bud tip (Figure 1.3).

Another form of branching has been described as internodal or lateral branching (Oliver, 1968). In this form of branching a lateral branch arises and bifurcates to form two new termini, neither of which branch, but their "stalks" give rise to the next generation of lateral branches. Recently, this form of branching has been directly observed by time-lapse fluorescent micrography (Srinivas, Goldberg et al. 1999; Srinivas, Wu et al. 1999). This system of branching has been proposed as a plausible mechanism for "filling in" space left by the terminal branching mechanism (Shah, Sampogna et al. 2004) (Figure 1.4)

The UB continues to go through approximately 15 dichotomous terminal branching events (in humans), after which there is a burst of nephron formation in which several nephrons form through serial lateral branches connected in "arcades". In this phase, dichotomous branching is less frequent (Shah, Sampogna et al. 2004) (Figure 1.4). Consecutive dichotomous branching of the UB occurs about 20 times during human gestation, generating the 300,000 to more than 1 million nephrons in each human kidney (Nyengaard and Bendtsen 1992). As is apparent, final nephron number is a complex function of the number of branching events that occur during fetal life. Loss of one initial branching event could result in half the total number of nephrons formed, and a subtle decrease (less than 1%) in branching efficiency can likewise, over many iterations of branching, reduce nephron number by as much as half. Thus, factors that regulate branching morphogenesis will in turn affect final nephron number.

Table 1.1 Nephrogenic time table

Comparison of the developmental stages in human and mouse nephrogenesis is shown (adapted from The Kidney, 2003, Chapter 21, page 378).

	Human	Mouse
Pronephros		
First appears at	22 days	9 days
Regresses by	25 days	10 days
Mesonephros		
First appears at	24 days	10 days
Regresses by	16 weeks	14 days
Metanephros		
First appears at	28-32 days	10.5 days
Nephrogenesis ceases	34-36 weeks	7-10 days after birth
Length of Gestation	40 weeks	20-21 days

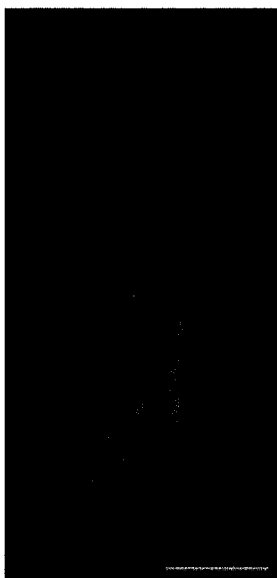
Figure 1.2 Early kidney development in *Hoxb7/Gfp* mouse kidney

Hoxb7-Gfp mice (generously provided by Dr Frank Costantini) express green fluorescent protein throughout the nephric duct and emerging ureteric bud.

A) T-bud stage: At E11.5 the ureteric bud has emerged from the caudally descended nephric duct at somite 26 and has undergone the first branching event after contacting metanephric mesenchyme (Dziarmaga, Quinlan et al. 2006).

B) Expanded ampullary tips: At E11.75, each ampullary tip of the T-shaped ureteric bud expands just prior to an additional bifurcation event. Scale bar=400 μ m.

A)



B)



Figure 1.3 Nephrogenesis from mesenchymal condensates

Embryonic (E)15 mouse kidney section allows visualisation of the different stages of mesenchymal condensates that will eventually fuse with the tips of a UB and form a nephron. Scale bar: 500um.



S-shaped
body

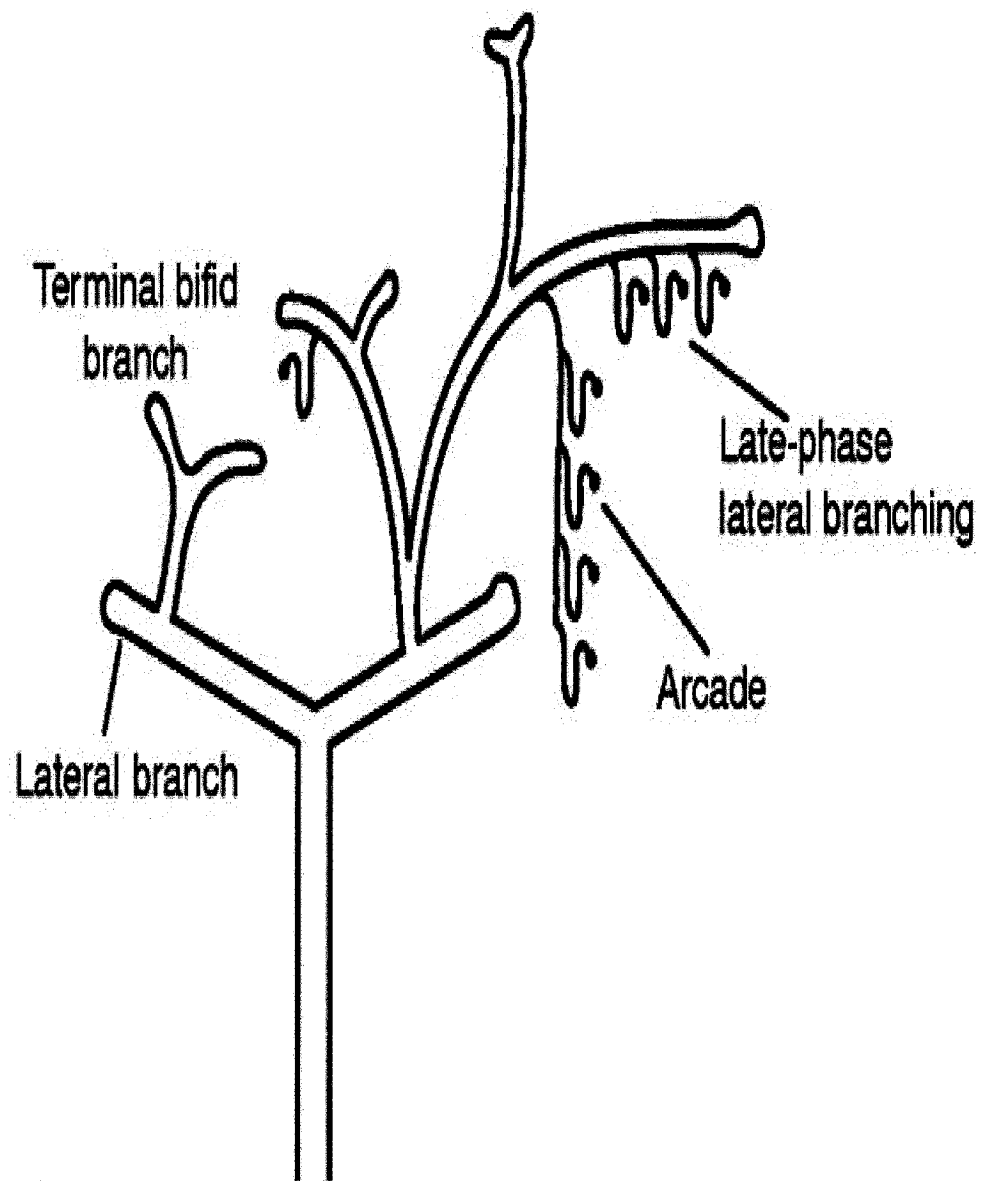
UB tips

Comma-
shaped
body

Although the molecular control of renal branching morphogenesis is complex, some key regulatory molecules play important roles in this process, while other players display secondary roles (Clark and Bertram 1999). The expression levels and/or gene dosage of certain molecules also appears to be critical in establishing an adequate nephron number in the kidney (Cullen-McEwen, Drago et al. 2001). It is conceivable that subtle variations in gene expression or function is amplified during the logarithmic arborization of the ureteric bud and could result in significant changes in final nephron number.

Figure 1.4 Types of renal branching morphogenesis

Nephron endowment is thought to be largely determined through branching of the UB. The UB adopts a strategy of lateral branching followed by bifurcation of a stem into two daughter branches (terminal bifid branching) to form the collecting system of the kidney. Nephrons are induced at UB tips but are also formed around the stem of elongated branches during the later branching iterations (arcades) and lateral branching (late-phase lateral branching.) (Shah et al. 2004)



1.5 PAX2

1.5.1 *Pax2* and branching morphogenesis

Renal branching morphogenesis is dependent on PAX2, a transcription factor critical to several developmental processes in the kidney. PAX2 is known to regulate a number of molecules, including other transcription factors, ligands, and receptors (Torres, Gomez-Pardo et al. 1995). Tight regulation of *Pax2* expression is important for proper renal development; homozygous mutations in *Pax2* cause renal agenesis, while heterozygous mutations cause renal hypoplasia. Inappropriate spatial expression or temporal overexpression of PAX2 may cause cancer or cystic phenotypes. Because PAX2 is known to play a critical role in branching, subtle variations in the PAX2 gene may affect final nephron number.

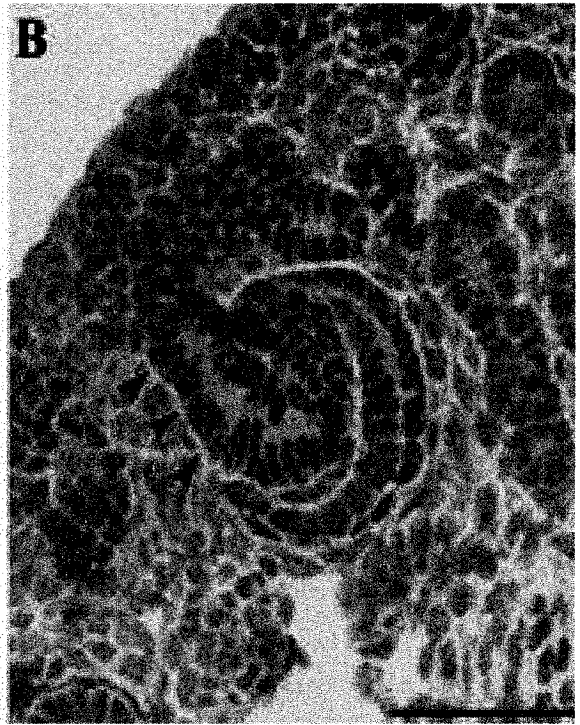
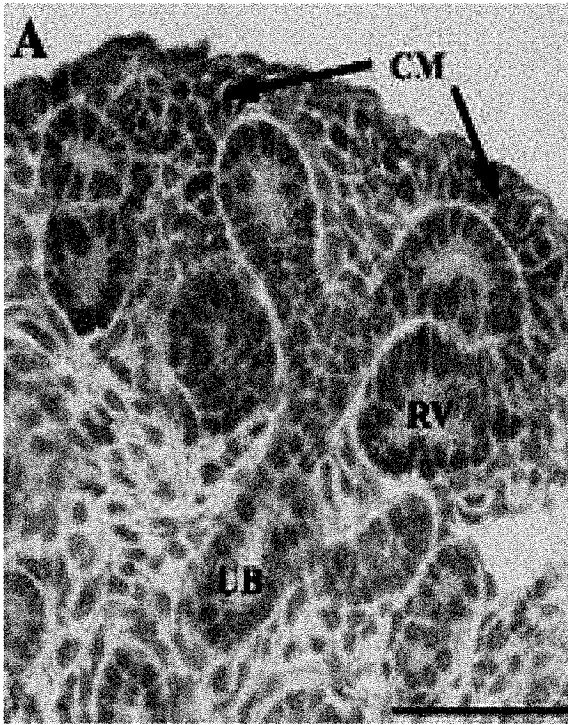
1.5.1.1 *Pax2* and its expression pattern

Pax2 is a member of the family of “paired-box” transcription factors. The *Pax2* gene is expressed in the midbrain-hindbrain region, spinal cord, eye, ear, and urogenital system (Porteous, Torban et al. 2000). *Pax2* expression is observed in early renal development: in the nephrogenic duct at the level of the pronephros and mesonephros (Torres, Gomez-Pardo et al. 1995). *Pax2* is later expressed in the Wolffian duct (Torres, Gomez-Pardo et al. 1995), and remains strongly expressed in the entire outgrowth of and the subsequent branching UB that will make up the metanephric kidney (Torres, Gomez-Pardo et al. 1995; Dressler, Deutsch et al. 1990). In uninduced mesenchyme, *Pax2* expression is low and is undetected by *in situ* hybridization and by immunohistochemistry (Dressler, Deutsch et al. 1990); however, once the mesenchyme begins to condense and form into vesicular clusters, *Pax2* expression can be detected (Dressler, Deutsch et al. 1990; Eccles 1998; Eccles, Wallis et al. 1992). *Pax2* plays a role in mesenchymal-to-epithelial transition (MET) as seen by its expression in early epithelial structures (the comma- and S-shaped bodies) derived from the induced mesenchyme. As S-shaped bodies begin to differentiate into what will become glomeruli, the proximal portions of these structures lose *Pax2* expression. At birth, *Pax2* mRNA is undetectable by *in situ* hybridization (Eccles, Wallis et al. 1992; Dressler, Deutsch et al.

1990). The expression of *Pax2* is imperative for the proper development of the urogenital system and although homozygous *Pax2* mutants initially form a nephric duct, all other urogenital structures fail to form (Torres, Gomez-Pardo et al. 1995).

Figure 1.5 Pax2 expression in development

(A) At E15.5 in the mouse, *Pax2* is strongly expressed in ureteric bud cells (*UB*) of the normal kidney. It is also seen in metanephric mesenchymal cells (*CM*) as they begin to condense around the tips of the ureteric bud (*arrows*) and in the renal vesicles (*RV*). (B) *Pax2* is expressed in the tubular anlage (distal to the glomerulus) portion of the S-shaped body (*arrows*). *Scale bar*=500 μm ((Dziarmaga, Quinlan et al. 2006).



1.5.1.2 *Pax2* regulates multiple developmental pathways

Several developmental roles for *Pax2* have been identified during nephrogenesis. Two *Pax* genes are expressed in early kidney development: *Pax2* and *Pax8* (Dressler, Deutsch et al. 1990; Plachov, Chowdhury et al. 1990). It was shown that *Pax2* is the member that influences early cell fate in nephric duct cells (Bouchard 2003; Bouchard, Souabni et al. 2002). This was done through experiments that compared *Pax* knock out mice: *Pax2*^{-/-} and *Pax8*^{-/-} mutants (Bouchard, Souabni et al. 2002). The homozygous *Pax2* mutants initially form a nephric duct, but all other urogenital structures fail to form (Torres, Gomez-Pardo et al. 1995). In the homozygous *Pax8* knockout mice, kidney development is unaffected (Mansouri, Chowdhury et al. 1998). In double mutant *Pax2*^{-/-}/*Pax8*^{-/-} embryos, the pronephros and later renal structure fail to form (Bouchard, Souabni et al. 2002). Through comparison of these mouse models, *Pax2* was identified as the *Pax* member that exerts the most powerful effect on early cell fate specification (Bouchard, Souabni et al. 2002).

In the MM, *Pax2* activates *Gdnf* expression (Brophy, Ostrom et al. 2001). GDNF is a secreted protein that binds to c-RET (Sariola and Saarma 2003), a tyrosine-kinase receptor expressed at the plasma membrane of epithelial nephric duct cells. Upon binding GDNF ligand, RET heterodimerizes with GFR α 1, initiating intracellular signals via the MAPK pathway. A mutation in any of these key molecules (*Ret*, *Gdnf*, *Gfr α 1*) precludes UB outgrowth and blocks subsequent development of the metanephric kidney (Schuchardt, D'Agati et al. 1994; Moore, Klein et al. 1996; Pichel, Shen et al. 1996; Sanchez, Silos-Santiago et al. 1996; Cacalano, Farinas et al. 1998; Enomoto, Araki et al. 1998). *Pax2* was shown to stimulate *Gdnf* transcription directly in the MM (Brophy, Ostrom et al. 2001). This stimulation is critical, as seen when *Gdnf* is absent and the UB fails to emerge (Moore, Klein et al. 1996; Pichel, Shen et al. 1996; Sanchez, Silos-Santiago et al. 1996; Schuchardt, D'Agati et al. 1996).

In order for the MM to respond to inductive signals from the UB, the expression of *Pax2* and at least one other transcription factor; Wilms tumour gene (*Wt1*), are required. The absence of these two factors in the uninduced mesenchyme results in a failure of UB outgrowth *in vitro* (Kreidberg, Sariola et al. 1993; Brophy, Ostrom et al. 2001). *Wt1* is expressed in the intermediate mesoderm that surrounds the nephric duct

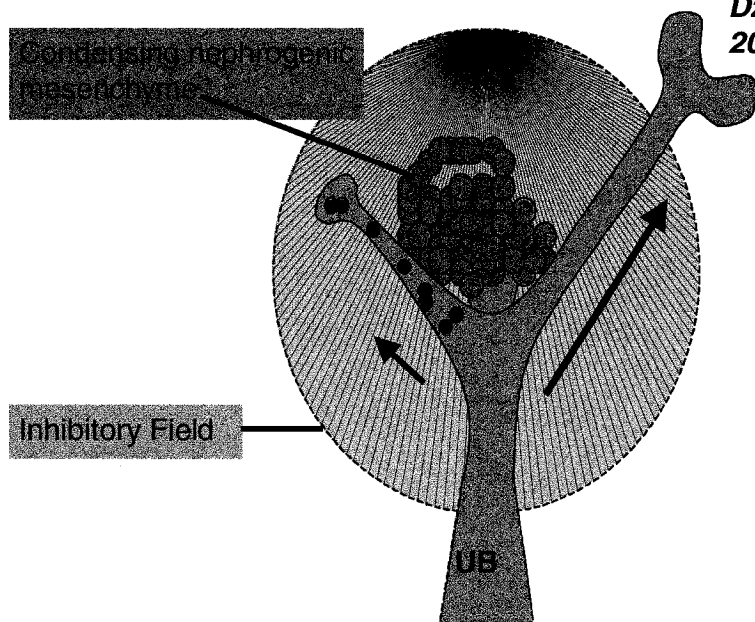
(Armstrong, Pritchard-Jones et al. 1993). Mice bearing homozygous null mutations of the *Wt1* gene, had no UB outgrowth, and the metanephric blastema underwent significant apoptosis (Kreidberg, Sariola et al. 1993). Furthermore, these mice no longer expressed *Pax2* in the metanephric blastemas (Kreidberg, Sariola et al. 1993). It was shown that PAX2 activates *Wt1* in the metanephric blastema (Dehbi, Ghahremani et al. 1996) suggesting a regulatory feedback loop between these two genes.

Pax2 has recently been reported to activate *Wnt4* (Torban, Dziarmaga et al. 2006). *Wnt4* is part of the Wnt family of secreted glycoproteins (Stark, Vainio et al. 1994; Kispert, Vainio et al. 1996; Lin, Liu et al. 2001) and is expressed in the induced MM and the renal vesicle as it progresses from a comma to an S-shaped body (Stark, Vainio et al. 1994; Kispert, Vainio et al. 1996). *Wnt4* mutants have initial branching of the UB, but are arrested at the condensation stage of nephrogenesis (Horster et al, 1999). Thus, by regulating *Wnt4*, *Pax2* plays a role in mesenchymal induction and in MET.

Pax2 was identified to have an anti-apoptotic function in the UB of the developing kidney. Haploinsufficiency of PAX2 leads to suboptimal UB arborization and elevated apoptosis of UB cells (Porteous et al, 2000; Torban et al, 2000). Recent work further established the anti-apoptotic role of *Pax2* (Clark, Dziarmaga et al. 2004; Dziarmaga 2003; Dziarmaga, Clark et al. 2003; Dziarmaga, Eccles et al. 2006) and identified a downstream anti-apoptotic target: NAIP, a caspase inhibitor (Dziarmaga, Hueber et al. 2006). Based on these observations, a model was proposed for the mechanism in which *Pax2* exerts its effect on branching. In this model, each branching event induces local mesenchymal cells to form an inhibitory field, which suppresses UB branching. In order for the next round of branching to occur, the UB needs to grow sufficiently to be lifted beyond this inhibitory field. The anti-apoptotic function of *Pax2* would optimize UB bud elongation and branching. Thus, when *Pax2* is limited, UB bud cells are no longer protected from apoptosis, reducing the rate at which the UB grows out of the inhibitory field. This model is in agreement with the *Pax2* mutant mouse observations that have a renal hypoplasia phenotype (Dziarmaga, Clark et al. 2003) (Figure 1.6).

Figure 1.6 Model of anti-apoptotic function of Pax2

This model hypothesizes that successive UB branching events are suppressed by an inhibitory field that is formed by local mesenchymal cells. Further rounds of branching can only occur once the UB has grown sufficiently to be lifted beyond this inhibitory field. Thus, the anti-apoptotic function of Pax2, which promotes UB cell growth, will regulate the rate of UB growth and influence the number of final branching events that occur (Dziarmaga, Clark et al. 2003).



*Dziarmaga et al 14:2767,
2003*

1.5.1.3 Human *PAX2* mutations and disease

At least ten mutations in the *PAX2* gene are associated with Renal-Coloboma Syndrome (RCS) (Sanyanusin, McNoe et al. 1995; Sanyanusin, Schimmenti et al. 1995). RCS is a rare autosomal dominant condition in which children have renal hypoplasia, ocular colobomas, vesico-ureteral reflux and brain malformations or ear defects (Sanyanusin, Schimmenti et al. 1995; Schimmenti, Cunliffe et al. 1997; Devriendt, Matthijs et al. 1998). The most common feature of RCS is renal hypoplasia (Sanyanusin, Schimmenti et al. 1995), and patients with RCS usually do not present with renal dysplasia. The most common *PAX2* mutation is an insertion of a single guanine nucleotide in exon 2 resulting in a frameshift mutation and null truncated protein (Eccles, Wallis et al. 1992).

Mutations in the *PAX2* gene are also seen in patients with “oligomeganephronia”, where the glomeruli and tubules are enlarged (Salomon, Tellier et al. 2001). In this condition, children have renal hypoplasia without evidence of renal dysplasia (Salomon et al. 2001). Furthermore, nephron structures appear normal, but are reduced in numbers and are hypertrophied (Royer, Habib et al. 1967). These observations suggest that mutations causing a reduction in *PAX2* are linked to nephron deficit.

Aberrant over-expression of *PAX2* may be involved in the pathogenesis of certain tumours. *PAX2* is normally downregulated in the kidney after completion of nephrogenesis (Eccles, Wallis et al. 1992; Dressler 1996). However, patients with Wilm’s Tumor, a childhood neoplasm of the kidney, have over-expression of *PAX2* (Eccles, Wallis et al. 1992; Dressler 1996). *PAX2* is also over-expressed in Renal Cell Carcinoma (RCC), an adult renal malignancy. A high proportion (73%) of RCC cell lines and primary RCC tumors express *PAX2* (Gnarra and Dressler 1995). Furthermore, *PAX2* is over-expressed in epithelial cells lining lumen in polycystic kidney disease (Eng et al, 1994). Conceivably *PAX2* could contribute to cell proliferation through activation of growth factors, such as GDNF and WNT4, or contribute to resistance of these tumours to chemotherapy through its anti-apoptotic effects.

1.5.1.4 Pax2 Mouse Models

There are three known *Pax2* mutant mouse models that help elucidate the role of *Pax2* in the development of the genitourinary system: *krd* mice (Keller, Jones et al. 1994), *Pax2* knock-out mice (Torres, Gomez-Pardo et al. 1995; Torres, Gomez-Pardo et al. 1996), and *Pax2*^{1Neu} mice (Favor, Sandulache et al. 1996). By far, the most useful of these models in studying the role of *Pax2* in renal hypoplasia is the *Pax2*^{1Neu} mouse (Favor, Sandulache et al. 1996).

The *Pax2*^{1Neu} mouse characterized by Favor et al. in 1996 has a spontaneous single guanine insertion in exon 2, causing a frameshift mutation that results in a premature stop codon and non-functional protein. This single base pair insertion is identical to the most commonly occurring mutation in RCS patients (Weaver, Cashwell et al. 1988; Sanyanusin, McNoe et al. 1995; Sanyanusin, Schimmenti et al. 1995; Schimmenti, Cunliffe et al. 1997). Homozygous *Pax2*^{1Neu} mice have complete renal agenesis, severe ocular and auditory anomalies, as well as loss of the mid- to hindbrain region, and die within hours of birth. Heterozygous *Pax2*^{1Neu} mice have a similar phenotype as patients with RCS, including renal hypoplasia and ocular colobomas. Work on these mice has served as an excellent tool for understanding the role of *Pax2* in renal hypoplasia. It is believed that the anti-apoptotic function of *Pax2* is the cause of sub-optimal nephron formation.

1.5.2 Are common variants in the human PAX2 gene associated with subtle renal hypoplasia in the normal population?

PAX2 is an important regulator of nephrogenesis with rare *PAX2* mutations causing autosomal dominant renal hypoplasia from haploinsufficiency. Thus, common variants in the *PAX2* gene might account for the decrease in nephron number of individuals at the lower end of the nephron spectrum observed in the “normal” population.

1.5.2.1 The genetics of common complex diseases

Common complex diseases, such as Alzheimer’s disease, type 2 diabetes, and inflammatory bowel disease (Gragnoli, Milord et al. 2005; Pierik, Yang et al. 2005;

Slifer, Martin et al. 2006) are genetically heterogeneous. These diseases are common and affect more than 0.1% of the population. They are complex because they can be caused by multiple genes and are influenced by the environment; they don't follow classical Mendelian inheritance patterns; they are not fully penetrant. Although it has been difficult to identify the various genetic factors that cause common complex diseases, three main methods have contributed to our understanding of these medical conditions: candidate gene screening, linkage mapping (positional approach), and association studies (by case-control or family-based design).

The candidate gene approach requires existing knowledge of the disease. This enables the selection of genes that are likely involved in the disease. For example, prior knowledge of the expression of a gene in diseased tissue or knowledge obtained from animal models (for example knock out mice) enables prediction of potential candidate genes. These candidates are then sequenced to see if the affected patients possess mutations or polymorphism that are more common in the diseased individuals and less in the control individuals. This approach has been successful in identifying the *APOE* gene associated with Alzheimer's disease (McConnell, Sanders et al. 1999) and *HLA-DQB1* with type 1 diabetes (Undlien, Lie et al. 2001).

If there are no obvious gene candidates for the disease, a positional approach can be used. The positional approach utilizes genetic markers distributed throughout the genome to identify large DNA regions that cosegregate more frequently with the disease trait. Linkage analysis is used in identifying regions that are significantly linked with the disease. This statistical analysis is based on a LOD score that measures the logarithm of the odds that a marker is significantly linked with the disease. The disadvantages of this approach are that many markers must be analyzed and large multigenerational families need to be recruited. These analyses also require many statistical tests and result in a high chance of obtaining a type 1 error where an identified linkage is actually a false positive. To reduce type 1 errors, large cohorts are needed to ensure enough statistical power to identify linkages. The history of complex disease analysis has been marked by a succession of irreproducible results due to errors from these false positives.

Association is not specifically a genetic phenomenon; it is simply a statistical statement about the co-occurrence of an allele (alternative forms of a chromosomal

region) and phenotype. An association can have many different causes. Direct causation occurs when having allele A makes you more susceptible to disease D. Natural selection occurs when people with disease D might be more likely to survive and have children if they have allele A. If population stratification occurs, this could coincidentally cause both the disease and the allele to be particularly frequent in one subset of the population. An association can also occur because of linkage disequilibrium between the disease and the allele. Ultimately, case-control association studies look for differences in the frequencies in common genetic variants between ethnically matched cases and controls to find variants that are strongly associated with the disease. In any association study, the choice of the control group is crucial. One method that has been developed which uses internal controls is called the transmission disequilibrium test (TDT). The TDT method uses parents who have one or more affected offspring. To test if a marker is associated with the disease, parents who are heterozygous for the marker are used. The number of cases where such a parent transmits the marker to the affected offspring is compared with the number of cases when their other allele is transmitted. Thus, excellent internal controls are used in this method

When a genetic variant is associated with a complex disease, it confers only risk. Occurrence of the disease depends on the presence of other factors including life style and environment, as well as presence of other genetic susceptibility variants. For many common complex diseases, the combination of many genetic variants can play important roles through gene-gene interactions and gene-environment interactions. Nonetheless, association studies have helped in the initial dissection of common-complex diseases.

1.5.2.2 Study of common complex diseases – the Hap Map project

The recent sequencing of the human genome has identified common patterns of variation in different populations. It is believed that the frequency of these variants in a population's genome plays a powerful role in the etiology of common complex diseases. The International HapMap Project's (2003) goal is to describe common variations by identifying common single nucleotide polymorphisms [(SNPs) – variation in a single base pair] in major populations with African, European and Asian ancestry. It has been revealed that there are differences in the allele frequencies of individual SNPs across

population samples (Cavalli-Sforza and Piazza 1993). This finding emphasizes the importance of being population specific for association studies.

Through comparison of DNA sequences, certain genomic regions, i.e. alleles, cosegregate with other alleles more often than not. This nonrandom association is called linkage disequilibrium (LD). Many studies have found LD either in one or many gene regions, and it has been concluded that regions of LD are not evenly distributed along the genome. A simple pattern has been suggested: the genome is divided into LD blocks of variable length (each LD block is represented by a few common haplotypes) separated by sites of recombination, called hotspots (Figure 1.7). A haplotype is a conserved combination of alleles on a single chromosome observed in a population. LD blocks can span a region covering many genes, or can make up only a small portion of the gene, depending on the number of recombination events that have occurred in that region. In older populations (such as African populations), blocks will be shorter due to more recombination events, while younger populations (such as Caucasian populations) will have longer blocks. It is believed that when a new mutation arises, it occurs on a specific haplotype. Thus, it should be possible to track an ancestral mutation (variant allele) in the population by identifying (through the use of genetic markers) the particular haplotype on which it lies.

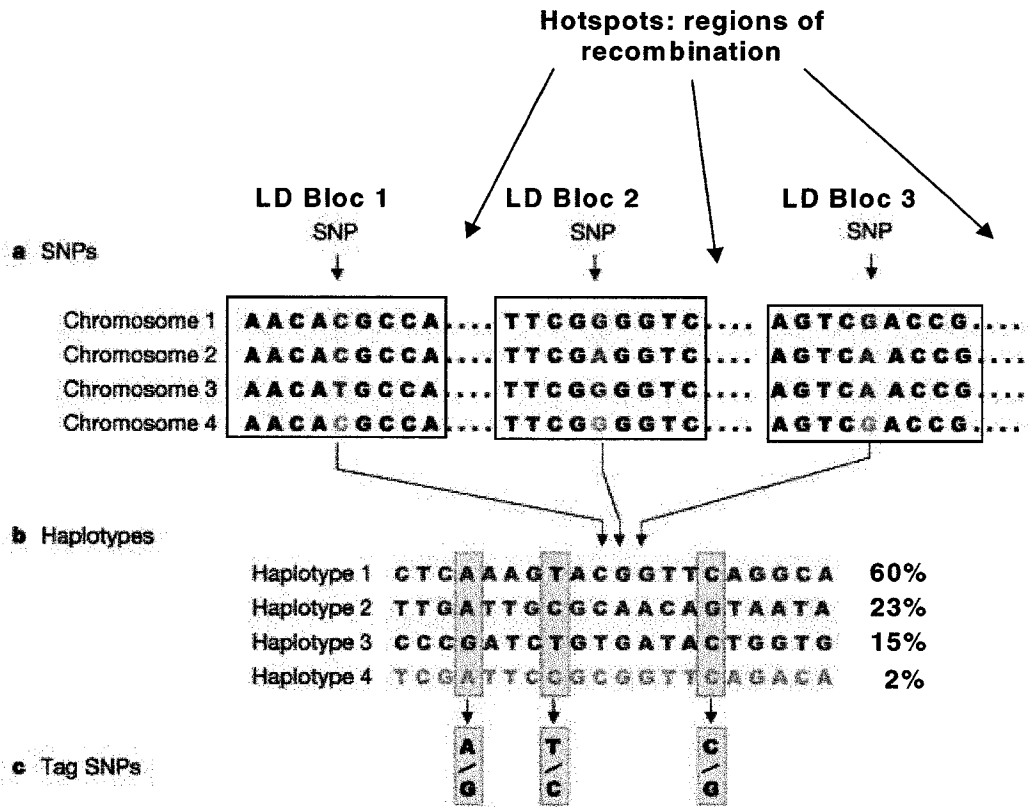
The major attraction of using haplotypes for association studies is the idea that common haplotypes can be identified through the careful selection of a small number of haplotype tagging SNPs (htSNPs) (Daly, Rioux et al. 2001; Carlson, Eberle et al. 2004). Within each LD block, a few common htSNPs can capture most haplotypes in that LD block for each population. Thus, only a few htSNPs need to be genotyped to predict the genotypes of the surrounding SNPs that are in the same LD block. This reduces the cost and time that would be required if each SNP had to be genotyped individually. The haplotype-based association method offers a powerful approach to common complex disease mapping (Gabriel, Schaffner et al. 2002).

Using HapMap data, it is now possible to use htSNPs to define specific blocks within a candidate gene and determine whether this region of the gene is associated with a clinical phenotype. New developments in genotyping enable automated multiplex PCR reactions, allowing multiple htSNPs to be analyzed simultaneously.

When a htSNP is associated with a disease, it may be a marker that identifies the haplotype on which the mutated allele is present, or it may be the causative SNP, also known as a functional SNP, for the disease. Functional SNPs can alter gene expression or change an amino acid to directly alter the protein. A SNP may occur in the gene promoter region, untranslated region (UTR), coding region, or intronic region. A promoter SNP may change gene transcription. A UTR SNP may change gene translation. Both coding SNPs and intronic SNPs can influence alternative splicing of a gene. A SNP in the gene coding region that causes an amino acid change is called a nonsynonymous SNP. Nonsynonymous SNPs that change protein function and are the most common types of disease-associated SNPs.

Figure 1.7 DNA sequence variations

LD blocks are spread throughout the genome at irregular spacings, separated by areas of recombination (hotspots). (a) Single nucleotide polymorphisms (SNPs) are identified in DNA samples from multiple individuals. Each distinct sequence of a chromosomal region is called an allele. For example, in LD block 1, the colored sequence has two alleles: C, or T. In each population, the frequency of each allele may vary. Thus, it is important to remain population specific in association studies. (b) The series of SNPs found along linked loci on the chromosome in each LD block make haplotypes. (c) "Haplotype tagging" (tag)SNPs can be genotyped to uniquely identify the haplotypes. By genotyping the three tag SNPs shown in this figure, the major haplotypes in the population can be differentiated, with only the first three haplotypes being common (greater than 5%). It has been estimated that 3-5 common haplotypes (greater than 5%) in each LD block allow 90% of all alleles to be identified (Modified from HapMap www.hapmap.org (2003)).



1.5.2.3 What is known about the *PAX2* gene and its variants?

The human *PAX2* gene is located close to the boundary of bands q24 and q25 on human chromosome 10 (10q24-25) (Narahara, Baker et al. 1997), and consists of 12 exons spanning approximately 70 kb (Sanyanusin, Norrish et al. 1996). The first four exons encode the paired box domain (Sanyanusin, Norrish et al. 1996), while the fifth exon contains a highly conserved motif called the octapeptide sequence (Sanyanusin, McNoe et al. 1995; Sanyanusin, Norrish et al. 1996). Three exons in *PAX2* are alternatively spliced in humans: exons 6, 10, and an alternative acceptor splice site located within exon 12 (Dressler, Deutsch et al. 1990; Ward, Nebel et al. 1994; Sanyanusin, Norrish et al. 1996; Tavassoli, Ruger et al. 1997). The exact function of the alternatively spliced exons in *PAX2* is not clear. The carboxyterminal portion of the *PAX2* protein, encoded by exons 7-12, is required for transcriptional activation of target genes by *PAX2* protein (Dressler 1996; Lechner and Dressler 1996), and has strong activating and inhibitory domains (Dorfler and Busslinger 1996; Dressler 1996; Lechner and Dressler 1996).

A number of rare *PAX2* mutations have been reported. Sanyanusin et al. (1996) identified a (CA)_n dinucleotide repeat polymorphism in *PAX2* which they mapped immediately upstream of exon 9. Schimmenti et al. (1999) described patients with *PAX2* homoguanine tract (7G) missense mutations and showed that this is a hotspot for spontaneous expansion and contraction mutations. Reports of other rare *PAX2* mutations include 11 other allelic variants identified in patients with renal-coloboma syndrome, most of which cause a truncated protein. Patients with renal coloboma syndrome having rare *PAX2* mutations have also been associated with vesicoureteric reflux (VUR). (www.ncbi.nlm.nih.gov/entrez/dispomim.cgi?id=167409). Shim, Nakamura et al. (1999) estimated the allele frequencies of two single nucleotide polymorphisms (1410 C --> T, 0.94C) and (1521 A --> C, 0.72A) in the coding region of exon 8 in *PAX2* from patients with renal-coloboma syndrome. It was suggested that these alleles are in Hardy-Weinberg equilibrium and jointly in linkage disequilibrium. Gelb, Manligas et al. (2001) identified two other polymorphisms in the *PAX2* gene. As recorded in NCBI dbSNP (BUILD 125), 248 SNPs have been found in the *PAX2* region. Among these SNPs, there are none that change amino acids (nonsynonymous SNP). Some SNPs have predicted function on gene

transcription and splicing. There are no studies examining *PAX2* variants associated with subtle renal hypoplasia.

1.6 Retinoic Acid

1.6.1 Retinoic acid and branching morphogenesis

Retinoic acid (RA) is the physiologic metabolite of vitamin A (Zile and Deluca 1965). Vitamin A is critical for kidney development (Ross, McCaffery et al. 2000) as seen in offspring from vitamin A deficient (VAD) rodents who have genitourinary tract anomalies, including renal agenesis (Lelievre-Pegorier, Vilar et al. 1998). These defects can be reversed with vitamin A supplementation given at the onset of renal organogenesis (Wilson, Roth et al. 1953). Even mild maternal vitamin A deficiency (50% reduction in circulating retinol level) causes renal hypoplasia among their offspring (Lelievre-Pegorier, Vilar et al. 1998) without any obvious effect on overall fetal growth (Wilson, Roth et al. 1953). Pregnant rats fed vitamin A-deficient diets bear pups with smaller kidneys that contain fewer nephrons than controls; postnatal (14 days) kidney weight is decreased by 24% and nephron number is reduced by 20% (Gilbert and Merlet-Benichou 2000; Gilbert 2002) (see Figure 1.8). Thus, vitamin A plays a crucial role in kidney organogenesis, presumably through the effects of RA. RA exists in different isoforms with the most common ones being all trans (at) RA and 9-cis (9cis) RA. The active physiological form is believed to be atRA (Zile and Deluca 1965; Zile, Inhorn et al. 1982; Zile 2001). In E14 fetal rat kidneys cultured *ex vivo*, atRA (0.1-1 μ M) accelerated new nephron formation 2-3 fold (Vilar, Gilbert et al. 1996). Nephron number correlated directly with (maternal) retinol concentration even into the low normal range (Wilson, Roth et al. 1953; Lelievre-Pegorier, Vilar et al. 1998; Gilbert and Merlet-Benichou 2000; Gilbert 2002).

Figure 1.8 Number of nephrons (glomeruli) as a function of fetal plasma vitamin A (retinol)

Term rat kidneys were isolated from embryos born from vitamin A replete mothers (closed circles) and from vitamin A deficient mothers (open circles). The number of glomeruli in the vitamin A deficient group was fewer than those in vitamin A replete group (Lelievre-Pegorier, Vilar et al. 1998).

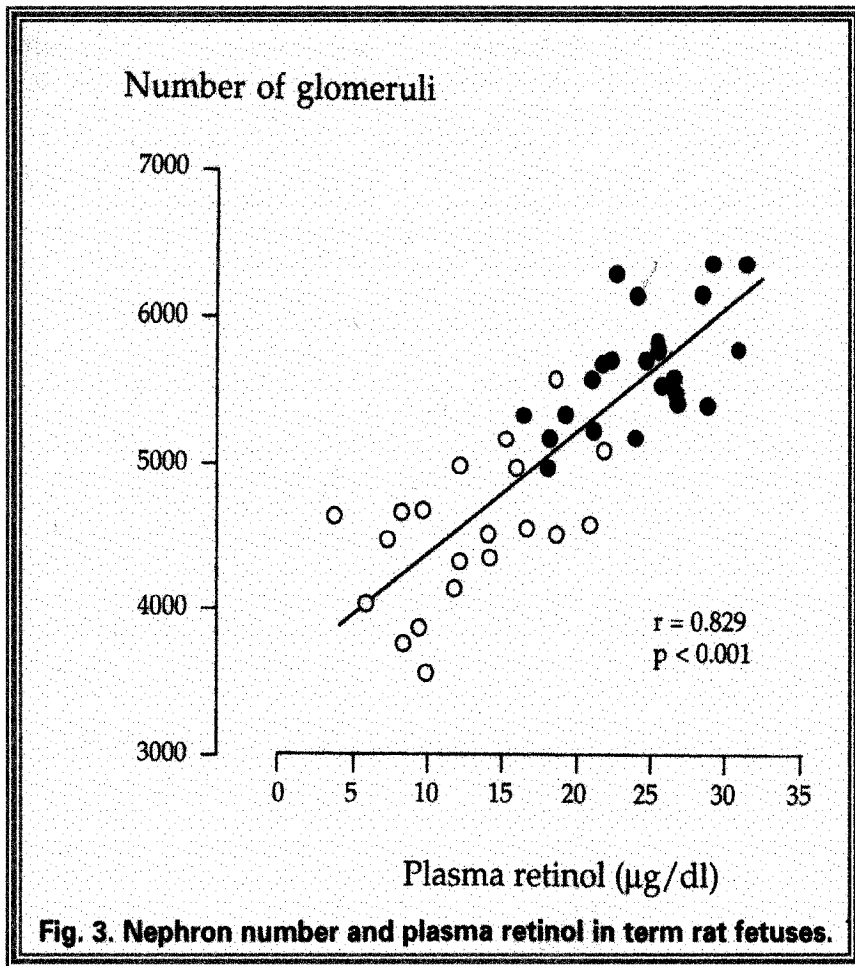


Fig. 3. Nephron number and plasma retinol in term rat fetuses.

1.6.1.1 Retinoid metabolism and mode of action in the kidney

Vitamin A is an inactive precursor acquired from the diet and is stored in the liver as retinylesters, where its release is controlled to allow for steady levels of plasma retinol. The conversion of retinol to RA occurs in a 2-step oxidative process: alcohol (retinol) dehydrogenase converts retinol to retinal; aldehyde dehydrogenase converts retinal to RA (Lee, Manthey et al. 1991; Bhat, Marcinkiewicz et al. 1998; Lee, Dohi et al. 1998) (Figure 1.9). In fetal kidneys, the conversion of retinal to RA is the rate-determining step. Presumably, by controlling expression of retinaldehyde dehydrogenase (RALDH), the level of available RA is regulated. Isoforms of RALDH are restricted to specific cell types in the kidney: RALDH1 and 2 are expressed in the metanephric mesenchyme (MM) while RALDH 1 and 3 are expressed in the ureteric bud (UB) (Ross, McCaffery et al. 2000). Recently, cytochrome P450 enzymes (CYP26A1, B1, and C1) have been identified as controlling the rate of RA degradation (Taimi, Helvig et al. 2004). Miss-regulation of either the RALDH or the CYP26 enzymes could cause RA insufficiency for the embryo.

RA binds to nuclear receptors (retinoic acid receptor RAR). The effects of atRA are mediated by three specific RARs (α , β , γ) encoded by distinct genes (Ross, McCaffery et al. 2000). When bound to atRA, RARs heterodimerize with a retinoid X receptor (RXR) protein partner, they enter the nucleus and regulate expression of target genes by binding recognition motifs in their enhancer elements (Figure 1.10). Differential mRNA splicing generates eight major RAR isoforms (RAR α 1-2, RAR β 1-4 and RAR γ 1-2). RAR α mRNA was identified in both tubular cells and mesenchyme of mesonephric kidney but expression in metanephric kidney was not well-defined (Leid, Kastner et al. 1992; Leid, Kastner et al. 1993; Leid 1994). The RAR β expression pattern is more clearly restricted to undifferentiated mesenchyme and stromal compartments (Leid, Kastner et al. 1992). RAR γ is expressed at levels barely detectable by in situ hybridization, making accurate comment impossible (Leid, Kastner et al. 1992). Data from retinoic acid receptor knockout mice is complex but, in short, there seems to be redundancy among RARs. Few malformations are seen in mice with homozygous inactivation of any one RAR gene, whereas double knockout RAR mice display severe malformations of multiple organs and die perinatally. Neither the *RAR α 1^{-/-}* nor the *RAR β*

^{-/-} knockout mice exhibit a dramatic renal phenotype (Mendelsohn, Mark et al. 1994), but double knockout *RARα*^{-/-} / *RARβ*^{-/-} mice have renal hypoplasia and arrested development of the stromal compartment (Mendelsohn, Lohnes et al. 1994).

Figure 1.9 Conversion of vitamin A to retinoic acid and its degradation

Vitamin A (retinol) is converted to retinaldehyde by an enzyme called alcohol dehydrogenase. Retinaldehyde is then converted to retinoic acid (RA) by tissue specific retinaldehyde dehydrogenases (RALDH) in the rate determining step. Recently, cytochrome P415 was shown to be important in degrading RA into metabolites. (Ross, McCaffery et al. 2000).

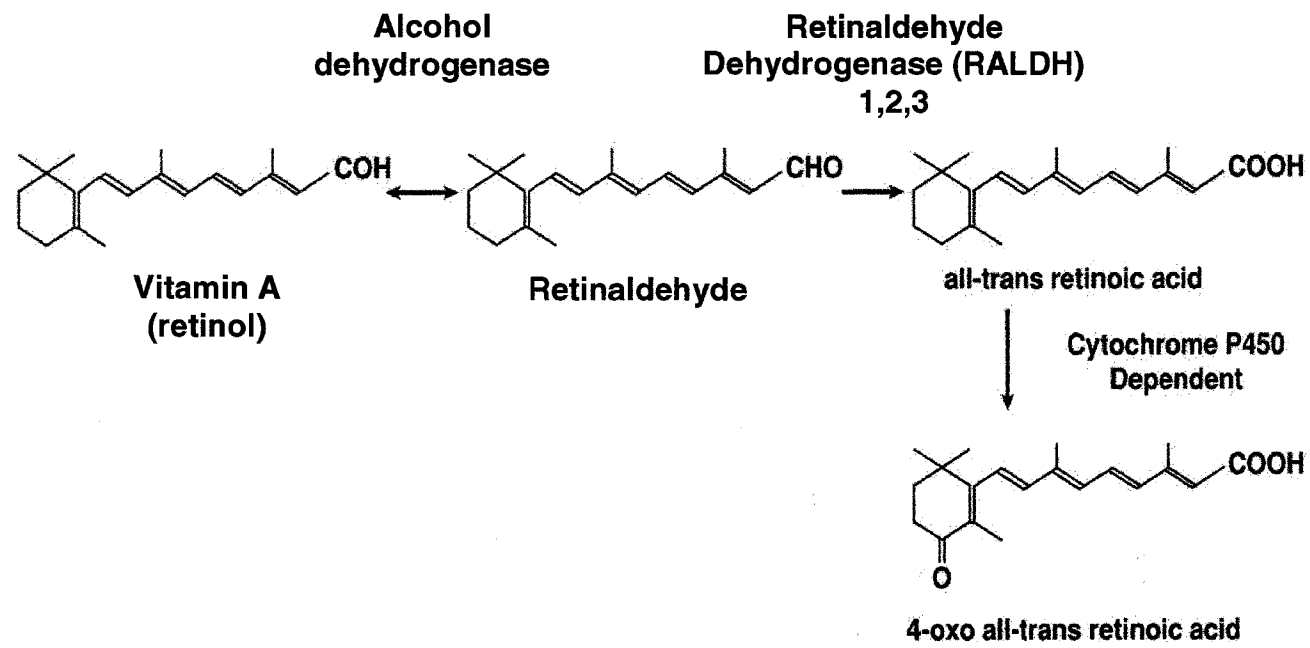
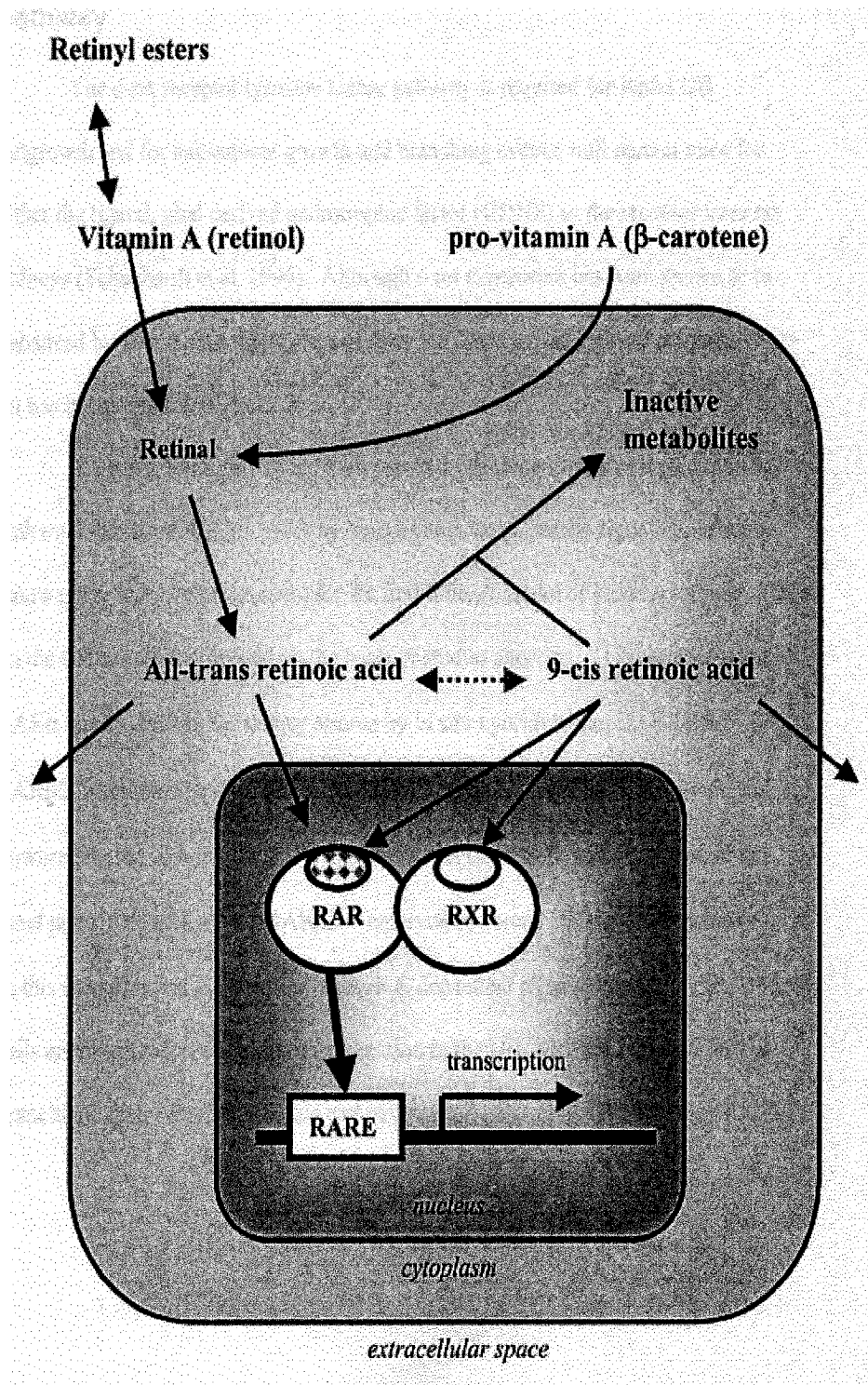


Figure 1.10 Retinoic acid action in cells

Vitamin A is obtained from the diet and is converted to its physiologically active metabolites: all trans retinoic acid (atRA) and 9cisRA, which bind to nuclear receptors RAR and RXR. RAR and RXR heterodimerize and activate specific gene targets containing retinoic acid response elements (RARE) in their promoter regions (Ross, McCaffery et al. 2000)

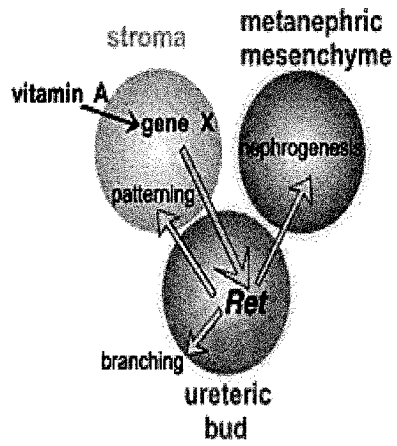


1.6.1.2 Retinoic acid maintains c-ret expression in the UB via an indirect pathway

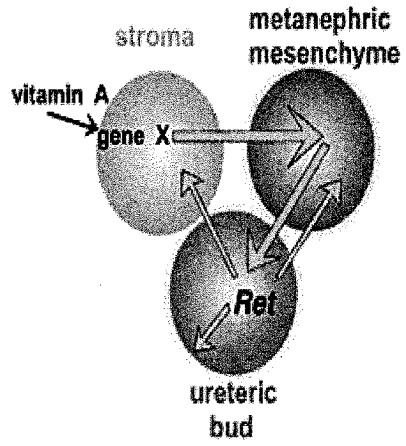
In 2001, Batourina et al. proposed a model for the indirect effects of RA on the UB (Batourina et al. 2001). Initial work identified co-localization of RAR α and RAR β 2 in the kidney stroma. In knock out *RAR α ^{-/-}; RAR β 2^{-/-}* embryos, it was observed that the mesenchymal stromal cell patterning was altered, the UB outgrowth was impaired, and c-ret in the UB tips was down-regulated. Interestingly, they were able to rescue the renal phenotype of *RAR α ^{-/-}; RAR β 2^{-/-}* embryos when they over-expressed c-ret in the UB. Based on these results, they proposed a model of how RA indirectly stimulates the UB to branch. In this model, it is proposed that an unknown molecule expressed in the mesenchymal stroma is activated by RA which is secreted and induces UB branching and c-ret expression (Batourina, Gim et al. 2001) (Figure 1.11).

Figure 1.11 Model of indirect effects of RA on UB branching

A schematic diagram is shown, illustrating a reciprocal signaling loop between stromal cells and the ureteric bud. Vitamin A signaling induces expression of gene X, whose product is secreted by stromal cells and acts on ureteric bud epithelial cells inducing *Ret* expression (yellow arrow). In the reciprocal direction, *Ret* signaling is required for generating secreted ureteric bud signals important for patterning stromal mesenchyme, nephron differentiation and ureteric bud branching. In an alternative model shown at the right, vitamin A signaling induces gene X in stromal cells. Gene X acts first on metanephric mesenchyme, and metanephric mesenchyme generates signals inducing *Ret* expression in ureteric bud cells (yellow arrows). *Ret*-dependent signals are required in the ureteric bud for branching, nephron differentiation and stromal cell patterning (gray arrows) (Batourina, Gim et al. 2001).



stroma \Rightarrow ureteric bud



stroma \Rightarrow metanephric mesenchyme \Rightarrow ureteric bud

1.6.2 How does the effect of RA on nephrogenic mesenchyme induce branching of the ureteric bud? Lessons from other organs.

Epithelial branching is a common feature of mammalian organogenesis. It is fundamental in proper development of the kidney, lung, mammary gland, salivary (submandibular) gland, pancreas, and prostate. In all cases, morphogenesis begins when an epithelial “bud” forms from a preexisting epithelium, either by evagination (kidneys, lungs, salivary glands) or by invaginating from the ectoderm (sweat glands, mammary glands), with new branches successively occurring to give rise to a treelike structure of interconnected tubes (Metzger and Krasnow 1999). Based on common events that occur during this process, it has been proposed that branching organs may share common molecular pathways (Hu and Rosenblum 2003). Given the number of common molecules involved in the branching process of both the kidney and the lung (Table 1.2), we have focused our attention on possible additional similarities in their development.

1.6.2.1 Pulmonary mesenchymal cells stimulate branching morphogenesis of the epithelial lung bud.

The lung begins to develop with the emergence of an epithelial structure, the lung bud (Perelman, Engle et al. 1981). This initial branching event is followed by 23 generations of branches via invasion of the surrounding mesenchyme and dichotomous bifid branching. Asymmetrical branching in the lung begins at week 7 of gestation in humans resulting in the right side with three lobes (four in mouse), and the left side with two (one in mouse). Lung development comprises multiple stages, but can be roughly divided into early and late events (Roth-Kleiner and Post 2005) with overall lung development going through eight stages (Figure 1.12). In early lung development of humans, the epithelial lung bud undergoes repetitive, dichotomous branching, beginning at around week 3 and slowing down at around week 34. In later stages of development (~36 weeks of gestation), the lung begins to mature to form the terminal gas exchange units, the alveoli. At this time, airway branching comes to completion, airspaces widen, the mesenchyme thins, surfactant is produced, and cells undergo final differentiation (Roth-Kleiner and Post 2003). By 3 years of age, the overall morphology of the lung has been established

and subsequent expansion occurs through a proportional growth of all lung components until adulthood (<http://www.ana.ed.ac.uk/anatomy/lungbase/lungdev.html>).

Morphogenesis and differentiation of the fetal lung is dependent upon complex interactions between the epithelium and the mesenchyme. Two important molecules that regulate lung development are retinoids and glucocorticoids (GC). RA stimulates initial lung branching of the primary lung bud (Wilson, Roth et al. 1953; Mollard, Ghyselinck et al. 2000). *RAR α ^{-/-}/RAR β ²^{-/-}* KO mice showed agenesis of the left lung and hypoplasia of the right lung (Mendelsohn, Lohnes et al. 1994). However, RA appears to be downregulated during later stages of lung development (Mollard, Ghyselinck et al. 2000).

In early lung development, GC has been found to induce growth retardation (Torday, Zinman et al. 1986), and to distort branching by causing proximal tubules to be dilated (Oshika, Liu et al. 1998). In late stages of lung development, GC stimulates terminal maturation and differentiation of the alveoli (Garbrecht, Klein et al. 2006). The effects of GC are most often indirect (Garbrecht, Klein et al. 2006); GC acts on receptors in pulmonary fibroblasts (mesenchyme) to stimulate the release of a secreted factor which drives maturation of the epithelial lung bud. This paradigm is reminiscent of the retinoic

Table 1.2 Molecules in common between the kidney and other branching organs

Molecule	Kidney	Lung	Mammary	Pancreas	Prostate	Salivary
Activin	Y				Y	
ALKs	Y	Y		Y		
Bcl-2	Y			Y		
Bek (FGF2 splice variant)	Y	Y	Y	Y		Y
Bmps	Y	Y	Y	Y		
Cadherins	Y		Y			
Collagen	Y	Y		Y		Y
Desmin	Y				Y	
EGF	Y	Y	Y	Y		Y
EGFR	Y	Y				Y
Fas ligand	Y	Y		Y	Y	Y
FGFs	Y	Y	Y	Y		Y
FGFRs	Y	Y		Y		Y
Fibronectin	Y	Y				Y
Heperan Sulphate Proteoglycan	Y	Y	Y			
HBF	Y	Y		Y		Y
Hox genes	Y	Y		Y		
11-beta-HSD2	Y	Y				
IGF-1	Y	Y	Y			
IGFBP3	Y	Y	Y			
IGF type 1 Receptor	Y	Y	Y			
Integrins	Y	Y	Y			Y
KGf/FGF7	Y	Y	Y	Y	Y	Y
KGFR	Y	Y	Y	Y		Y
Laminins	Y	Y				Y
LEF-1	Y		Y			
c-met	Y		Y	Y		
Midkine	Y	Y				Y
n-myc	Y	Y				
Nidogen	Y	Y				
Pax genes	Y					Y
PDGFR-alpha	Y	Y	Y			Y
c-Ret	Y					Y
Retinoic Acid	Y	Y				Y
RAR	Y	Y				Y
Ron	Y	Y				
c-ros	Y	Y				
Shh	Y	Y				
Syndecan	Y	Y		Y		
TGF beta	Y	Y	Y	Y		Y
TGF-beta Receptor	Y	Y				Y
VEGF	Y	Y				
Vimentin	Y			Y	Y	Y
Wnts	Y		Y			

(adapted from glandular organ database: www.ana.edu.ac.uk/anatomy/orghome.html)

Figure 1.12 Development of the human lung

The development of the lung can be divided into eight stages. In early lung development (from ~3 weeks of gestation to ~34 weeks of gestation), pulmonary branching morphogenesis occurs. Late lung development (~36 week to after birth), comprises of maturation events (Roth-Kleiner and Post 2005; Perelman, Engle et al. 1981).

Gestational Age	Lung Morphology	Changes
3-4 Weeks	<p>Lung Bud First Division</p>	<p>Lung bud appears. First Branching of the airway Trachea and esophagus separate.</p>
5-6 Weeks	<p>Beginning of Pseudoglandular Period</p>	<p>Elongation to form the mainstem bronchi. Further division to form lobar bronchi.</p>
7 Weeks	<p>Further Airway Divisions</p>	<p>Cartilage is present in the trachea. Bronchi have segmented and subsegmental branches appear</p>
8-10 Weeks	<p>Closure of Pleuroperitoneal Canals</p>	<p>Pleuroperitoneal canals closed. Continued branching of the airways. Airway cartilage extends distally.</p>
16 Weeks	<p>Beginning of Canalicular Period</p>	<p>Bronchi segmentation is complete. Pulmonary acinus formation begins. Airways lined with ciliated columnar epithelium.</p>
20 Weeks	<p>Pulmonary Vascularization</p>	<p>Cuboidal epithelium lines canalized airways. Mesenchyme decreases. Capillaries penetrate early saccules.</p>
26 Weeks	<p>Beginning of Terminal Sac Period</p>	<p>Transitional ducts give rise to respiratory saccules (s). Septae formed by attenuation of epithelium.</p>
32-36 Weeks	<p>Type II Pneumonocytes</p>	<p>Type II pneumonocytes with lamellar bodies increase in number. Potential airspaces filled with fetal pulmonary fluid.</p>

acid idea (Batourina, Gim et al. 2001) in the kidney. Thus, it is tempting to speculate that the glucocorticoid dependent relationship between pulmonary mesenchyme and the epithelial lung bud may share common pathways with the retinoic acid dependent relationship between the mesenchyme and UB in the developing kidney.

1.6.2.3 LGL1 was identified as a branching morphogen in lung mesenchyme

A novel gene, late gestation lung protein 1 (*Lgll*), was recently identified in the lung by using differential display PCR to screen for genes induced by GC in late gestation lung tissue (Kaplan, Ledoux et al. 1999). Characterization of *Lgll* identified that the mRNA was detected in fetal lung mesenchyme, and pulse-chase experiments determined that LGL1 was a secreted glycoprotein of 52kDa that acted on the epithelia (Oyewumi, Kaplan et al. 2003). Antisense oligodeoxynucleotides directed against LGL1 inhibited airway branching in fetal lung buds in explant culture, establishing a role for *Lgll* in lung branching morphogenesis (Oyewumi, Kaplan et al. 2003). Interestingly, Northern blot analysis identified *Lgll* in other organs, including the kidney (Kaplan, Ledoux et al. 1999). Based on the similarities between airway and renal branching morphogenesis, it is of interest to determine if *Lgll* plays a role in renal development.

1.6.2.4 LGL1, a candidate RA-induced branching morphogen in kidney?

As a prelude to the project, we screened the *Lgll* promoter for response elements and found putative retinoid response elements in addition to the expected glucocorticoid response element (GRE). We hypothesized, therefore, that LGL1 might function as a mesenchymally derived branching morphogen in the developing kidney, paralleling its function in the lung. If so, we speculate that *Lgll* might be regulated by RA and GC.

CHAPTER 2

THESIS PROPOSAL

2.1 Thesis Proposal

Humans are born with the total number of nephrons they will have for life. The number of nephron at birth is a direct reflection of the number of branching events that occurred *in utero* (Hinchliffe, Sargent et al. 1991). The importance of sufficient renal branching morphogenesis is evident in cases where its absence or gross reduction cause renal agenesis or severe hypoplasia. Recent studies have suggested that even a mild reduction in branching events has clinical consequences, resulting in essential hypertension and end-stage renal disease (Brenner, Garcia et al. 1988; Brenner and Milford 1993; Cullen-McEwen, Kett et al. 2003; Keller, Zimmer et al. 2003). However, the genetic determinants responsible for nephron formation remain largely unknown. Nonetheless, two important pathways have been implicated in nephron formation: the *PAX2* pathway (Dziarmaga, Quinlan et al. 2006) and the retinoic acid pathway (Gilbert and Merlet-Benichou 2000). In the present thesis, these two pathways and their effects on renal branching morphogenesis will be studied.

The first objective of my project was to focus on the *PAX2* pathway and subtle renal hypoplasia. Although the control of nephrogenesis is complex, *PAX2* is known to play an important role in final nephron number, with mutations in this gene causing agenesis and renal hypoplasia (Favor, Sandulache et al. 1996; Eccles 1998; Eccles and Schimmenti 1999; Eccles, He et al. 2002; Dziarmaga, Quinlan et al. 2006). Thus, we postulated that mild variations in *PAX2* could cause a subtle reduction in nephron number. For this reason, we proposed to examine common polymorphic variations in the *PAX2* gene to see if they accounted for a subtle reduction in newborn renal volume, a surrogate measure of nephron number. We proposed to study healthy, term Caucasian newborns, from which we would collect cord blood for DNA extraction, serum for cystatin C measurement, and renal ultrasounds to establish a surrogate nephron measurement. The DNA would be used to genotype haplotype tagging single nucleotide polymorphisms (htSNPs) in the *PAX2* gene region to determine a possible association between individual htSNPs and renal volume or cystatin C measurements. By choosing htSNPs, we hoped to construct a haplotype on which we postulate an ancestral variant could account for the subtle renal hypoplasia observed in the normal population.

The second objective of this thesis focused on the retinoic acid (RA) pathway and its effects on renal branching. Although the importance of RA on kidney development is well established (Lelievre-Pegorier, Vilar et al. 1998; Gilbert and Merlet-Benichou 2000; Gilbert 2002), the downstream targets of RA that induce UB branching have yet to be identified (Batourina, Gim et al. 2001). Our knowledge of lung development helped to identify a potential candidate- *Lgll* (Kaplan, Ledoux et al. 1999; Oyewumi, Kaplan et al. 2003). We hypothesized that *Lgll* may exert a role on kidney branching morphogenesis that is similar to its role in the developing lung. Initial screening of the reported *Lgll* promoter identified potential RA binding motifs, among others, and thus, we hypothesized that *Lgll* may be a potential RA target. We proposed to characterize *Lgll* expression in the developing kidney, its response to RA and its effect on renal branching morphogenesis.

CHAPTER 3

COMMON htSNPs IN PAX2 ASSOCIATE A HAPLOTYPE WITH SUBTLE RENAL HYPOPLASIA

3.1 INTRODUCTION

Branching morphogenesis is critical for kidney development; the number of embryonic branching events reflects the final number of nephrons an individual will have for life (Hinchliffe, Sargent et al. 1991). Defects in branching will thus compromise the functional capacity of the mature kidney, with even a subtle decrease in nephron number causing susceptibility to acquired renal diseases and essential hypertension later in life (Cullen-McEwen, Kett et al. 2003; Keller, Zimmer et al. 2003).

In the “normal” population, nephron number varies widely, ranging from 300,000 to over one million per kidney (Nyengaard and Bendtsen 1992). Although this was once dismissed as a benign reflection of human diversity, recent evidence suggests that subtle reduction in nephron number may be of considerable clinical importance. Observations in mice with heterozygous *Gdnf* mutations show that as little as a 30% decrease in total nephron number caused glomerular hypertrophy and hypertension as adults (Cullen-McEwen, Drago et al. 2001; Cullen-McEwen, Kett et al. 2003). Concurrent with these findings, Keller *et al.* described patients with essential hypertension to have roughly 50% fewer nephrons than age-matched controls (Keller, Zimmer et al. 2003). Taken together, these observations suggest that humans born with a subtle reduction in nephron numbers may be at increased risk of developing “essential” hypertension and acquired renal disease as adults.

The genetic determinants of final nephron number remain unknown. However, *PAX2*, a transcription factor, has profound effects on nephron formation. Mutations in *PAX2* have been reported to cause autosomal dominant renal hypoplasia (Renal-Coloboma Syndrome (RCS)) (Sanyanusin, McNoe et al. 1995; Eccles and Schimmenti 1999; Porteous, Torban et al. 2000), and glomerular hypertrophy (Salomon, Tellier et al. 2001), while homozygous mutations cause renal agenesis. Several roles for *PAX2* have been described during kidney development with recent work implicating its anti-apoptotic function as the mechanism by which it optimizes UB growth and renal branching morphogenesis (Dziarmaga, Clark et al. 2003; Dziarmaga, Eccles et al. 2006; Dziarmaga, Hueber et al. 2006). These observations suggest that *PAX2* is centrally involved in determining nephron number.

For these reasons, we chose *PAX2* as a candidate gene involved in subtle renal hypoplasia. We hypothesised that common variations in *PAX2* may account for a subtle reduction in final nephron number observed in normal individuals born into the lower end of the nephron endowment spectrum.

We used the HapMap project data (2003) to identify common haplotype-tagging single nucleotide polymorphisms (htSNP) in the *PAX2* gene. We examined the possibility that htSNPs associate a haplotype with subtle congenital renal hypoplasia in healthy Caucasian newborns. We hypothesized that such a haplotype may contain an ancestral polymorphism that causes subtle renal hypoplasia in normal individuals.

Rare *PAX2* mutations have been associated with severe conditions such as Renal Coloboma syndrome (Sanyanusin, McNoe et al. 1995; Sanyanusin, Schimmenti et al. 1995). A few studies have examined polymorphisms in *PAX2* exons or its promoter (Shim, Nakamura et al. 1999; Gelb, Manligas et al. 2001).

As recorded in NCBI dbSNP (BUILD 125), 248 SNPs have been found in the *PAX2* region. Among these, some SNPs have predicted function on gene transcription and splicing, but none change amino acids. To our knowledge, we are the first to examine *PAX2* variants that are associated with subtle renal hypoplasia.

3.2 MATERIALS AND METHODS

3.2.1 Study subjects

Subjects in this study were healthy Caucasian infants born to women with uncomplicated pregnancies that were recruited with informed consent at their final prenatal clinical visit at the Royal Victoria Hospital (N=300) in Montreal, QC. Mothers with twins, diabetes, intrauterine growth restriction, genetic abnormalities, renal malformations or hydronephrosis, delivery <36 weeks and who had newborns with low serum albumin were excluded. At birth, cord blood was obtained for DNA isolation (10 mls in EDTA at room temperature) and for serum cystatin C determination (5 mls at 4°C). Newborn length, weight, sex and gestational age as recorded in the hospital post partum unit records was collected.

3.2.2 Renal Volume

Renal volume was measured by an experienced ultrasonography technician within the first 3 days of life. Renal volume was calculated from measures of maximal longitudinal length, transverse width, and height of the kidney, using software for estimation of an eliptoid solid installed on the ultrasonography machine. The equation that was used is the following:

Volume = $4/3 \pi$ (length/2) (height/2) (width/2) (Beyer, et al. 1987, page 131). Left, right, and total kidney volumes were measured. Body surface area was estimated: [body length (cm) x weight (kg)/3600]^{1/2} according to Mosteller (Mosteller et al. 1987). The final study parameter was mean total renal volume normalised by body surface area.

3.2.3 Serum cystatin C measurement

Serum was separated by centrifugation (1000 rpm for 2-3 min) from 5 ml of cord blood stored at 4°C in EDTA-free tubes for 12-24 hours after delivery and frozen at -70°C for cystatin C assay by nephelometry (Filler et al. 1999).

3.2.4 Genomic DNA isolation

Genomic DNA was isolated from cord blood samples containing EDTA using the FlexiGene DNA kit (Qiagen, Maryland) according to the manufacturer's protocol. DNA quality was confirmed by spectrophotometry (260/280 ratio 1.8-2.0) and was quantified using the Quant-iT™ PicoGreen® dsDNA Assay Kit *2000 (Invitrogen).

3.2.5 Choice of htSNPs in the PAX2 gene region

Haplotype-tagging single nucleotide polymorphisms (htSNPs) were chosen from a region spanning the *PAX2* gene (70kb) plus 10 Kb at both the 5' and 3' flanking segments (total chromosome location: Chr10:102,160,274-102,260,517), using the HapMap human genome database (www.hapmap.org, NCBI_35, dbSNP_b135). All known SNPs (N=248) from the CEPH population (Caucasians from Western Europe settling in Utah) for the *PAX2* gene region were downloaded into Haploview (ver 3.32) and a plot of linkage disequilibrium between SNPs was obtained. Using Haploview's "Tagger" program, set for pairwise tagging, we chose 23 htSNPs occurring in at least 5%

of the population which spanned the three major linkage disequilibrium blocks ($r^2 > 0.8$) in the region. These htSNPs are indicated in Table 3.1.

3.2.6 PAX2 htSNP genotypes

For each subject, 15ng of genomic DNA was used for multiplex genotyping reactions, using Sequenom iPLEX PCR technology (Sequenom, San Diego CA, USA). This system involves extension of the PCR amplicon with modified nucleotides to distinguish SNP alleles by Matrix Assisted Laser Desorption Ionization-Time Of Flight (MALDI-TOF) technology. Primers for SNP detection were designed using MassARRAY AssayDesign software (Sequenom). Briefly, the assay conditions were as follows: PCR reactions were performed using 1.25 X PCR buffer, 1.625mM MgCl₂, 0.5mM dNTPs, 0.1 uM PCR primer pool, 0.1 U/ul Quiagen Hotstar TAQ, and 15ng DNA. Cycling conditions included an initial denaturation at 95°C for 15min, 45 cycles of denaturation (95°C for 20sec), annealing (56°C for 30sec) and extension (72°C for 60sec), followed by final extension of 72°C for 3 min. To each PCR product, a shrimp alkaline phosphatase (SAP) reaction was performed using 1X SAP buffer and 1U/ul of SAP and incubated at 37°C for 40min followed by enzyme denaturation at 85°C for 10min. A single base pair extension was performed on the clean PCR products using 10.20% (v) of probe mix, 1mM of iPlex Terminator, 1X iPlex Buffer, and 0.655 U/ul iPlex Thermo Sequenase. The cycling conditions were performed with an initial denaturation of 95°C for 30sec, followed by 45 cycles of [denaturation at 95°C for 5sec followed by 5 cycles of annealing at 52°C for 5sec and extension at 80°C for 5sec] and a final extension of 72°C for 3min. A list of the primers and probes used in the Sequenom reaction is attached in the appendix.

3.2.7 PAX2 Haplotypes

Of the 5 htSNPs identified in the preliminary analysis as independently associated with total renal volume normalised for body surface area, 3 htSNPs (rs11599825, rs11190688 and rs11190702) were found to be in tight linkage disequilibrium with each other based on HapMap data using the CEPH population ($D' = 0.911$, $r^2 = 0.795$). These htSNPs occurred at similar frequencies in the CEPH population (major allele frequency =

~0.70). Thus it was possible to consider these htSNPs as belonging to one LD block and were used to reconstruct haplotypes: GGG or AAA. These *PAX2* haplotypes were assigned to individuals in the Caucasian cohort based on the 3 htSNP genotypes.

3.2.8 Statistical Analysis

Data was analysed using a statistical software programme (SPSS for Windows, ver. 11.0, SPSS Inc., Chicago, USA). The distribution of each clinical endpoint in our cohort was tested for skewness. Genotype frequencies for each htSNP were examined for divergence from Hardy–Weinberg equilibrium.

Of the 300 subjects recruited, complete data sets were obtained for 200. Of these, the first 180 subjects were genotyped for 23 htSNPs. In preliminary analyses, mean total renal volume, total renal volume normalised for body surface area and cord serum cystatin C was established for each htSNP genotype (homozygous rare allele, heterozygous and homozygous common allele). Association between htSNP genotype and each variable was assessed by one-way analysis of variance (ANOVA). A post-hoc t-test (independent samples) was performed to identify significant differences between genotype groups if the ANOVA was close to being significant ($p < 0.05$). For relatively rare alleles with few homozygous subjects, t-tests were performed to compare subjects homozygous for the common allele with subjects homozygous or heterozygous for the uncommon allele.

Of the 180 genotyped subjects, it was possible to establish *PAX2* haplotypes for a subset of 168, using three tightly linked htSNPs. Association between *PAX2* haplotypes and total renal volume normalised for body surface area was assessed by ANOVA followed by post-hoc t-tests as above.

Table 3.1 Choice of *PAX2* htSNPs

SNP	Position	Variation	Location	% in CEPH
rs10786606	chr10:102492138	R		19(A)
rs10883537	chr10:102485687	Y		33(C)
rs11190688	chr10:102514460	R	intron	26(A)
rs11190702	chr10:102532515	R	intron	26(A)
rs11592735	chr10:102518253	R	intron	3(A)
rs11598208	chr10:102512526	M	intron	2(A)
rs11599825	chr10:102510165	R	intron	28(A)
rs11812391	chr10:102551180	Y	intron	4(T)
rs11816136	chr10:102581444	R		11(G)
rs12266644	chr10:102549048	K	intron	3(T)
rs12781220	chr10:102536387	K	intron	3(T)
rs2077642	chr10:102555459	Y	intron	42(C)
rs2476968	chr10:102585910	R		28(A)
rs2495762	chr10:102559952	K	intron	5(T)
rs3862028	chr10:102566118	R	intron	1(A)
rs3923992	chr10:102518799	Y	intron	5(T)
rs4244341	chr10:102498567	K	intron	20(T)
rs4278454	chr10:102486475	R		31(A)
rs4601695	chr10:102504071	Y	intron	1(T)
rs4917911	chr10:102549411	R	intron	12(G)
rs6421335	chr10:102497329	Y	intron	25(C)
rs927638	chr10:102560105	R	intron	2(A)
rs996359	chr10:102580743	M		23(A)

3.2.9 *PAX2* allele expression assay

Human renal carcinoma cell lines were screened for heterozygosity of a *PAX2* exonic SNP (rs1800898) tightly linked ($D' = 0.827$, $r^2 = 0.63$) to the htSNPs (rs1559828, rs1119068) used to establish the *PAX2* haplotypes. Cells were grown in RPM1 or minimal eagle media (MEM) supplemented with 5% fetal calf/5% fetal bovine serum, 1% penicillin/streptomycin and incubated at 37°C in humidified 5% CO₂ in air. Cells were trypsinized, pelleted and washed in PBS for genomic DNA isolation using the Wizard Genomic DNA Purification Kit (Promega). DNA was amplified by PCR using specific primers flanking the rs1800898 SNP and sequenced by HPLC (Genome Centre, Montreal, QC).

PCR reactions included 1ul of a 100ng stock of each primer, 0.5ul of 10mM dNTPs, 0.75ul of 50mM MgCl₂, 2.5ul 10X PCR Buffer, 16.95ul ddH₂O, 0.3ul Taq polymerase, and 2ul of DNA (total volume 25ul). The PCR cycling conditions were performed using an initial denaturation step at 96°C for 3min, followed by 35 cycles each consisting of denaturation (94°C for 30sec), annealing (55°C for 30sec), and extension (72°C for 30sec). Synthetic oligodeoxynucleotides pairs spanning the SNP yielded a 230bp product. The following sets of PCR primers were used:

DNA Fwd Primer: TGATGAAGTCAAGTCGAGTCTAT

DNA Rev Primer: AAGCACCTGGTTTTAGAAG

One heterozygous cell line was obtained and used to establish the level of *PAX2* mRNA expression from each allele. Total cellular RNA was isolated using Qiagen RNeasy Mini Column extraction kit (Qiagen, Maryland, USA), reverse-transcribed and amplified in a one-step RT-PCR reaction using the Qiagen OneStep RT-PCR kit (Qiagen, Maryland, USA), following the manufacturer's recommendations. RT-PCR reactions were performed using 30 minutes at 50°C, 15 minutes at 95°C, 35 cycles each consisting of denaturation (94°C for 30sec), annealing (55°C for 30sec), and extension (72°C for 30sec). Synthetic oligodeoxynucleotides pairs were designed to span the SNP and yielded a 250bp product. The following sets of primers were used:

RNA Fwd Primer: ACGTCTTCCAGGCATCAGAG

RNA Rev Primer: AGGGTGGAGGTGGGGTAG

PCR and RT-PCR products were run on a 1% (wt/vol) agarose gel and visualized by ethidium bromide staining to confirm amplicon size.

Relative levels of mRNA expression from each allele were estimated by quantitative HPLC sequencing (Genome Quebec, Montreal, QC) of the RT-PCR amplicon as described by Pastinen *et al.* 2005. In this method, the relative amplitude of cDNA from the normalised SNP nucleotide peak from the RT-PCR products are standardized to the relative amplitude of gDNA from the normalised SNP nucleotide peak from the PCR product. Normalization of each allele peak to the surrounding peak heights in the sequenced area was performed with Peak Picker, a program developed by the Genome Centre, Montreal, QC (Pastinen, Ge et al. 2006). Standardization of the cDNA to gDNA was performed by using the following formula:

Allelic imbalance (AI) = $(\text{RT-PCR peak}_A / \text{PCR peak}_A) \div [(\text{RT-PCR peak}_A / \text{PCR peak}_A) + (\text{RT-PCR peak}_C / \text{PCR peak}_C)] * 100\%$.

PCR reactions were performed on two separate occasions, with each performed in triplicate. RT-PCR reactions were performed in replicates of 5X. The sequencing reactions were performed in duplicate for each PCR and RT-PCR reaction.

3.3 RESULTS

3.3.1 Linkage disequilibrium in the PAX2 gene +/- 10kb region of the CEPH population

In Figure 3.1, the amount of LD between single nucleotide polymorphisms (SNPs) in the PAX2 +/- 10kb gene region from the CEPH population was obtained using Haploview. A total of 248 SNPs were downloaded with 124 SNPs capturing the three major LD blocks. With this information, 23 haplotype tagging SNPs (htSNPs) were chosen to be genotyped in our cohort of Caucasian infants.

3.3.2 Characteristics of study subjects

The characteristics of the study subjects are presented in Table 3.2 (A). Among all study subjects, the average gestational age was 39.6 weeks with a range of 37.14 to 42.24 weeks, and slightly less than half of the study subjects were female (49.4%). Average weight, height and body surface area are 3.58 kg +/- 0.46 SD, 51.08 cm +/- 2.51 SD, 0.225 m² +/- 0.018 SD.

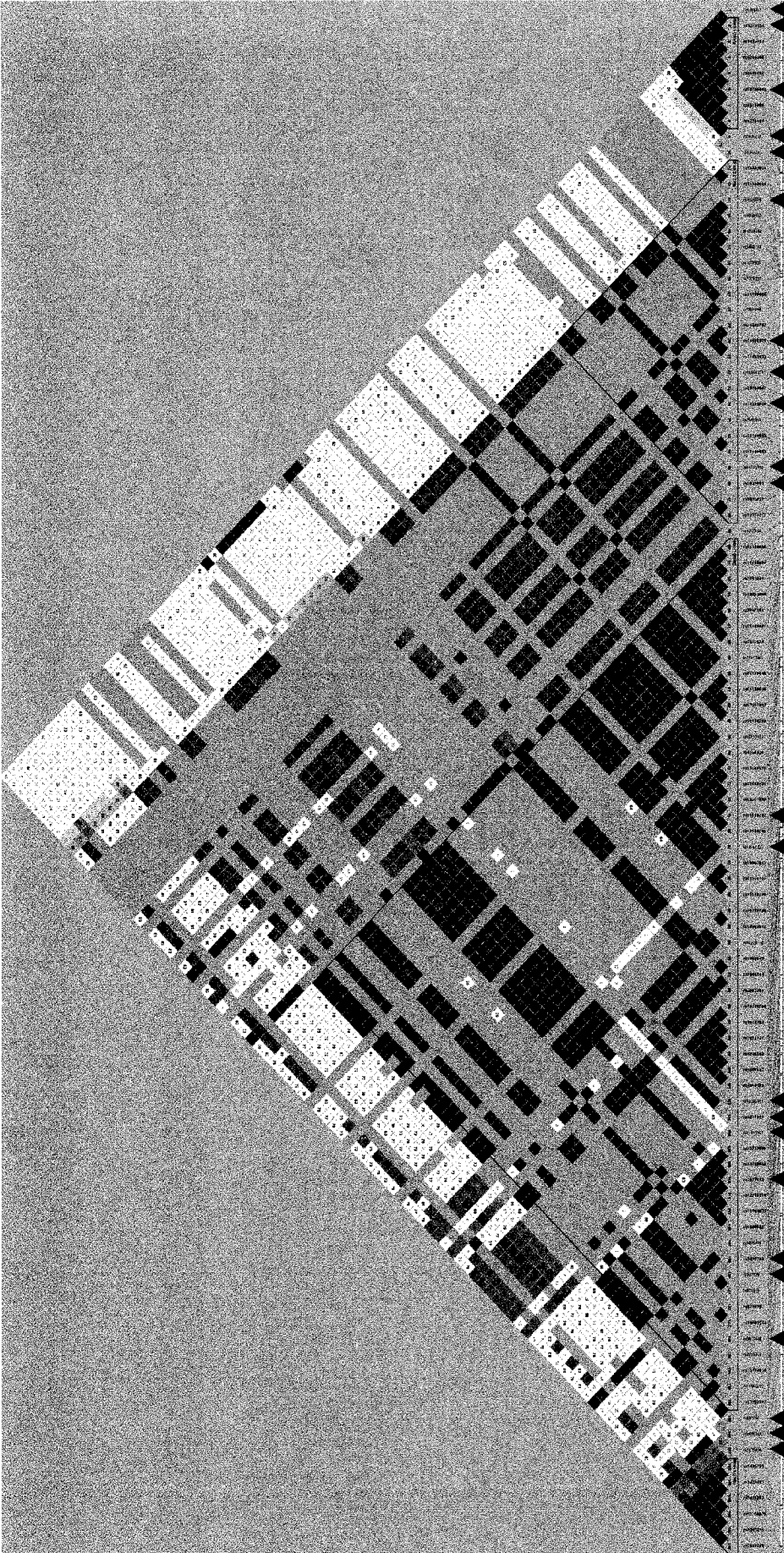
The renal volumes and cystatin C values are presented in Table 3.2 (B). Unadjusted left, right, and total kidney volume were 14.45cc +/- 3.86 SD, 15.41cc +/- 3.89 SD, and 29.56 +/-6.96 SD. These values are all similar to a previous report that examined a large Danish cohort of newborns within the first 5 days of life (Schmidt, Main et al. 2004). Renal volume was corrected for body surface area (BSA) and the mean normalised left kidney/BSA, right kidney volume/BSA, and mean total kidney volume/BSA were 63.36cc/m² +/- 16.04 SD, 68.82 cc/m² +/- 16.59 SD, and 132.17 cc/m² +/- 28.9 SD. The mean levels of serum cystatin C were 1.92 mg/L +/- 0.32 SD.

The distribution of the characteristics in our cohort approached normality and the total kidney volume, total kidney volume normalised for BSA, and cystatin C distributions were plotted as histograms (Figures 3.2 (A), (B), (C)). The conversion of the data to a natural log scale was thus not required (skewness was less than 2 for all characteristics).

The distribution of total renal volume was correlated with body surface area (BSA) ($R^2 = 0.11$, Pearson correlation = 0.332, $p < 0.01$) (Figure 3.3 (A)). The correlation between cystatin c and total kidney volume is shown in Figure 3.3 (B) (Pearson correlation = -0.317, p (2 tailed) < 0.01 , $R^2 = 0.101$) and the correlation between cystatin C and total kidney volume normalised for body surface area is shown in 3.3 C (Pearson Correlation = -0.305, p (2 tailed) < 0.01 , $R^2 = 0.093$).

Figure 3.1 Linkage disequilibrium between SNPs in the PAX2 gene region of CEPH population

23 htSNPs were chosen to span the PAX2 gene +/- 10 Kb to capture the majority of other common alleles.



rs10883537
rs4278454

rs10786606

rs6421335
rs4244341

rs4601695

rs11599825

rs11598208

rs11190688

rs11592735
rs3923992

rs11190702

rs12781220

rs1226664
rs4917911
rs11812391

rs2077642

rs2495762
rs927638

rs3862028

rs996359
rs11816136
rs2476968

Table 3.2 Characteristics of study subjects

A) Characteristics of study subjects

The mean weight, length, body surface area (BSA), gestational age, and sex for the cohort of Caucasian newborns are presented.

B) Study end point parameters

Mean kidney volumes, normalized mean kidney volumes, and mean serum cystatin C measurements are presented. For the total kidney volume measurement, the minimum and maximum volume spans a ~3 fold range and the normalized total kidney volume/BSA spans ~3.6 fold range.

A

Characteristics of study subjects

	Weight (kg)	Length (cm)	Body surface area (m ²)	Gestation Age (weeks)	Sex
N	166	162	162	150	166
Mean	3.58	51.08	0.225	39.6	49.4% female
SD	0.466	2.51	0.018	1.13	

B

Table of renal volume and cystatin C

	Left kid vol (cc)	Right kid vol (cc)	Total kid vol (cc)	Left kid vol/ BSA (cc/m ²)	Right kid vol/ BSA (cc/m ²)	Total kid vol/ BSA (cc/m ²)	Serum cystatin C (mg/L)
N	169	169	169	160	160	160	168
Mean	14.14	15.42	29.56	63.36	68.83	132.17	1.92
SD	3.86	3.89	6.96	16.04	16.59	28.9	0.32
Minimum	3.31	7.44	15.05	13.43	29.73	60.14	1.22
Maximum	26.1	28.54	50.33	109.7	121.64	217.5	2.85

Figure 3.2 Distribution of study parameters

All study parameters were distributed normally with minimal skewness. In A) the total renal volume distribution for 169 subjects is shown. The mean value was 29.6 cc +/- 6.96 SD. In B) the total renal volume normalized for body surface area distribution for 160 subjects is shown. The mean value was 132.2 cc/m² +/- 28.9 SD. In C) the distribution of serum cystatin C in 150 patients is shown. The mean value was 1.92 mg/L +/- 0.32 SD.

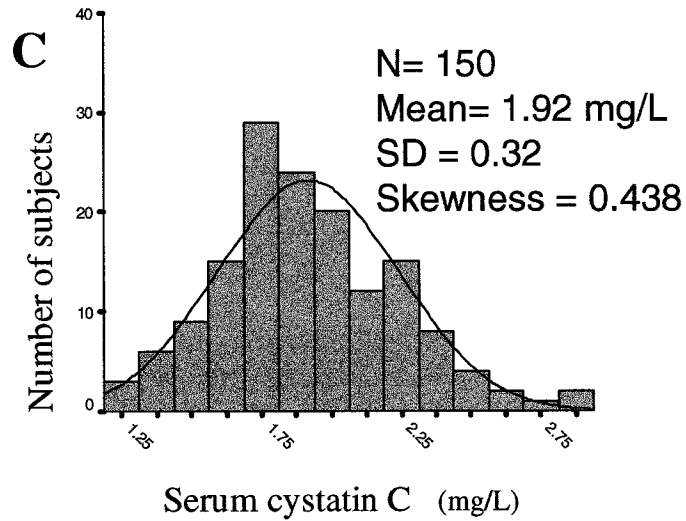
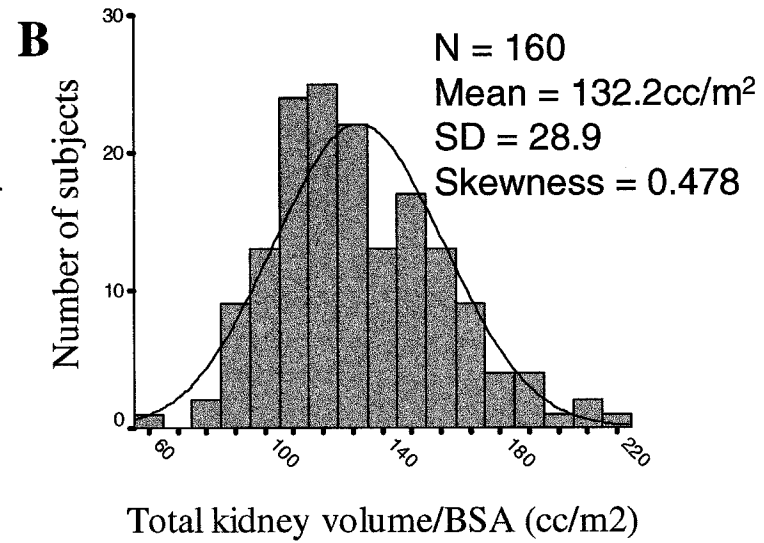
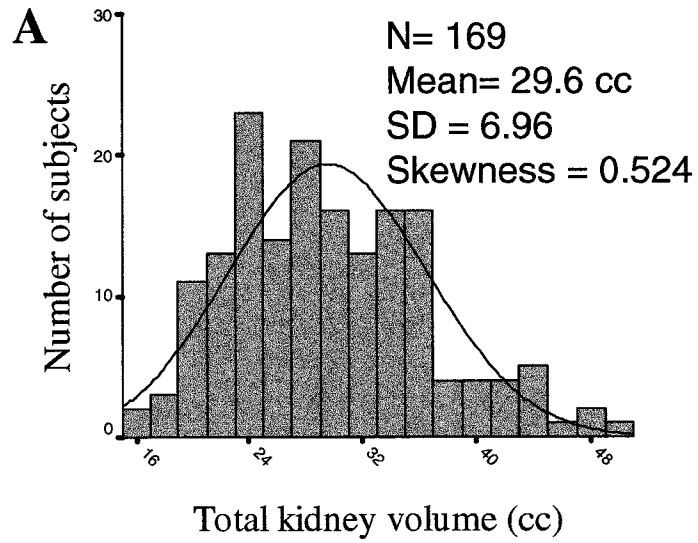
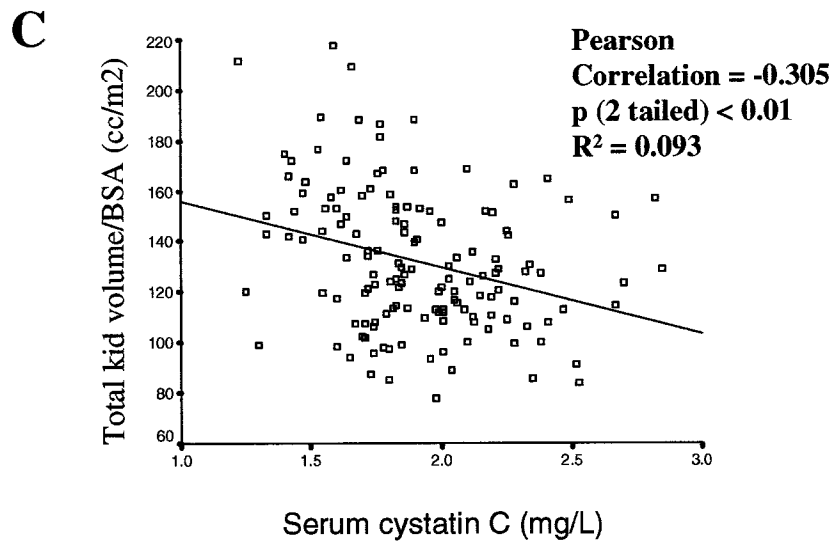
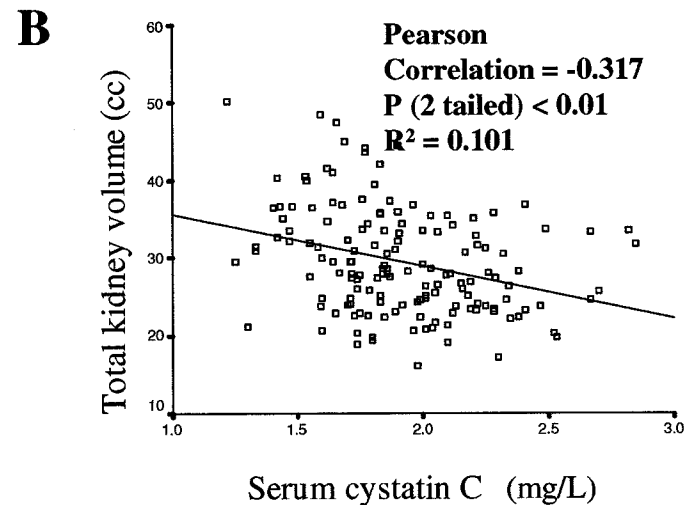
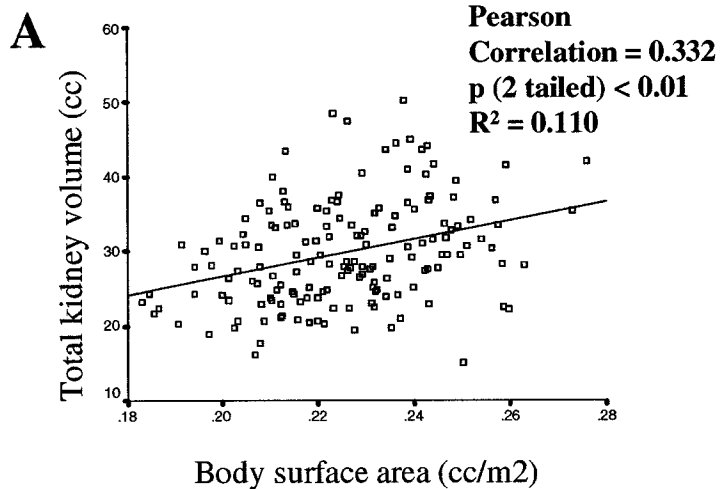


Figure 3.3 Correlation between study parameters

In figure A) the correlation between total renal volume (N=169) and body surface area (N= 162) is shown. In B) the correlation between total renal volume (N= 169) and serum cystatin C (N= 168) is shown. In C) the correlation between total renal volume normalised for body surface area (N=160) and serum cystatin C (N= 168) is shown.



3.3.3 Frequencies of PAX2 variants in study subjects and level of LD between htSNPs

The frequency of the PAX2 SNP genotypes and alleles in the newborn Caucasian cohort (N=180) are presented in Table 3.3. Genotype distributions for all variants were in Hardy-Weinberg equilibrium. These frequencies are similar to those predicted from the CEPH population listed on Hapmap (www.hapmap.org). The level of linkage disequilibrium between htSNPs was obtained by using the software on Haploview (version 3.32) and is shown in Figure 3.4. The level of LD between htSNPs was measured as D' and r^2 . D' is related to the recombination fraction and r^2 is related to the statistical association.

3.3.3 Genetic association analyses

Mean values of study parameters (total kidney volume and total kidney volume/BSA) are presented by PAX2 SNP genotype for significant associations in Table 3.4. One-way ANOVA was performed and p values are indicated. Post-hoc independent sample t test was performed between each genotype and their p values are shown in the middle of the table. Rare alleles were combined with heterozygous alleles to compare them to the common alleles. The mean values of the study parameters for these comparisons are presented in the last columns of Table 3.4 with their corresponding p values.

3.3.4 PAX2 haplotypes

PAX2 haplotypes are presented in Figure 3.5. The common haplotype, GGG has a frequency of 77.6% in our cohort, with a frequency of 63.7% occurring homozygously (GGG/GGG) and 13.9% occurring heterozygously (GGG/AAA). The less common haplotype occurs in 18.9% of the cohort with 4.8% being homozygous AAA/AAA. The patients with the homozygous common haplotype (GGG/GGG) have a mean total kidney volume of 30.34 cc, a mean total kidney volume normalised for BSA of 134.87 cc/m² and a mean serum cystatin C level of 1.91 mg/L. The patients with the heterozygous GGG/AAA haplotype have a mean total kidney volume of 27.74 cc and total kidney volume normalised for BSA of 123.44 cc/m², which is similar to the patients with homozygous AAA/AAA haplotype who have a total kidney volume of 27.45 cc and total

kidney volume normalised for BSA is 124.09 cc/m². In 3.6% of the cohort (6 individuals), haplotypes were not able to be assigned confidently.

In Table 3.5, the association between haplotypes and study parameters was examined by performing an ANOVA and post-hoc t-test. A significant difference between the homozygous GGG/GGG haplotype and the homozygous common haplotype (GGG/AAA) for both total renal volume and normalised renal volume/BSA was identified ($p < 0.024$, 0.011). When the homozygous AAA/AAA haplotype and the heterozygous AAA/GGGG haplotype were combined and compared to the homozygous GGG/GGG haplotype, a significant difference was observed in the total renal volume ($p = 0.015$) and the total renal volume/ BSA ($p = 0.007$).

3.3.5 Allelic Imbalance

The human renal cell carcinoma cell line A498 was found to be heterozygous for SNP rs1800898. In Figure 3.6 A, the chromatogram of the sequence surrounding the exonic SNP rs1800898 is shown for the PCR reaction (genomic DNA (gDNA)) and for the RT-PCR reaction (coding DNA (cDNA)). The arrow points to the rs1800898 C/A SNP. As is obvious, the height of the peaks corresponding to the C and A alleles for the cDNA are not proportional to the gDNA. Thus, allelic imbalance for *PAX2* is occurring. After normalising by the mean values of the surrounding peak intensities and standardizing for the gDNA, the *PAX2* expression was shown to be almost two fold greater for the common A allele (65.5% +/- 3.7 SD) in the exonic SNP than the rare C allele (34.5 +/- 3.7 SD) ($p < 0.001$).

Table 3.3 Frequencies of htSNPs in PAX2 in Caucasian cohort

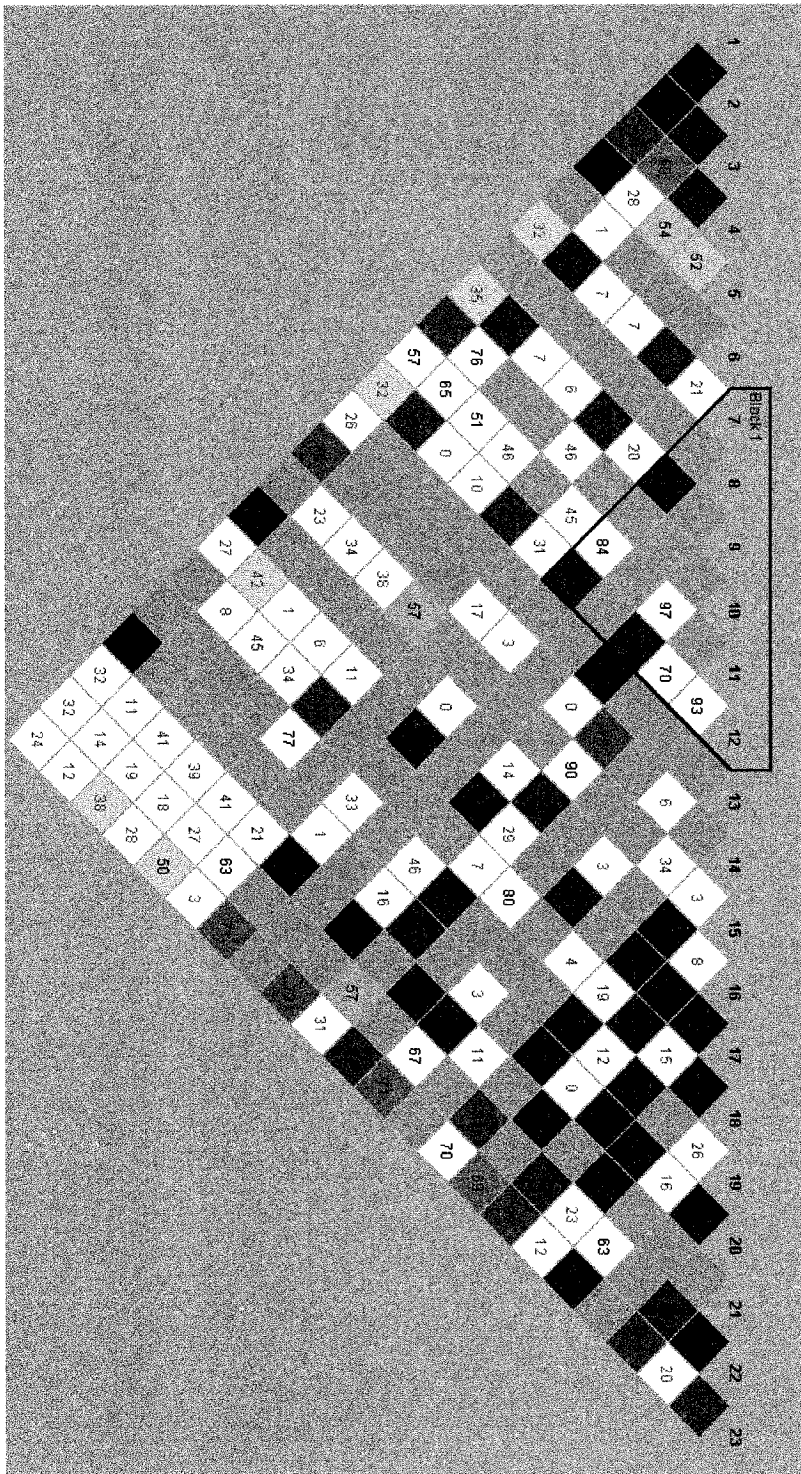
The frequencies of the htSNPs were similar in our cohort compared to those of the CEPH population. The genotype frequency is shown in the columns on the left, while the allele frequencies are shown in the columns on the right.

SNP	Genotype	Genotype		Allele	Allele	
		Frequency (%)	N		Frequency (%)	N
rs10786606	AA	9(5.84%)	154	A	23.70%	
	AG	55(35.71%)		G		76.30%
	GG	90(58.44%)				
rs10883537	CC	12(7.84%)	153	C	27.45%	
	CT	60(39.22%)		T		72.55%
	TT	81(52.94%)				
rs11190688	AA	8(4.76%)	168	A	19.64%	
	AG	50(29.76%)		G		80.36%
	GG	110(65.48%)				
rs11190702	AA	8(5.19%)	154	A	19.48%	
	AG	44(28.57%)		G		80.52%
	GG	102(66.23%)				
rs11592735	AA	1(0.59%)	169	A	5.62%	
	AG	17(10.06%)		G		94.38%
	GG	151(89.35%)				
rs11598208	AA	0(0%)	170	A	0.29%	
	AC	1(0.59%)		C		99.71%
	CC	169(99.41%)				
rs11599825	AA	8(5.03%)	159	A	18.87%	
	AG	44(27.67%)		G		81.13%
	GG	107(67.30%)				
rs11812391	CC	150(92.02%)	163	C	96.01%	
	CT	13(7.98%)		T		3.99%
	TT	0(0%)				
rs11816136	AA	118(71.95%)	164	A	84.76%	
	AG	42(25.61%)		G		15.24%
	GG	4(2.44%)				
rs12266644	GG	151(90.42%)	167	G	95.21%	
	GT	16(9.58%)		T		4.79%
	TT	0(0%)				
rs12781220	GG	152(95.60%)	159	G	97.80%	
	GT	7(4.40%)		T		2.20%
	TT	0(0%)				
rs2077642	CC	28(16.87%)	166	C	38.55%	
	CT	72(43.37%)		T		61.45%
	TT	66(39.76%)				
rs2476968	AA	19(12.10%)	157	A	35.67%	
	AG	74(47.13%)		G		64.33%
	GG	64(40.77%)				
rs2495762	GG	148(90.24%)	164	G	95.99%	
	GT	15(9.15%)		T		4.01%
	TT	1(0.61%)				
rs3862028	AA	149(91.98%)	162	A	95.99%	
	AG	13(8.02%)		G		4.01%
	GG	0(0%)				
rs3923992	CC	152(91.10%)	167	C	95.51%	
	CT	15(8.98%)		T		4.49%
	TT	0(0%)				
rs4244341	GG	98(59.76%)	164	G	78.05%	
	GT	60(36.59%)		T		21.95%
	TT	6(3.66%)				
rs4278454	AA	23(14.65%)	157	A	36.62%	
	AG	69(43.95%)		G		63.38%
	GG	65(41.40%)				

rs4601695	CC	154(97.47%)	158	C	98.73%
	CT	4(2.53%)		T	1.27%
	TT	0(0%)			
rs4917911	AA	120(76.92%)	156	A	87.82%
	AG	34(21.80%)		G	12.18%
	GG	2(1.12%)			
rs6421335	CC	7(4.93%)	142	C	24.65%
	CT	56(39.43%)		T	75.35%
	TT	79(55.63%)			
rs927638	AA	0(0%)	157	A	1.27%
	AG	4(2.55%)		G	98.73%
	GG	153(97.45%)			
rs996359	AA	13(8.81%)	160	A	27.19%
	AC	61(38.13%)		C	72.81%
	CC	86(53.75%)			

Figure 3.4 Linkage disequilibrium in PAX2 htSNPs in Caucasian cohort

The amount of linkage disequilibrium (LD) between the htSNPs of *PAX2* in the study subjects is indicated by the intensities of the colors (red = in tight LD, white = little LD). LD is measured by D' .



rs10883537

rs4278454

rs10786606

rs6421335

rs4244341 *

rs4601695

rs11599825 *

rs11598208

rs11190688 *

rs11592735 *

rs3923992

rs11190702 *

rs12781220

rs12266644

rs4917911

rs11812391

rs2077642

rs2495762

rs927638

rs3862028

rs996359

rs11816136

rs2476968

Haplotype

Table 3.4 Association of individual htSNPs in PAX2 with study parameters

The significant (or borderline significant) associations observed between individual htSNPs and total renal volume or total renal volume normalised by body surface area (BSA) are indicated by ANOVA and T-tests. The T-tests were performed between all three htSNP genotypes (T-test (individual genotypes)), or between grouped (rare and heterozygous) genotypes and common genotypes (T-test (grouped genotypes)).

ANOVA

T test (individual genotypes)

T test (grouped genotypes)

		Homozygous	Hetero	Homo	p	p values							
		rare		common		Rare vs htz	Hetero vs common	Rare vs Common	Rare		Common	p	
Total renal volume (cc)						Total renal volume (cc)			Total renal volume (cc)				
rs1190688	Mean	27345	28.17	30.5	0.096	0.78	0.051	0.233	rs1190688	Mean	28.07	30.5	0.031
	N	8	50	108						N	58	108	
rs11190702	Mean	26.33	28.82	30.81	0.09	0.356	0.118	0.077	rs11190702	Mean	28.44	30.81	0.047
	N	8	44	100						N	52	100	
rs11592735	Mean	21.07	32.93	29.149	0.059	0.17	0.042	0.224	rs11592735	Mean	32.272	29.33	0.09
	N	1	17	149						N	18	149	
rs11599825	Mean	27.45	28.31	30.75	0.09	0.734	0.053	0.205	rs11599825	Mean	28.18	30.75	0.03
	N	8	44	105						N	52	105	
rs4244341	Mean	31.87	30.97	28.94	0.167	0.759	0.079	0.381	rs4244341	Mean	31.04	28.95	0.061
	N	5	60	97						N	65	97	
Total renal volume/BSA (cc/m2)						Total renal volume/BSA (cc/m2)			Total renal volume/BSA (cc/m2)				
rs1190688	Mean	124.09	125.38	136.54	0.061	0.901	0.029	0.243	rs1190688	Mean	125.19	136.54	0.018
	N	8	47	102						N	55	102	
rs11190702	Mean	120	128.22	137.65	0.079	0.465	0.079	0.098	rs11190702	Mean	126.93	137.65	0.033
	N	8	41	95						N	49	95	
rs11592735	Mean	99.25	150.55	131.11	0.021	0.105	0.012	0.259	rs11592735	Mean	147.35	131.11	0.031
	N	1	15	142						N	16	142	
rs11599825	Mean	124.09	125.56	137.79	0.044	0.878	0.022	0.207	rs11599825	Mean	125.34	137.79	0.012
	N	8	41	99						N	49	99	
rs4244341	Mean	137.49	139.67	129.09	0.088	0.862	0.029	0.536	rs4244341	Mean	139.5	129.09	0.028
	N	5	56	92						N	61	92	

Figure 3.5 Schematic depiction of haplotypes in Caucasian cohort

Haplotypes composed of three htSNPs were assigned to individuals in the study population. The common GGG haplotype occurs most often in the homozygous state (GGG/GGG, frequency = 63.7%). The AAA is the less common haplotype and occurs heterozygously (GGG/AAA, frequency = 27.8%) or homozygously (AAA/AAA, frequency = 4.8%). In 6 individuals, a haplotype was not able to be confidently assigned. (GNN/ANN, frequency = 3.6%). The mean value of the study parameters were calculated and are shown for total kidney volume, total kidney volume normalised for body surface area, and cystatin C.

Haplotypes

rs1159825 ↓	rs11190688 ↓	rs11190702 ↓
G	G	G
G	G	G
G	G	G
A	A	A
A	A	A
A	A	A
G	N	N
A	N	N

Haplotypes Frequencies

N	Frequency	Total kid vol	Total kid vol/BSA	Cystatin C
107	63.70%	30.34	135.87	1.91
47	27.80%	27.74	123.44	1.92
8	4.80%	27.4525	124.09	2.03
6	3.60%	35.54	156.16	2.01

Table 3.5 Association of haplotypes with study parameters

Association between haplotype and study parameter was performed by ANOVA and post-hoc T-tests. The GGG/GGG haplotype significantly differs from the GGG/AAA haplotype ($p = 0.024, 0.011$) and from the combined rare and heterozygous haplotypes (GGG/AAA + AAA/AAA) ($p = 0.015, 0.007$) for total renal volume and total renal volume normalised for body surface area, respectively.

ANOVA

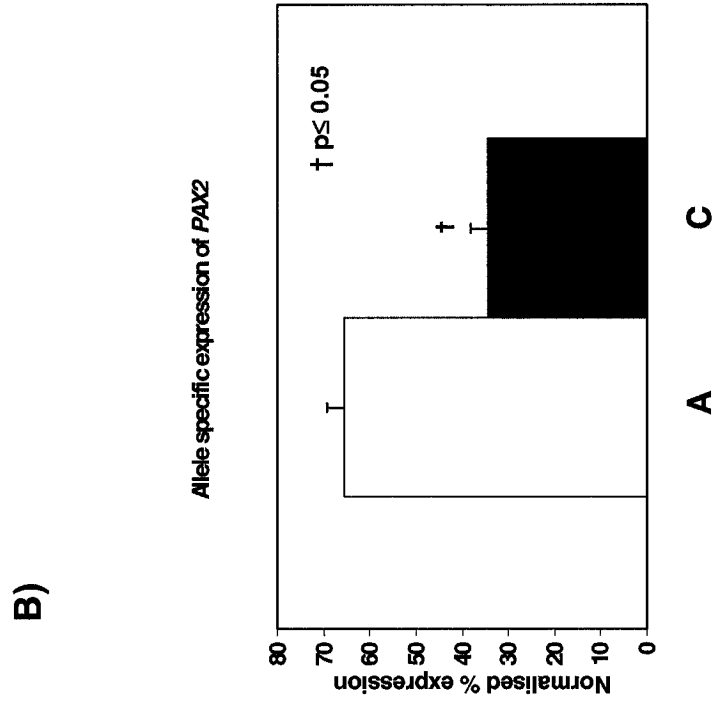
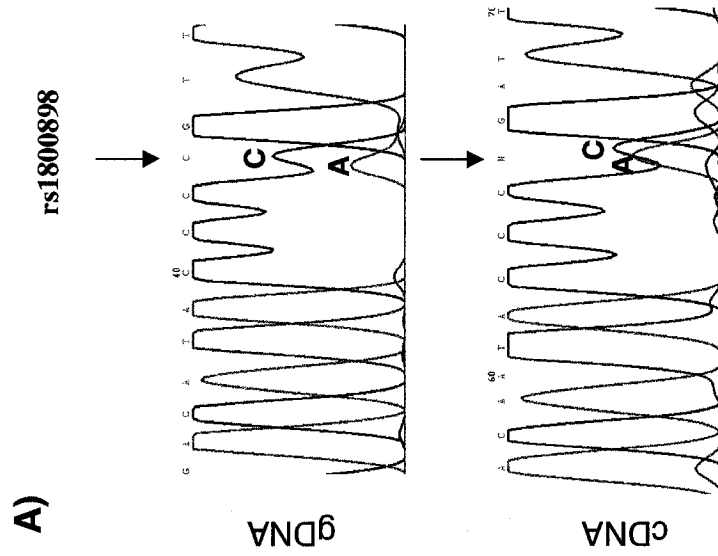
Total renal volume (cc)			p
GGG/GGG	Mean	30.45	0.01
	N	104	
GGG/AAA	Mean	27.74	
	N	47	
AAA/AAA	Mean	27.45	
	N	8	
Others	Mean	35.4	
	N	6	
Total renal volume/BSA (cc/m2)			p
GGG/GGG	Mean	136.4	0.004
	N	98	
GGG/AAA	Mean	123.44	
	N	44	
AAA/AAA	Mean	124.09	
	N	8	
Others	Mean	0.16	
	N	6	
Serum cystatin C (mg/L)			p
GGG/GGG	Mean	1.9	0.722
	N	88	
GGG/AAA	Mean	1.92	
	N	45	
AAA/AAA	Mean	2.03	
	N	8	
Others	Mean	2.01	
	N	6	

T test

Total renal volume (cc)		p
GGG/GGG vs GGG/AAA		0.024
GGG/GGG vs AAA/AAA		0.237
GGG/GGG vs (one AAA)		0.015
Total renal volume/BSA (cc/m2)		p
GGG/GGG vs GGG/AAA		0.011
GGG/GGG vs AAA/AAA		0.241
GGG/GGG vs (one AAA)		0.007
Serum cystatin C (mg/L)		p
GGG/GGG vs GGG/AAA		0.797
GGG/GGG vs AAA/AAA		0.317
GGG/GGG vs (one AAA)		0.565

Figure 3.6 Allele specific expression of *PAX2*

In A) the chromatogram of the sequence surrounding the exonic SNP rs1800898 is shown for genomic DNA (gDNA) and for coding DNA (cDNA). The arrow points to the C/A SNP. It is obvious that the height of the peaks corresponding to the C and the A allele for the cDNA are not proportionally similar to the heights shown in the gDNA. Thus, allelic imbalance is occurring. In B) the normalised C and A allele expression are shown after standardization for gDNA. The A allele accounts for 65.5% +/- 3.7 SD of the *PAX2* expression, nearly two fold greater than the C allele of 34.5% +/- 3.7 SD. This difference is statistically significant ($p < 0.001$).



3.4 DISCUSSION

It is widely accepted that the number of fetal branching events reflects the total number of nephrons formed during kidney development. Thus, optimal renal branching morphogenesis is important for an individual's functional nephron endowment they will have for life (Hinchliffe, Sargent et al. 1991).

Nephron number appears to vary widely in the normal human population, ranging from 300,000 to over 1 million per kidney in one study (Nyengaard and Bendtsen 1992). Although this variance in nephron number was once considered to be normal without any significant clinical consequences, an autopsy study performed by Keller *et al.* showed that middle-aged patients with documented "essential" hypertension had roughly 50% fewer nephrons compared to their age-matched normotensive controls (Keller, Zimmer et al. 2003). Moreover, Australian Aborigines have a higher incidence of end-stage renal disease (Cass, Cunningham et al. 2001) that was later associated with decreased glomerular number (Samuel, Hoy et al. 2005) when compared to Australian Caucasians. Thus, reduced glomerular number is a risk factor for renal dysfunction later in life (Brenner, Garcia et al. 1988; Brenner and Milford 1993; Keller, Zimmer et al. 2003; Samuel, Hoy et al. 2005).

Concurrent with this hypothesis, studies in rodents that examined heterozygous *Gdnf*^{+/-} knock-out mice showed that a 25% reduction in kidney size and a 30% decrease in nephron number (Cullen-McEwen, Drago et al. 2001) caused 14 month old mice to develop hypertension and compensatory glomerular hypertrophy (Cullen-McEwen, Kett et al. 2003). In the *Pax2*^{1^{Neu} +/-} mutant mouse (Favor, Sandulache et al. 1996), a heterozygous mutation causes reduction in total kidney mass, sub-optimal nephron number, and increased cystatin C levels in aged mice (Dziarmaga, Eccles et al. 2006). These observations support the argument that reduced nephron number causes renal dysfunction later in life.

The molecular control of renal branching morphogenesis is complex, but is now known to be clinically important, with even subtle reductions in branching being significant (Hughson, Farris et al. 2003; Keller, Zimmer et al. 2003; Hoy, Hughson et al. 2005; Hoy, Hughson et al. 2006; Hughson, Douglas-Denton et al. 2006). However,

prospective studies examining the effects of reduced branching and nephron number have been difficult to perform since a modest reduction in nephron number at birth may be masked in postnatal life by compensatory hypertrophy, which normalizes renal mass. In 1-week-old *Pax2*-mutant mice, kidney mass was correlated with congenital nephron number (Dziarmaga, Clark et al. 2003): the mutants had 60% kidney size correlating to 65% of the nephron number of wildtype littermates (Dziarmaga, Clark et al. 2003). Furthermore, in 14-day-old rat pups exposed to moderate maternal retinol deficiency, nephron number correlates with kidney weight (74% and 80% of controls, respectively) (Lelievre-Pegorier, Vilar et al. 1998). However, in humans, compensatory hypertrophy results soon after birth to obscure this relationship. Because nephron number cannot be counted in living human beings, the number of studies done on humans is limited.

In order to overcome this problem, we measured newborn volume prior to compensatory hypertrophy as a surrogate of nephron number. We found a correlation in total renal volume with body surface area (BSA) and with renal function. As our final study parameter, we normalised renal volume measured at birth for body surface area (BSA), establishing a good surrogate of congenital nephron number.

Both environmental and genetic factors influence kidney development in utero. Severe vitamin A deficiency (VAD) can cause renal agenesis in experimental animals but the same degree of VAD is uncommon in human populations. On the other hand, even moderate maternal VAD in rodents caused a 24% decrease in kidney weight and a 20% decrease in nephron number (Lelievre-Pegorier, Vilar et al. 1998). Subtle renal hypoplasia is also associated with low birth weight in humans (Tulassay and Vasarhelyi 2002). These observations may be particularly important in developing countries where malnutrition and maternal VAD are common. However, both in Europe and in North America, where maternal malnutrition is not normally a problem, nephron number nevertheless varies widely (Clark and Bertram 1999). Presumably, the diversity in Western populations is more attributable to variations in genes regulating nephron formation.

Since the cause of subtle renal hypoplasia is complex, it most likely results from multiple genes, similarly to other complex traits (Austin, Talmud et al. 2004; Kitamura, Okumura et al. 2004), where phenotype variation is caused by multiple gene interactions.

Thus identifying candidate genes that contribute a significant portion of the phenotype is one method that can be used in identifying the genetic basis of subtle renal hypoplasia.

One interesting candidate gene for subtle renal hypoplasia is *PAX2*. *PAX2* mutations are associated with Renal Coloboma Syndrome (RCS) that causes renal hypoplasia. (Sanyanusin, McNoe et al. 1995; Sanyanusin, Schimmenti et al. 1996). RCS patients don't always present with a coloboma of the optic nerve, presumably because the kidney is more sensitive than the eye to reduction in *PAX2* expression (Salomon, Tellier et al. 2001). In animal models with homozygous *Pax2* mutations, renal agenesis occurs (Favor, Sandulache et al. 1996). The *Pax2* gene is normally expressed equally from both alleles and elimination of one allele results in haploinsufficiency with a 50% reduction in *PAX2* protein in fetal kidneys (Eccles, Wallis et al. 1992). Thus, the *Pax2* mutation causes a dominant form of renal hypoplasia. *Pax2*^{+/-} mutant mice have an overall reduction in renal cross sectional area and a 65 % reduction in nephron number (Dziarmaga, Clark et al. 2003). It is believed that the anti-apoptotic role of *PAX2* in ureteric bud (UB) cells during fetal life optimizes UB branching to influence final nephron number (Porteous, Torban et al. 2000; Dziarmaga, Clark et al. 2003; Dziarmaga, Eccles et al. 2006; Dziarmaga, Hueber et al. 2006). For these reasons, we considered *PAX2* as an excellent candidate gene responsible for subtle renal hypoplasia in the normal population.

To determine whether common polymorphic variants in *PAX2* are associated with subtle renal hypoplasia in healthy, term, Caucasians, we examined what was known about the *PAX2* gene. In humans, *PAX2* is located on chromosome 10 within the boundaries of q24 and q25 (Narahara, Baker et al. 1997) and consists of 12 exons spanning over 70 Kb of genomic DNA (Sanyanusin, Norrish et al. 1996). The largest 5' flanking region of the *Pax2* gene studied to date is an 8.5 Kb region upstream of the *Pax2* start site which drives *Pax2* expression in the pronephric duct, the Wolffian duct and its derivatives (Kuschert et al 2001). Thus, we included 10 Kb upstream and downstream of the coding region when searching for SNPs to be included in our study. As recorded in NCBI dbSNP (BUILD 125), 248 single nucleotide polymorphisms (SNPs) have been found in the *PAX* +/- 10 Kb region. Among these SNPs, some have a predicted effect on gene transcription and splicing, but none change amino acids. With the help of the

HapMap project, we chose htSNPs across the *PAX2* gene region including potential regulatory sites for possible associations.

SNP choice was based on information available from the CEPH population (individuals representative of the European American population obtained from the “Centre d’Etude du Polymorphisme de l’Humain”). Genotyping of our cohort showed similar SNP frequencies and confirmed that there was no appreciable genetic drift in our cohort from the CEPH population. Furthermore, our study population include Caucasians from diverse European background, eliminating anomalies from Founder effects that might occur in isolated groups.

In our Caucasian cohort, we were able to identify a cluster of htSNPs localised between exon 2 and exon 5 of *PAX2* that were significantly associated with a reduction in kidney volume ($p < 0.05$), with htSNPs at the outer limits of the *PAX2* gene not significantly associated. Thus we focused our attention on this region. Several of the htSNPs present in the localized region were in tight linkage disequilibrium (LD) in the CEPH population, suggesting a conserved haplotype block with minimal recombination events. We hypothesized that an ancestral polymorphism arose on a common haplotype spanning this region that would partially account for reduction in renal volume. With the CEPH population data available on the HapMap site (2003), we were able to identify 3 htSNPs that were in tight LD with each other and spanned the specified region. We observed that the frequencies of these 3 htSNPs in our population were similar to their frequencies in the CEPH population. Thus, using these 3 htSNPs, we were able to construct haplotypes and reliably assign them to 162 out of the 168 subjects. The frequencies of the haplotypes in our cohort were similar to those predicted from the CEPH population. We found that the less common haplotype (AAA) (18.7%) was significantly associated with lower total renal volume ($p = 0.024$) and with lower total renal volume/BSA ($p = 0.011$). Mean newborn renal volume in subjects bearing at least one AAA haplotype (homozygous AAA or heterozygous AAA) was 10% smaller than that of the most common haplotype (homozygous GGG). This suggests that a common *PAX2* polymorphism present on the AAA haplotype reduces nephron number by 10%. The magnitude of this effect is shown in comparison to the reported percent decrease in

nephron number observed in individuals with essential hypertension (Keller, Zimmer et al. 2003) (Figure 3.7).

We postulate that additional genes are involved in the reduction of nephron number that was associated with essential hypertension in the report by Keller *et al.* (Keller, Zimmer et al. 2003).

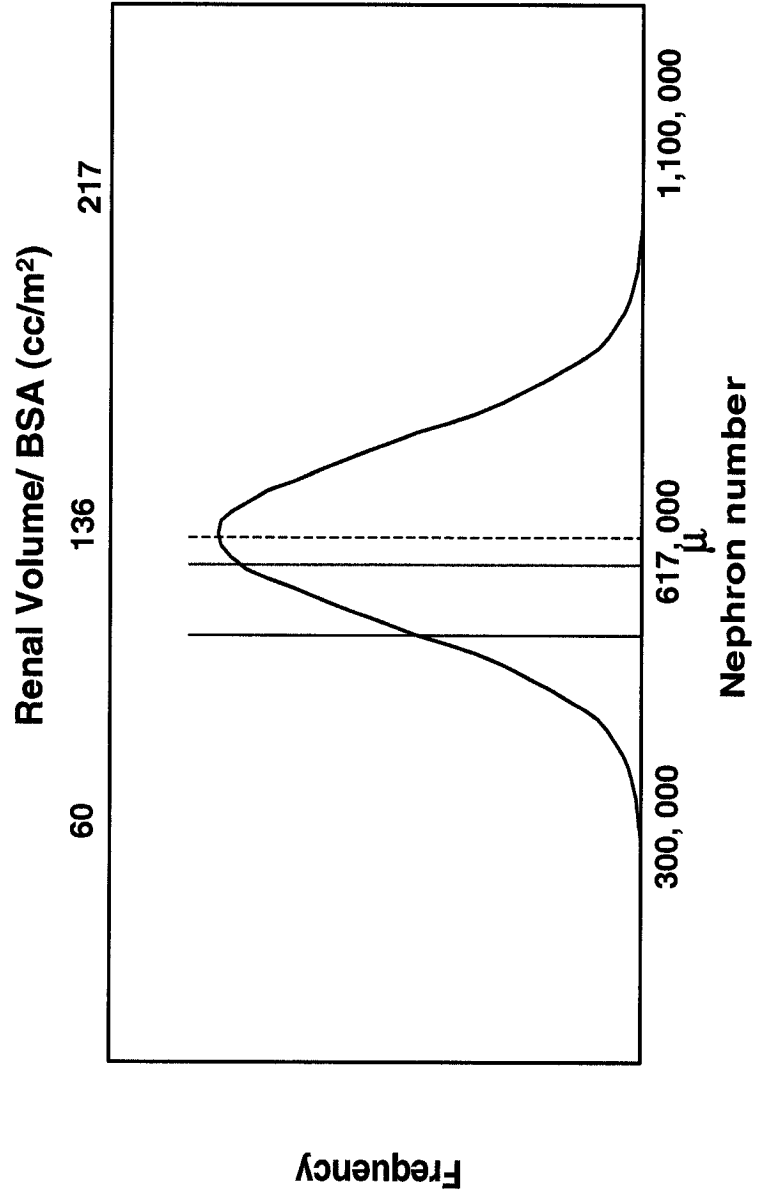
Since no known common polymorphism in the *PAX2* gene has been observed to change an amino acid, we hypothesize that the ancestral polymorphism on the less common *PAX2* haplotype (AAA) affects regulation of *PAX2* expression and its prevalence among Caucasians is presently about 20%.

To test if *PAX2* expression is altered by this haplotype, we examined allele specific *PAX2* expression in a cultured cell line that was heterozygous for an exon 8 SNP (rs1800898). The C allele of this SNP is in tight linkage disequilibrium (LD) ($D' = 0.827$, $r^2 = 0.63$) with the htSNPs defining the AAA haplotype. This exonic SNP doesn't change an amino acid; the C allele occurs in 29% of the population. We found that the human renal cell carcinoma cell line (A498) was heterozygous for the exonic SNP (Figure 3.5 A) and confirmed that it was also heterozygous for the htSNP (rs11599825). In order to measure the allele specific expression, we normalized each allele intensity by the mean of the corresponding allele peak intensities and standardized for genomic DNA (Pastinen, Ge et al. 2006). We show that *PAX2* expression is almost 2X greater for the common (A) allele compared to the rare (C) allele for the exonic SNP. Thus, the *PAX2* allele (rs1800898 C) associated with the AAA haplotype is expressed at a 50% reduced level and might explain the effect of this haplotype on renal volume.

In conclusion, we have linked a common *PAX2* haplotype to reduced newborn kidney volume and have shown that the haplotype is associated with reduced *PAX2* expression.

Figure 3.7 Normal distribution of nephron number

The distribution of nephron number in the normal human population varies widely (Nyengaard and Bendtsen 1992). In this schematic diagram, the *PAX2* AAA haplotype (in red) shifts total kidney volume normalized for body surface area by 10% of the mean (μ). This haplotype is only partially responsible for the 50% reduction in nephron number observed among patients with essential hypertension reported by Keller, Zimmer et al. (2003) (in black). Thus, we predict that other genes are involved in this effect.



ACKNOWLEDGEMENTS

This study was supported by an operating grant from the Canadian Institutes of Health Research (MOP 12954) and by a Pilot Project Grant from the Montreal Children's Hospital. Dr. Paul Goodyer is the recipient of a James McGill (CIHR) Research Chair.

Appendix

Table 3.6 List of primers and probes used in Sequenom

Primer	Sequence
rs996359_CA-F	ACGTTGGATGTTTCAAGTGGGAGGAAGCTG
rs927638_GA-F	ACGTTGGATGACAGTTGTACCAGTACAGCC
rs11190702_AG-F	ACGTTGGATGCTTAGGGCCTTCCCACAAC
rs12781220_GT-F	ACGTTGGATGAAGGTAGGTTGATGCCTGTG
rs10786606_AG-F	ACGTTGGATGTACTGCCGGCCTGGTTTTCT
rs11592735_GA-F	ACGTTGGATGTTACCGAAGCCTATAGCAG
rs11599825_GA-F	ACGTTGGATGACAGTAGACATCCTGATGGG
rs4601695_CT-F	ACGTTGGATGGACACCCTTATGTGTCAGCTC
rs11816136_GA-F	ACGTTGGATGGCAGAACTCCTGACTATTGC
rs11190688_GA-F	ACGTTGGATGGCCCCTTTGTCAACTTTGAG
rs11598208_CA-F	ACGTTGGATGTGCATGCCTGTGTGTTTAGC
rs2476968_AG-F	ACGTTGGATGAACCCCAAATGGAGAGGAG
rs2495762_GT-F	ACGTTGGATGAGACACTGAGGCGTTACCTG
rs3923992_CT-F	ACGTTGGATGTGCGGCTAACCATGAGTAG
rs11190710_CA-F	ACGTTGGATGCTTTCGGCACCAAAGACTTC
rs6421335_CT-F	ACGTTGGATGGGCTCTCTGTCTAAACAC
rs2077642_TC-F	ACGTTGGATGGAACCAGGTGACCAAGAAAC
rs4244341_GT-F	ACGTTGGATGTTGGCCGAAAGAGCAAAAGC
rs12266644_GT-F	ACGTTGGATGATTGCACAGCTGGCAAGAAG
rs10883537_CT-F	ACGTTGGATGCGAGAAAGTCTCAACACAC
rs4278454_AG-F	ACGTTGGATGAAAAGCTCAGGTGGCCACAG
rs11812391_CT-F	ACGTTGGATGTGGCATGAGCACTCTCAAGG
rs4917911_AG-F	ACGTTGGATGCACCTACACTCATCAACCTC
rs12773509_TC-F	ACGTTGGATGGCAATCACACACAGACACAC
rs4278455_AT-F	ACGTTGGATGGCAGATAGGGAGGAGTTTTTC
rs3862028_AG-F	ACGTTGGATGCTAAAAAGCTTAGTGCTGGG
rs996359_CA-R	ACGTTGGATGTCCCACACTCTTGTCAACAC
rs927638_GA-R	ACGTTGGATGCTGCATTTGAGCCTGAGCTG
rs11190702_AG-R	ACGTTGGATGTATCAAACCGATTTGGCCG
rs12781220_GT-R	ACGTTGGATGTAGTGTGCGTGCTTGGAGAG
rs10786606_AG-R	ACGTTGGATGTGCGTGGGTACACTCGAGGT
rs11592735_GA-R	ACGTTGGATGTATCCTCTCCCATGCATGTG
rs11599825_GA-R	ACGTTGGATGTCACATCCCCAAACTTGTGC
rs4601695_CT-R	ACGTTGGATGCCTCCTTTGAAAGAACAGGC
rs11816136_GA-R	ACGTTGGATGATGAGGGCAGTGTTCCTGAG
rs11190688_GA-R	ACGTTGGATGCAATAGCAGGCTTCCAAGAG
rs11598208_CA-R	ACGTTGGATGGGGTACATGTACGAAGTCAC
rs2476968_AG-R	ACGTTGGATGGTTAATGTAGGGTGGTGCTG
rs2495762_GT-R	ACGTTGGATGTAGAGTGGGCGGTGCCTGTT
rs3923992_CT-R	ACGTTGGATGCTCTTCTATTCAAGCCTAGC
rs11190710_CA-R	ACGTTGGATGCTCAAAGGACACAAGCAAGG
rs6421335_CT-R	ACGTTGGATGGAAAACCTCCTCCCTATCTGC
rs2077642_TC-R	ACGTTGGATGTGTGGATGCCTCTATGCCCT
rs4244341_GT-R	ACGTTGGATGGCGAGTTAATAACTCTCGGG
rs12266644_GT-R	ACGTTGGATGCGCTTTTCTCTTTCTTCCC
rs10883537_CT-R	ACGTTGGATGGGTGTCTCTAAACCTTCTG
rs4278454_AG-R	ACGTTGGATGTCTAGCTTCTGACCCAATC
rs11812391_CT-R	ACGTTGGATGAGTTTTGACTCAGCAGTTTG
rs4917911_AG-R	ACGTTGGATGTTCTAGCTGTGCAGTGTG
rs12773509_TC-R	ACGTTGGATGATTGCGTGTCTACGCGCTTG
rs4278455_AT-R	ACGTTGGATGTATGCCATGTCTTTAGCTTG
rs3862028_AG-R	ACGTTGGATGTACGGGACCCTTTGGTTTC

Probe	Sequence
rs996359_CA-Pa	TCCTTCTGTGCCCTG
rs927638_GA-Pa	GCCCTGTCAGTTTTCC
rs11190702_AG-P	TGGTTGTTTTGGCGGC
rs12781220_GT-P	GGGTGTGACTGTGTGA
rs10786606_AG-P	tCGACACCTACACCCAG
rs11592735_GA-Pa	CCATGCATGTGCCATAG
rs11599825_GA-Pa	TGTACCTTTCAGAACCCC
rs4601695_CT-P	tGGTTACTGACAATCCCC
rs11816136_GA-Pa	AACTTCCAGAAACGTACT
rs11190688_GA-Pa	TCCAAGAGAAGGAATGTG
rs11598208_CA-P	AAACCGGCTTTATGCCAAG
rs2476968_AG-P	TTGAAGAGTTAGAGAGACC
rs2495762_GT-P	taccGTTCCCTGCCTTTGCC
rs3923992_CT-P	CCTCTCATAGATTCTACCAT
rs11190710_CA-Pa	GCCCTAAGTATGCTTGTTTA
rs6421335_CT-P	gCACAAGGAACTTTAGACC
rs2077642_TC-Pa	acgtCCTCTGTCTCCAACCTA
rs4244341_GT-Pa	tgcaGACCCAAACCCGACTCG
rs12266644_GT-P	agatGTCATTTTCTGCCTGCG
rs10883537_CT-P	aaCTCTAAACCTTCTGAAACTT
rs4278454_AG-P	gcctcGGGCCTTGTCCTCCACTG
rs11812391_CT-P	agTGACTCAGCAGTTTGTTTAAT
rs4917911_AG-P	CCTTTTCTAGAAAATGAGAGTA
rs12773509_TC-Pa	gattcatAGATAAACAAGGGTCTGC
rs4278455_AT-P	gattaTTTGCAGGCTTTTTTTTT
rs3862028_AG-P	ggttacatAGGGGAATTCTCCAAAAA

CONNECTING TEXT FOR CHAPTERS 3 AND 4

In the first section of this thesis, *PAX2*, an important genetic determinant of nephron formation that influences the rate of branching morphogenesis, was examined. We linked a common *PAX2* haplotype with subtle renal hypoplasia and showed that the haplotype is associated with reduced *PAX2* allele specific expression.

In the second part of this thesis, a second pathway involved in renal branching morphogenesis was studied: the retinoic acid (RA) pathway (Lelievre-Pegorier, Vilar et al. 1998; Gilbert and Merlet-Benichou 2000; Batourina, Choi et al. 2002; Gilbert 2002). Based on previous research involving the lung (Kaplan, Ledoux et al. 1999; Oyewumi, Kaplan et al. 2003; Oyewumi, Kaplan et al. 2003), we proposed a candidate gene, *Lgl1*, as a potential downstream target of RA involved in nephron formation.

CHAPTER 4

LGL1, A NOVEL RA INDUCIBLE RENAL BRANCHING MORPHOGEN

4.1 INTRODUCTION

Development of the metanephric kidney begins when the ureteric bud (UB) emerges from the nephric duct and grows into the adjacent metanephric mesenchyme (MM). Signals from the tips of the UB induce the metanephric mesenchyme (MM) to condense and form nephrons in a process called branching morphogenesis (Pohl, Stuart et al. 2000). The number of embryonic branching events reflects the final number of nephrons an individual will have formed for life (Hinchliffe, Sargent et al. 1991), and any defects will compromise the functional capacity of the mature kidney. Even a subtle decrease in nephron number increases susceptibility to acquired renal disease and essential hypertension later in life (Brenner, Garcia et al. 1988; Brenner and Milford 1993; Cullen-McEwen, Kett et al. 2003; Keller, Zimmer et al. 2003).

Epithelial branching is a common feature of mammalian organogenesis and is fundamental in the formation of the kidney, as well as in the formation of the lung, mammary gland, submandibular gland, pancreas, and prostate (Pohl, Stuart et al. 2000; Hu and Rosenblum 2003). Based on common events that occur during branching morphogenesis, it has been proposed that common molecular pathways are shared by these organs which regulate this process (Hu and Rosenblum 2003). A review of shared molecules focused our attention on similarities between development of the kidney and of the lung (<http://www.ana.ed.ac.uk/anatomy/database/orghome.html>). During late stages of lung development, glucocorticoids (GC) act on receptors in pulmonary fibroblasts (mesenchyme) to stimulate the release of a secreted factor, which drives maturation of the epithelial lung bud (Garbrecht, Klein et al. 2006). This paradigm is reminiscent of the postulated effects of retinoic acid (RA), the metabolite of vitamin A, on kidney branching (Batourina, Gim et al. 2001). In this hypothesis, RA induces UB branching through stimulation of an unknown molecule in the metanephric mesenchyme (MM) (Batourina, Gim et al. 2001). Thus, it is tempting to speculate that the GC-dependent relationship between pulmonary mesenchyme and the lung epithelium may share common pathways with the RA dependent relationship between the MM and UB in the developing kidney.

Interestingly, a novel molecule, late gestation lung protein 1 (*Lgll*), was recently identified in lung fibroblasts as a GC-induced gene (Kaplan, Ledoux et al. 1999). *Lgll* mRNA was detected in fetal lung mesenchyme and pulse-chase experiments determined

that LGL1 was secreted as a 52kDa glycoprotein that acted on the epithelia (Oyewumi, Kaplan et al. 2003). When antisense oligodeoxynucleotides were directed against *Lgll*, branching of fetal lung explants was inhibited (Oyewumi, Kaplan et al. 2003). These results suggest that *Lgll* is a GC induced molecule secreted by mesenchymal cells that affect epithelial development in the lung. Screening of various tissues for *Lgll* expression by Northern blot analysis identified the transcript in adult kidney (Kaplan, Ledoux et al. 1999). Thus, we considered the possibility that LGL1 might function as a branching morphogen in the developing kidney, paralleling its role in the lung.

As a prelude to the project, we screened the *Lgll* promoter for response elements and found putative retinoid response elements in addition to the expected glucocorticoid response element. Thus, we hypothesized that *Lgll* may be the mesenchymal molecule that is induced by RA to stimulate UB branching in the kidney.

4.2 MATERIALS AND METHODS

4.2.1 Reverse Transcriptase-Polymerase Chain Reaction Analysis

Total RNA was prepared from fetal mice kidney tissue following the Qiagen RNeasy Mini Column extraction kit (Qiagen, Maryland, USA). Briefly, whole mouse kidneys were dissected using RNase free techniques with RNAlater. The kidneys were homogenized using mortar and pestle and the extracted RNA was dissolved in RNase-free water. The RNA was then treated with RNase free DNase 1 (Ambion). One microgram of total RNA was used for reverse transcription-polymerase chain reaction (RT-PCR). RT-PCR reactions were performed using 30 minutes at 50°C, 15 minutes at 95°C, 35 cycles each consisting of denaturation (94°C for 1min), annealing (55°C for 1min), and extension (68°C for 1min). Synthetic oligodeoxynucleotides pairs were designed by aligning conserved sequences of the mouse diencephalon *Lgll* cDNA to the mouse *Lgll* cDNA sequence in the pancreas, yielding a 490bp product. The following sets of PCR primers were used:

Lgll forward primer: 5'ATGCTTCACAACAAGCTGC 3';

Lgll reverse primer: 5'GCTGGATGGACACTCAGAGC3'.

RT-PCR products were separated on a 1.5% (wt/vol) agarose gel and visualized by ethidium bromide staining.

4.2.2 Cell Culture

Murine inner medulla collecting duct (IMCD) (Rauchman et al. 1993), mK3 (murine mesenchymal cells), and mK4 (murine mesenchymal cells in epithelial transition) (kind gift from Dr. Potter and described by Valerius, Patterson et al. 2002), were maintained in DMEM containing 10% (v/v) FBS/FCS, 1% penicillin and streptomycin at 37°C in humidified 5% CO₂ in air. Cell pellets were collected, washed in cold PBS (RNase free) and used for RNA isolation and RT-PCR reactions as described above.

4.2.3 In Situ Hybridization

Nonradioactive *in situ* hybridization (ISH) was performed as described by Oyewumi *et al.* (2003), using a 1.4-kb *Lgll* digoxigenin-labeled RNA probe (vector was a kind gift from F. Kaplan and described by Oyewumi et al 2003). Rat *Lgll* cDNA flanked by Kpn1 and Sma I sites, subcloned into pBluescript KS, was used as a template for *in vitro* transcription. Riboprobes were generated after linearization with Asp718 (antisense) and Sma1 (sense) and *in vitro* transcription by T3 and T7 polymerase labeled in the presence of dig-UTP. Briefly, tissue sections were deparaffinized, rehydrated, and washed in phosphate buffered saline (PBS). Pretreatment included fixation with 4% paraformaldehyde (PFA) (10 min at room temperature 25°C), proteinase K digestion (1ug/ml, 10 min at 37°C), postfixation in 4% PFA (5 min at room temperature 25°C), and acetylation using 0.1M triethanolamine and acetic anhydride (15 min at room temperature). Sections were then washed in PBS and prehybridized for 1 h at 65°C. Riboprobes were added to hybridization solution (10mM Tris pH7.5, 600mM NaCl, 1mM EDTA, 0.25% SDS, 10% Dextran Sulfate, 1X Denhardt's, 200ug/ml yeast tRNA (Gidco), 50% formamide) at a concentration of 1.5ng/ul. Following denaturation at 85°C for 3 min, the probe was incubated with tissue sections at 65°C for 18 h. Tissues were washed in 50% formamide and 1X SSC at 65°C, RNase (Roche) treated (20ug/ml in TNE buffer (10mM Tris pH7.5, 500mM NaCl, 1mM EDTA)) for 30 min at 37°C, and washed

in MABT buffer (100mM Maleic Acid, 150mM NaCl, pH brought to 7.5, 0.1% Tween-20) for 2X 5min at room temperature. The slides were blocked with 20% heat inactivated sheep serum, and incubated with anti-DIG-AP antibody (1:000, Roche) overnight at 4°C. BM-purple (Roche Diagnostics, Mannheim, Germany) was used for immunologic detection of the hybridized probe. Tissues were dehydrated and mounted with Cytoseal 60 (Richard-Allan Scientific, Kalamazoo, MI). Images were captured using a Zeiss microscope.

4.2.4 HEK 293 transient transfections

HEK 293 (human embryonic kidney) cells were maintained in DMEM containing 10% (v/v) FBS/FCS, 1% penicillin and streptomycin at 37°C in humidified 5% CO₂ chamber in air. Cells were transfected at 50% confluency using LIPOFECTAMINETM 2000 (Invitrogen) with 0, 10, 20 ug *Lgl1* cDNA per 10cm diameter dish. Cells were grown for 48 h and harvested for Western blotting experiments.

4.2.5 Electrophoresis and Western blot immnuanalysis

At 48 h after transfection, HEK 293 cells grown in 10 cm diameter dishes were washed twice with cold PBS. Cells were scraped in 500ul of cold PBS and spun down to pellet cells. Postnatal (P) day 1 C3H/HeN mouse kidneys (supplied by Charles River Laboratories) were dissected and washed in cold PBS. Cell pellets and kidneys were lysed in hypotonic buffer (10 mM HEPES (pH 7.9), 10 mM KCl, 0.1 mM EDTA, 0.1 mM EGTA, 1 mM DTT, 0.5 mM PMSF, Aprotinin, Pepstatin, Leupeptin) and incubated 15 min on ice. NP40 was added to the lysates (10%) and vigorously vortexed for 10s. The supernatant was collected by centrifugation at maximal speed for 3 min at 4°C.

The total protein concentration of lysates was determined according to the BCA Protein Assay (PIERCE). Proteins (50ug) diluted in sample buffer were boiled for 5 min and loaded in each well on a SDS/10% (w/v) polyacrylamide gell and transferred on a nitrocellulose membrane (Bio-Rad Laboratories, Hercules, CA, USA). Membranes were blocked by incubation with 5% (w/v) non-fat dried milk in PBS-tween (PBS/0.05% (v/v) Tween) at room temperature (25°C) for 1 h to prevent non-specific binding. The membrane was incubated with rabbit anti-LGL1 antibody (1:500 dilution in 2% bovine

serum albumin/TBS-tween (TBS/0.05% (v/v) Tween); kind gift from F. Kaplan) at 4°C overnight, washed three times for 10 min with TBS-tween (TBS/0.05% (v/v) Tween) and incubated with HRP (horseradish peroxidase)-conjugated goat- anti-rabbit IgG (Cell Signaling with a 1:1000 dilution) in PBS-tween containing 5% (w/v) non-fat dried milk. After 3X TBS-tween washes, blots were detected with enhanced chemiluminescence detection system (Amersham, Picataw, NJ), and exposed to autoradiography film (Kodak BiomaxMR Film).

4.2.6 Immunohistochemistry

C3H/HeN (supplied by Charles River Laboratories) embryos were obtained at embryonic (E) day 13.5, E15, E18, post natal (P) day 1 and adult tissues. The embryos or kidneys were microdissected, washed in PBS, fixed overnight in 4% paraformaldehyde (PFA), dehydrated, and embedded in paraffin. Tissue sections were immunostained according to Oyewumi et al. (2003) with minor changes. In short, 8µm sections were deparaffinized, rehydrated and boiled in 10mM sodium citrate (pH 6) for 4 min. Endogenous peroxidase activity was quenched with 1% (v/v) hydrogen peroxide in methanol for 15 min. Nonspecific binding sites were blocked using 5% (v/v) normal goat serum and 1% (wt/v) bovine serum albumin in PBS-triton X (0.03%) for 1 h at room temperature. Preliminary experiments determined optimal antibody concentrations. Rabbit polyclonal antibody against LGL1 was used at a 1:100- 1:500 dilution overnight at 4°C. Secondary goat anti-rabbit (Cell Signaling) was used at a 1:300 dilution and incubated for 1 h at room temperature. Vectastain ABC Universal Kit (Vector Laboratories, Burlingame, CA) was used as described by the manufacturer, followed by incubation with 3, 3'-diaminobenzidine (DAB) (Vector Laboratories Burlingame, CA). Sections were counterstained with Gill's hematoxylin (Sigma-Aldrich Canada Ltd, Oakville, ON) and Scott's tap water, dehydrated and mounted with Permount (Fisher Scientific, Pittsburg, PA).

4.2.7 Lgl1 Promoter Region: Putative binding site detection

The 872 bp fragment upstream of the *Lgl1* start site that is expected to be the *Lgl1* promoter region (kind gift of Dr. F. Kaplan) was analysed for potential transcription factor binding sites using Genomatix (<http://www.genomatix.de>).

4.2.8 Lgl1 Transfection and Reporter Gene Assays with RA and GC

Functional promoter assays using the *Lgl1* reporter gene construct were performed by transient transfections into mK3 cells. Cells in 24 well plates were seeded at 70% confluence. The next day, cells were transfected in serum and antibiotics free DMEM using lipofectamine 2000 transfection reagent, at the following concentrations: 0.8µg *Lgl1*-pGL3Basic or empty pGL3Basic, 16ng pRL-tK, and 1.0ul lipofectamine 2000. After 6 hours the media was changed to antibiotics free DMEM/10% FBS and the cells were incubated with 10⁻⁶M atRA (Sigma) in DMEM/1% FBS/FCS, 10⁻⁶M 9cisRA (Sigma) in DMEM/1% FBS/FCS, 10⁻⁷M cortisol (GC) (Sigma) in DMEM/1% FBS/FCS, or in combination of atRA+GC, or 9cisRA + GC for 48 h at 37°C in a humidified 20% O₂/ 5% CO₂ chamber. After 48 hours, the cells were washed with cold 1 x PBS and lysed by scraping in 100 µl of 1 x passive lysis buffer (Promega). The cell extract was centrifuged and the cleared supernatant was used for both firefly luciferase and firefly renilla assays. Luciferase activity was determined on 20µL of supernatant at room temperature in 100 µl of luciferase reagent (Promega) for 10 seconds after a 2-sec delay in a Monolight 3010 luminometer. Renilla activity was also determined in the same manner, using the same 20µl supernatant aliquot after addition of 100µl of Stop and Glow buffer (Promega). Reporter assays were normalized for transfection efficiency based on the firefly/renilla activity.

4.2.9 RA and GC stimulation of Lgl1 mRNA measured by real-time RT-PCR

mK3 and mK4 cells were grown in media with minimal serum (DMEM + 1% FBS/FCS + 1% pen/strep) in the presence or absence of all-trans retinoic acid (atRA 10⁻⁶ M), 9-cis retinoic acid (9cisRA 10⁻⁶M), and/or cortisol (GC 10⁻⁷ M) for 48 h. After 48 h, cells were washed with PBS and total RNA was isolated using the RNeasy kit (Qiagen, Maryland) as per manufacturer's recommendations. Samples were resuspended in 40 ul

of RNase free water and treated with RNase-free DNase1 (Ambion) as per manufacturer's recommendations.

RNA samples were analyzed for levels of *Lgl1* by real time RT-PCR using the One-Step RT-PCR SYBR Green kit (Qiagen, Maryland, USA) as per manufacturer's recommendations on an ABI prism 7000 machine. Mouse *Lgl1* primers were designed to span an intron and mouse β -2-microglobulin (B2M) primers were used as a normalising control. The sequences are as follows:

Lgl1: F: 5' GACCAAGAAGACCCCAGTCA 3'

R: 5' CATCGATGACACCGTAGTGG 3'

RT-PCR Product Size: 206bp

B2M: F: 5' TGCAGAGTTAAGCATGCCAGTATGG 3'

R: 5' TGATGCTTGATCACATGTCTCG 3'

RT-PCR Product Size: 75bp

100ng of total RNA was used per reaction and RT-PCR conditions were as follows; a 30 minute reverse transcription step at 50°C proceeded by 95°C for 15 minutes. A total of 35 cycles were performed at 94°C for 30 sec, 58°C for 30 sec, 72°C for 30sec. Melt curves for each amplicon showed a single peak, indicating absence of primer dimerization or non-specific PCR products. Samples were run on a 1% agarose gel. Each sample was run in duplicate. The comparative CT method was used for relative quantification between treated and nontreated cells after standardization using the housekeeping gene B2M (Livak and Schmittgen 2001).

4.2.10 Fetal Kidney Explant Cultures

E11.5 *Hoxb7/Gfp* mouse (generously provided by Dr. Frank Costantini) kidney rudiments were dissected under sterile conditions and transferred to 0.4 μ M floating filters (Millipore, Bedford, MA, USA) suspended above a layer of DMEM 1% FBS/FCS 1% Pen/Strep +/- atRA (10^{-6} M), +/- GC (10^{-7} M). Fetal explant kidneys were cultured in a sterile 37°C incubator under 5% CO₂/air for 96h in the dark. Images were captured using Leica Microscope under fluorescent light after 0 h, 24 h, 48 h, 96 h in culture. Explant growth was calculated as a percent difference of the number of UB tips at each specified hour compared to that of the media control.

4.2.11 Counting UB tips of *Lgl*^{+/-}/*Hoxb7*/*Gfp* embryos

Lgl^{+/-} mice (generously provided by Feige Kaplan) (on a mixed C3H/HeN/C57 Black background) were mated to *Hoxb7*/*Gfp* mice (on a C3H/HeN background) to allow visualization of the UB. E12.5-E13 embryos were obtained from timed matings and the kidneys were microdissected and photographed under fluorescent light using Leica microscope. Images were captured at 32X magnification. The number of branching events was obtained by counting the number of UB tips. A section of each embryo was used for genotyping. Genomic DNA was isolated using the Wizard Genomic DNA Purification Kit (Promega) and genotyping was performed using the following PCR primers and conditions:

Lgl F (5'PCR-F3): 5' CACTGCTCCGTGTATCAAGCATAAC 3'

Lgl R (5'PCR-R3): 5' CAGGTCTGGCTCTGAGGTTCTTGCA 3'

Lgl Neo primer (Neo-1): 5' GACAATCGGCTGCTCTGATG 3'

The PCR reactions were performed with an initial denaturation step for 5 minutes at 94°C followed by 3 cycles consisting of 1 minute at 94°C and 3 minutes at 72°C, 3 cycles consisting of denaturation (1minute at 94°C), annealing (1minute at 66°C) and extension (3 minutes at 72°C), that was repeated with each block of 3 cycles having a decrease in the annealing temperature by 2°C until 56°C is reached. Final extension was performed at 72°C for 7 minutes.

PCR Program:

Initial Denaturation	94°C	5min	
	94°C	1min	3X
	72°C	3min	
Denaturation	94°C	1min	
Annealing	66°C	1min	3X
Extension	72°C	3min	
	...		
Denaturation	94°C	1min	
Annealing	56°C	1min	14X

Extension	72°C	3min
Final extension	72°C	7min

... Represents repeating the block 3X with a decrease in the annealing temperature by 2°C until 56°C is reached.

PCR products were run on a 1.5% agarose gel and visualized with ethidium bromide staining. The wildtype allele was a 0.8 Kb product, while the mutant allele was 1 Kb product (Figure 4.1).

4.2.12 Cystatin C measurements in aged *Lgll* heterozygotes

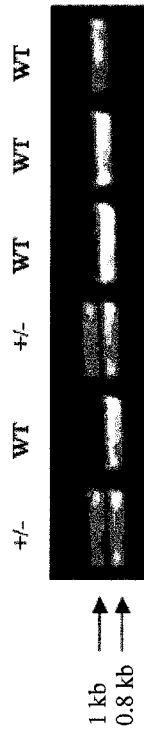
Lgll^{+/-} and wildtype C3H/HeN adult mice were sacrificed at 8 months of age and 300ul of blood was collected by cardiac puncture. Blood was centrifuged at 10,500 rpm for 10 minutes at room temperature in capillary blood collection tubes (Sarstedt, Nunbrecht, Germany). After centrifugation, the serum was removed and stored at -20°C. Serum cystatin C was measured by nephelometry in wildtype (n=5) and *Lgll*^{+/-} (n=4) animals (Filler et al. 1999).

4.2.13 Data presentation and Statistical Analysis

All data are presented as mean value ± standard deviation (SD), or as the mean value ± standard error of the mean (SEM). Statistical significance was determined using Microsoft Excell software. Comparisons between two groups were made using Student's t-Test. Significance was defined as *p < 0.05 or as †p < 0.001.

Figure 4.1 *Lgll*^{+/-} genotyping PCR reactions

DNA was extracted from embryos or from mice for PCR reactions and products were run on a 1.5% agarose gel. The *Lgll*^{+/-} mice have a Neo cassette inserted in one of their alleles disrupting the LGL1 protein. The mutant allele is observed as a 1 Kb band, and the wild type allele is a 0.8 Kb band. (Kaplan et al. SPR abstract, San Francisco 2005)



4.3 RESULTS

4.3.1 *Lgl1* mRNA is expressed in the kidney

The expression of *Lgl1* was examined during renal development by RT-PCR. Total RNA was isolated from C3H/HeN mouse kidneys. *Lgl1* mRNA was detected as early as embryonic (E) day 12 and was identified at E15, E18 and postnatal day (P) 1 (Figure 4.2 A).

To develop preliminary understanding of whether renal *Lgl1* is selectively expressed in mesenchymal cells (as in lung) versus epithelial cells, we screened various cultured kidney cell lines for *Lgl1* mRNA by RT-PCR. We found that the *Lgl1* transcript was present in murine mesenchymal cells (mK3 and mK4) (Valerius, Patterson et al. 2002) but was conspicuously absent from murine inner medullary collecting duct (IMCD) cells (Rauchman, Nigam et al. 1993) (Figure 4.2 B).

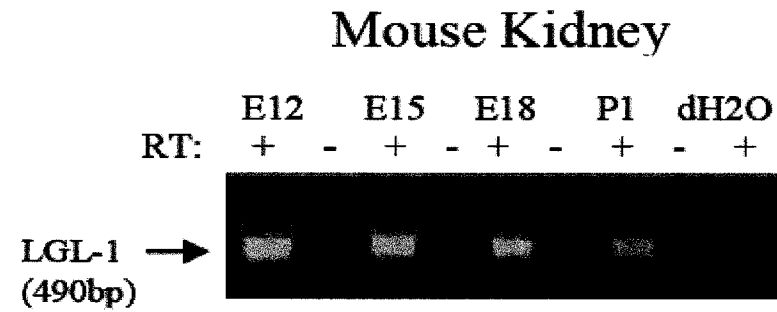
By *in situ* hybridization (ISH), *Lgl1* mRNA was localized to mesenchymal cells of C3H/HeN E12.5 mouse kidney, mesenchymal structures surrounding epithelial branches of the developing lung and the mesenchymal cells around the developing mid gut epithelial lining (Figure 4.3).

Figure 4.2 *Lgl1* mRNA expression

A) RT-PCR on total RNA from mouse kidney at E12 +/- RT, E15 +/- RT, E18 +/- RT, P1 +/- RT, and dH₂O + RT. *Lgl1* PCR product size: 490bp.

B) RT-PCR on total RNA from mK3, mK4, and IMCD cells. mK3 cells: *Lgl1* +/- RT, E12 + RT (control), dH₂O + RT. mK4 cells: *Lgl1* +/- RT, E12 + RT (control), dH₂O + RT. IMCD cells: *Lgl1* +/- RT, GAPDH +/- RT (control), dH₂O + RT. *Lgl1* PCR product size: 490bp.

A)



B)

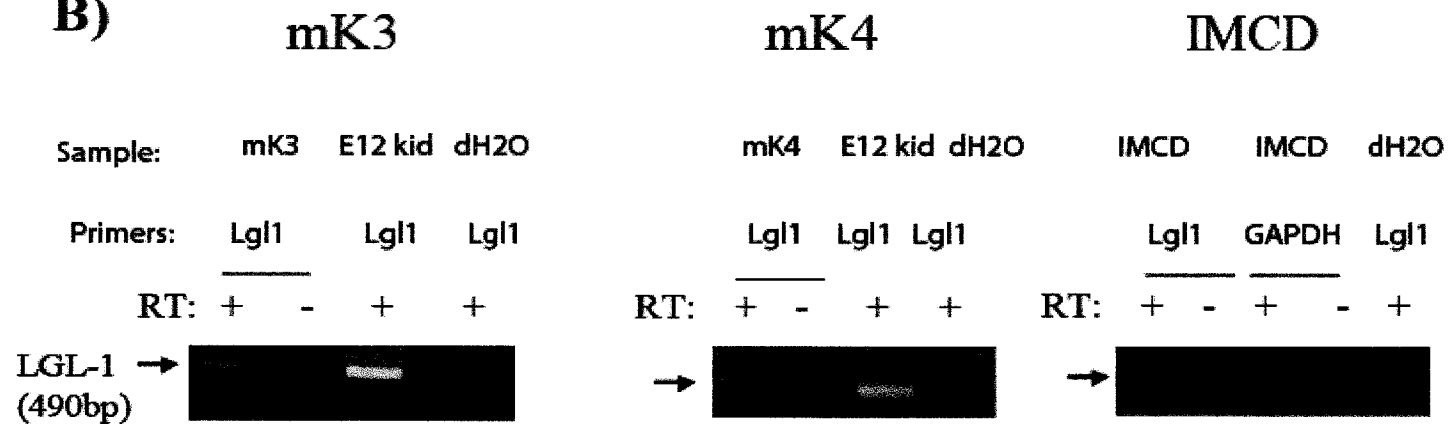
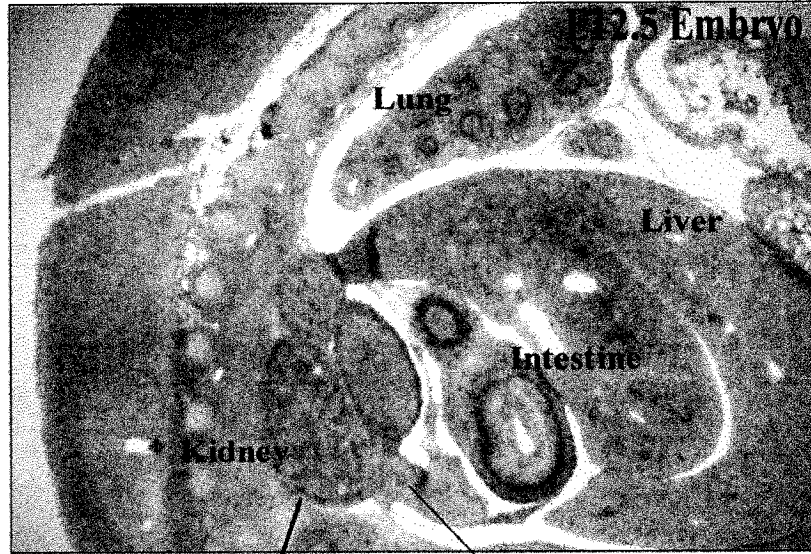


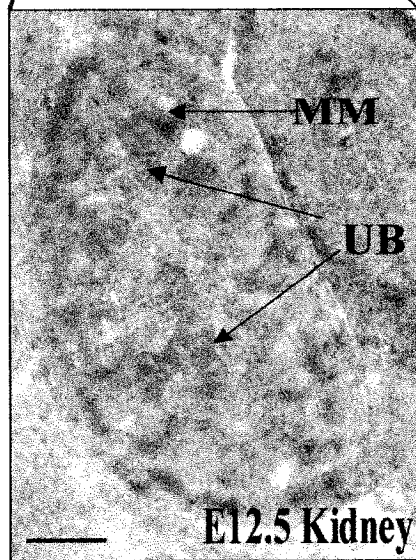
Figure 4.3 *Lgl1* mRNA expression pattern

In situ Hybridization (ISH) on E12.5 embryo using antisense *Lgl1* dig-labeled probe. 40X magnification of the embryo identified staining in the lung, intestine and kidney (blue staining) (Figure 4.3 A). 100X magnification of the kidney showed staining in mesenchymal cells (Figure 4.3 B).

A)



B)



4.3.2 LGL1 protein is present in the developing mouse kidney

Protein was extracted from whole P1 C3H/HeN mouse kidney and from human embryonic kidney (HEK) 293 cells transiently transfected with 0, 10, 20 ug of the full-length murine *Lgll* expression vector (kind gift from F. Kaplan) by homogenization in a hypotonic buffer (HEPES buffer with protease inhibitors and NP40). Western blots (40ug protein/lane) were probed with rabbit antiserum raised against murine LGL1 peptide (Oyewumi et al 2003). The expected 52 kDa LGL1 protein band was identified in P1 mouse kidney extracts. Extracts of HEK 293 cells transfected with murine *Lgll* cDNA produced the expected immunoreactive band at 52kDa (Figure 4.4).

LGL1 protein was also detected by immunohistochemistry in fetal (E13.5-E18.5) and postnatal (adult) mouse kidney (Figure 4.5). At E13.5, LGL1 protein was localized to mesenchymal cells in the nephrogenic zone and in stromal cells surrounding the ureteric bud trunk. At E15.5, LGL1 protein was seen in stromal cells; LGL1 was not evident in nephrogenic mesenchyme at the S-shaped body stage, but was clearly seen in more differentiated tubules derived from nephrogenic mesenchyme. At E18.5 and in adult mice, LGL1 protein was evident in maturing proximal tubules but not in glomeruli.

4.3.3 *Lgll* promoter analysis

A 872 bp fragment upstream of the rat *Lgll* start site was obtained from Dr. F Kaplan (unpublished). Initial screening of this sequence revealed sites homologous to consensus sequences for retinoic acid response elements (RARE), as well as the expected glucocorticoid response element (GRE) (Figure 4.6 A).

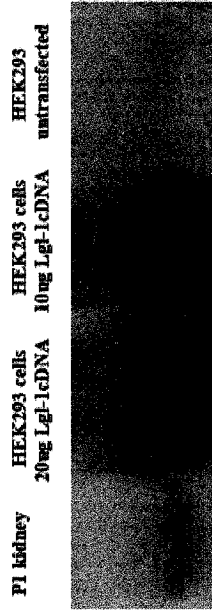
4.3.4 Regulation of *Lgll* promoter activity

To determine whether the *Lgll* promoter was activated by retinoic acid (RA) or cortisol (GC), a 901 bp fragment of the rat *Lgll* 5' flanking sequence cloned into a luciferase reporter vector (kind gift of F. Kaplan) was used. mK3 cells were transiently transfected with the *Lgll* promoter reporter and luciferase activity was measured after 48 hours incubation with RA and GC (Figure 4.6 B). Under basal conditions, minimal luciferase activity was detected. However, when transfections were performed in the presence of 9 cis-retinoic acid (9cisRA; 10^{-6} M) or all-trans retinoic acid (atRA; 10^{-6} M),

Lgl1 promoter activity was easily detected (0.61 +/- 0.08 SD luciferase/renilla units (p< 0.0006) or 0.69 +/-0.19 SD luciferase/renilla units (p<0.005), respectively. A similar level of stimulation of *Lgl1* promoter activity was induced by cortisol (GC; 10⁻⁷M), mean value of 0.62 +/- 0.33 SD luciferase/renilla units (p< 0.03). No additive effects were noted in this assay when these agents were combined: GC + 9cisRA = 0.67 +/- 0.22 SD luciferase/renilla units; GC + atRA = 0.68 +/- 0.04 SD luciferase/renilla units (Figure 4.6 B). No statistically significant difference was observed between any of these groups. Transfection experiments were done on two separate days, in duplicates.

Figure 4.4 LGL1 protein expression

Western Blot (WB) for LGL1 protein in P1 kidney, HEK 293 cells transiently transfected with 20 ug of *Lgll* cDNA, HEK 293 cells transiently transfected with 10 ug *Lgll* cDNA, and untransfected cells is shown. LGL1 protein is 52 kDA.



LGL-1 protein
52kDa

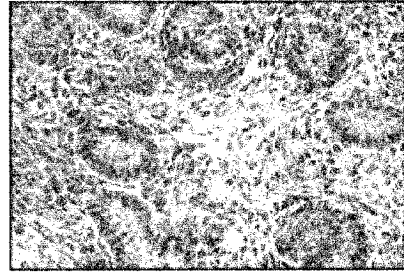
Figure 4.5 LGL1 protein expression pattern

LGL1 protein expression in mouse kidney sections at E13.5, E15.5, E18.5 and adult stages is observed as brown staining. Negative control is represented as no primary antibody. Images are shown at 200X and 400X magnification. At E13.5, LGL1 protein was localized to mesenchymal cells (MM) in the nephrogenic zone and in stromal cells (STR) surrounding the ureteric bud (UB) trunk. At E15.5, LGL1 protein was seen in stromal cells (STR); LGL1 was not evident in nephrogenic mesenchyme at the S-shaped body stage, but was clearly seen in more differentiated tubules (RT) derived from nephrogenic mesenchyme. At E18.5 and in adult mice, LGL1 protein was evident in maturing proximal tubules (PT) but not in glomeruli (G).

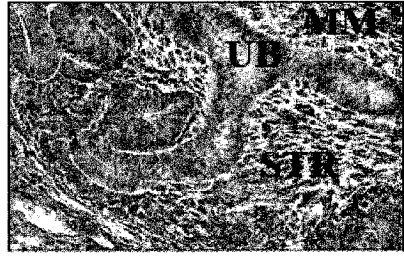
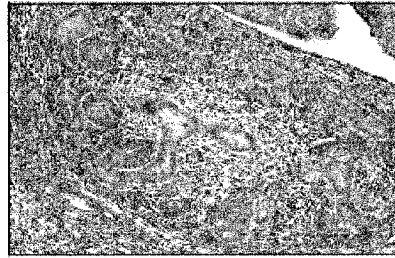
200X

400X

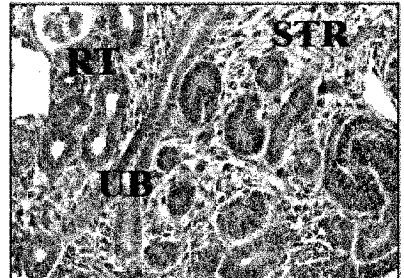
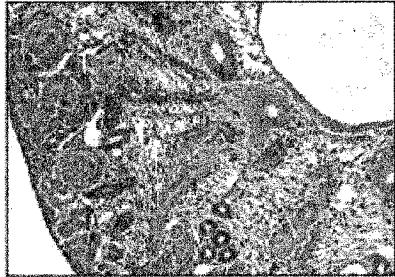
Negative
Control



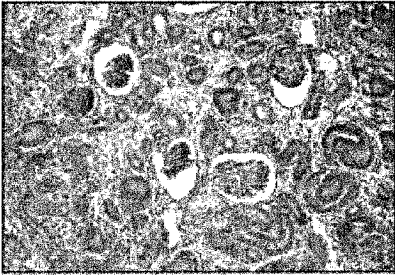
E13.5



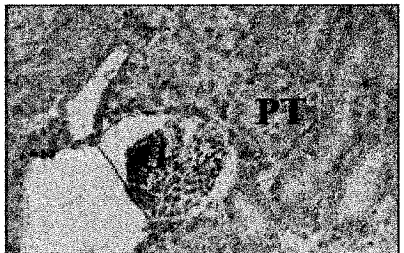
E15.5



E18.5



Adult



4.3.5 Lgl1 mRNA expression is increased by retinoids and/or glucocorticoids

To determine whether the effects of retinoids and glucocorticoids on *Lgl1* promoter activity correlate with changes in mRNA, *Lgl1* transcript levels were measured in mK3 cells after stimulation with 9cisRA, atRA, and/or GC for 48h. mK3 cells represent early metanephric mesenchyme in fetal mouse kidney, expressing markers such as *HoxAll*, *Emx2*, vimentin, *Fgf7*, (Potter Mech of Develop 2002). Total RNA was isolated and real-time RT-PCR was used to quantify *Lgl1* mRNA normalized for *beta-2 microglobulin*. In mK3 cells, 9cisRA increased *Lgl1* mRNA levels twofold (2.13 +/- 0.789 SD (p<0.064)). atRA increased *Lgl1* mRNA levels similarly (2.29 +/- 0.534 SD (p<0.017)). The effect of GC stimulation was significantly greater, increasing *Lgl1* mRNA levels to 5.62 +/- 2.15 SD times the level in untreated cells (p<0.023) (Figure 4.7). Cell stimulation experiments were performed on four separate occasions, with real time-RT-PCR reactions done in duplicates.

mK4 cells represent metanephric mesenchyme at a later developmental stage, as it undergoes epithelial conversion to form the structures of the nephron. mK4 cells express markers such as *Gdnf*, *Pax8*, *Eya2*, *Pax2* and *Wnt4*. In mK4 cells, 9cisRA increased *Lgl1* mRNA levels nearly twofold (1.71 +/- 0.54 SD) (p<0.041) and atRA increased *Lgl1* mRNA levels at least twofold (2.7 +/- 1.4 SD) (p<0.029) compared to untreated cells. Again, the effect of GC was more powerful, increasing *Lgl1* mRNA levels 8.3 +/- 1.6 SD times the level of untreated cells (p<0.0006). In combination, 9cisRA and GC had an additive effect on *Lgl1* mRNA level (10.1 +/- 2.7 SD) compared to untreated cells (p<0.007). atRA and GC acted synergistically, stimulating *Lgl1* mRNA about sixteen-fold (15.8 +/- 5.3 SD) compared to untreated cells (p<0.011). The difference between 9cis + GC stimulation was not significantly different from GC stimulation alone (p<0.256), but atRA + GC stimulation differed significantly from GC alone (p<0.019) (Figure 4.8). Cell stimulation experiments were performed on four separate occasions, with real time-RT-PCR reactions done in duplicates.

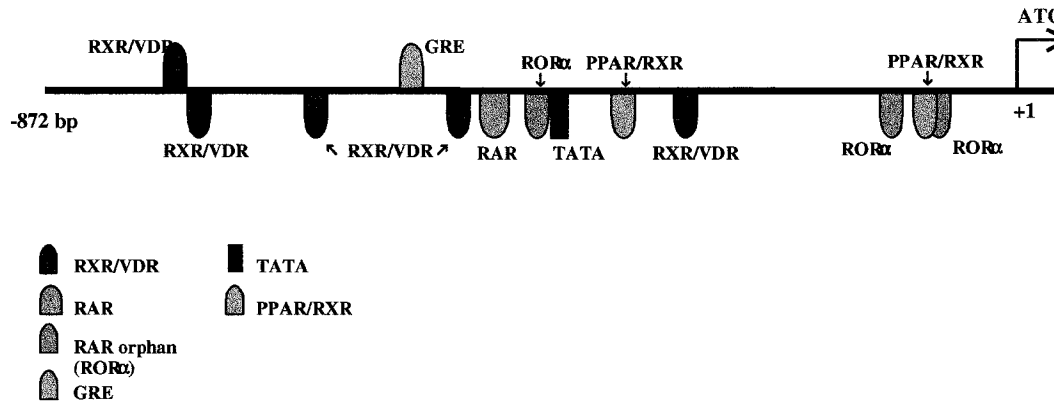
Figure 4.6 Potential binding sites in the 5' flanking sequences of *Lgl1* and promoter studies

A) The putative binding sites in the *Lgl1* promoter sequence were identified using Genomatix (<http://www.genomatix.de>). Comparison of the rat with the human and mouse sequences revealed ~11% homology with the human *Lgl1* promoter and ~14% homology with the mouse *Lgl1* promoter. Conserved transcriptional elements include a glucocorticoid response element (GRE) and retinoic acid response elements (RARE) sites, identified as RXR, RAR, and ROR α sites.

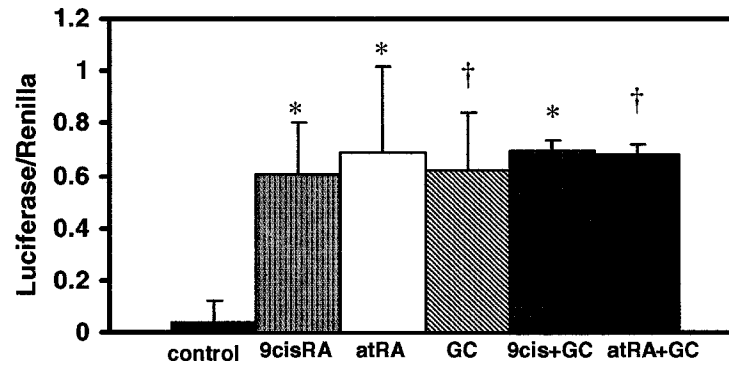
B) Stimulation of the *Lgl1* promoter

The *Lgl1* promoter- luciferase construct was transiently transfected into mK3 cells that were stimulated with retinoids (9cis retinoic acid (RA) 10^{-6} M), all trans (at) RA (10^{-6} M) and/or cortisol (GC, 10^{-7} M). The *Lgl1* promoter activity was significantly increased by these stimulants compared to non-treated control cells.

A)

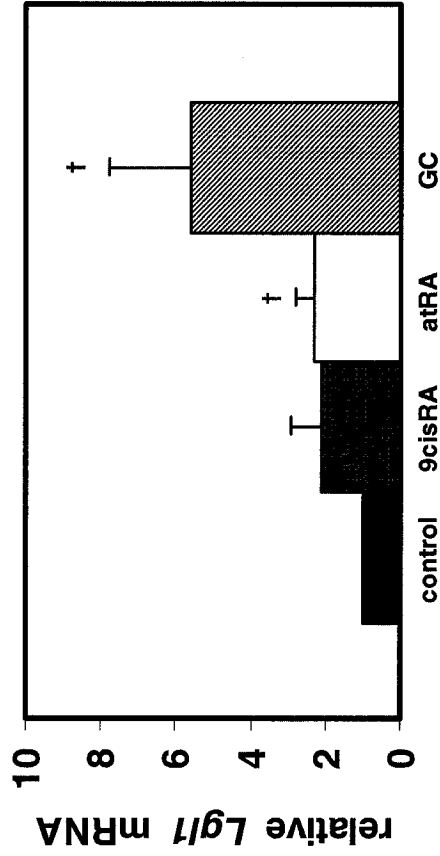


B)



† $p \leq 0.05$ vs Ctl
 * $p \leq 0.001$ vs Ctl

Figure 4.7 *Lgl1* mRNA expression in mK3 cells stimulated with retinoids and cortisol
mK3 cells were treated with retinoids (9cisRA (10^{-6} M); atRA (10^{-6} M) or cortisol (GC, 10^{-7} M) for 48hrs. Relative *Lgl1* mRNA was measured by real-time RT-PCR and standardized with β 2-microglobulin (B2M). Normalized *Lgl1* mRNA levels were increased by 2.13 +/- 0.789 SD after treatment with 9cisRA, by 2.28 +/- 0.534 SD after treatment with atRA, and by 5.62 +/- 2.15 SD after treatment with cortisol.

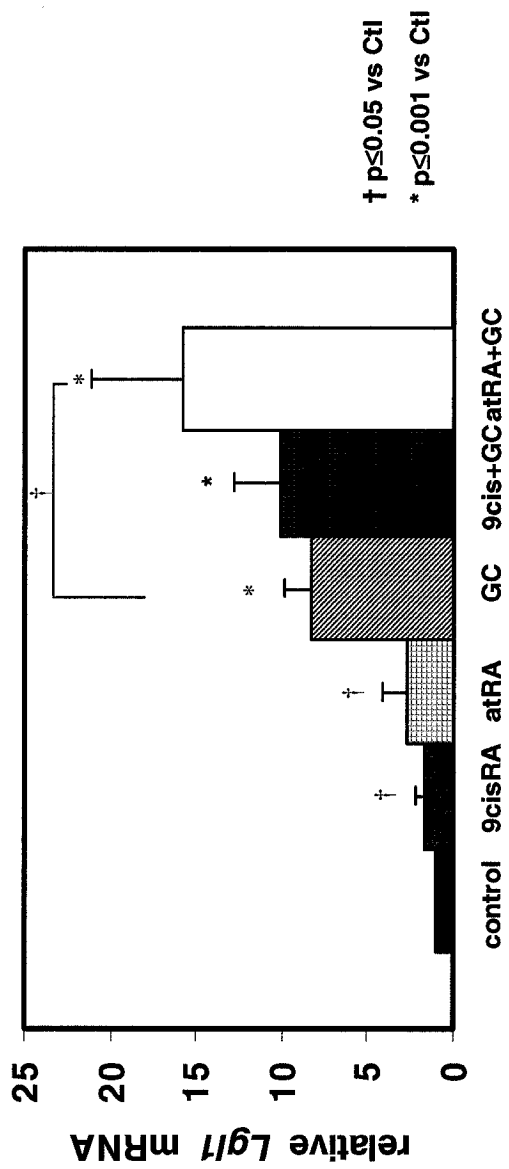


† p ≤ 0.05 vs Ctl

* p ≤ 0.001 vs Ctl

Figure 4.8 *Lgl1* mRNA expression in mK4 cells after retinoid and cortisol treatment

mK4 cells were treated with retinoids (9cis retinoic acid (RA) 10^{-6} M), all trans(at) RA 10^{-6} M) and/or cortisol (GC, 10^{-7} M) for 48hrs. Relative *Lgl1* mRNA was measured by real-time RT-PCR and standardized with a β 2-microglobulin (B2M). Normalized *Lgl1* mRNA levels were increased by 1.7 \pm 0.54 SD after treating cells with 9cisRA, by 2.7 \pm 1.4SD after treating with atRA, and by 8.3 \pm 1.6SD after treating with glucocorticoids. When cells were treated with 9cisRA in combination with GC, *Lgl1* mRNA was additively increased by 10.1 \pm 2.7 SD. However, when cells were treated with atRA in combination with GC, *Lgl1* mRNA was synergistically increased by 15.8 \pm 5.3 SD.



4.3.6 atRA increases UB branching and *Lgl1* mRNA in kidney explants, while GC decreases UB branching

Previous investigators have shown that all-trans retinoic acid stimulates branching morphogenesis of the ureteric bud in fetal mouse kidney explant cultures (Villar et al. 1996). To confirm atRA effects on UB branching are associated with a parallel increase in *Lgl1* mRNA, E11.5 fetal kidneys were isolated from *Hoxb7/Gfp* mouse embryos and grown in explant culture in medium with minimal fetal bovine (0.5%)/calf (0.5%) serum. Mice bearing the *Hoxb7/Gfp* transgene express green fluorescent protein throughout the ureteric bud, allowing visualization and quantification of terminal UB tips. The effect of GC on explant kidney branching was examined. Explants were grown in the presence of atRA (10^{-6} M) or GC (10^{-7} M) for 96 hours (Figure 4.9).

At 0, 24, 48 and 96 hours, explants were visualized under fluorescent light and the number of ureteric bud (UB) tips was counted for each explant. New branching events in each explant were identified by calculating the percent (%) change in UB tip number between time points compared to untreated controls (Figure 4.10). For untreated control explants, the mean % change in the number of UB bud tips after 24 h was 13.89% +/- 4.7 SEM, after 48 h was 19.47 % +/- 7.01 SEM, and after 96 h was 19.22% +/- 8.06 SEM. These values were set at 100% in comparisons with RA and GC stimulated explants. For explants treated with atRA (10^{-6} M), the mean % change in the number of UB tips compared to control was 107% +/- 7.02 SEM after 24 h ($p=0.18$), 130.82% +/- 6.7 SEM after 48 h ($p=0.0005$), and 158.5% +/-24.0SEM after 96 h ($p=0.01$). For explants treated with GC (10^{-7} M), the mean % change in the number of UB tips compared to control was 85.0% +/- 10.4 SEM ($p=0.08$) after 24 h, was 79.3% +/- 7.6SEM ($p=0.01$) after 48 h, and was 87.4% +/-10.4 SEM ($p= 0.13$) after 96 h. Explants were grown on three separate occasions for a total of 11 kidney rudiments in each group.

After 96 hours in culture, total RNA was isolated from kidney explants and *Lgl1* mRNA transcript levels were measured by real-time RT-PCR normalized for *beta-2 microglobulin* (B2M) mRNA. Explants treated with atRA (10^{-6} M) had nearly twice (1.77 +/- 0.5 SD) the amount of *Lgl1* mRNA compared to untreated explants ($p<0.06$). Four kidney rudiments were used for mRNA isolation after treatment with media and atRA for

96 hours and real-time RT-PCR experiment was performed on one occasion (Figure 4.11).

4.3.7 $Lgl1$ +/- / $Hoxb7/Gfp$ E12.5- E13 embryonic mouse kidneys have fewer UB branch tips than wildtype littermates

E12.5-E13 embryonic mouse kidneys were isolated under fluorescent light and the number of UB tips was counted (Figure 4.12 A). In Figure 4.12 B, $Lgl1^{+/-}$ heterozygous mice had a mean decrease of 20% +/- 14.11 SD in UB branch tips compared to wildtype littermates ($p=0.028$) (A total of 5 litters were examined, with $N=10$ $Lgl^{+/-}$ embryos, and $N= 17$ wildtype embryos).

4.3.8 Eight-month-old $Lgl1$ +/- mice do not have significantly increased levels of cystatin C

Serum cystatin C was measured as a surrogate of glomerular filtration rate at 8 months of age in $Lgl1$ +/- mice ($N= 4$) and in wildtype mice ($N= 5$) (Fig 4.13). $Lgl1$ +/- mice did not have significantly higher levels of serum cystatin C (mean 0.07 mg/L +/- 0.008 SD) than wildtype mice (mean 0.096 mg/L +/-0.015 SD) ($p=0.015$).

Figure 4.9 E11.5 *Hoxb7/Gfp* explants treated +/- all trans retinoic acid (atRA, 10^{-6} M) , +/- cortisol (GC, 10^{-7} M) for 96 h

Images of E11.5 *Hoxb7/Gfp* explants were taken after 0 h, 24 h, 48 h, and 96 h in culture. Explants grown in the presence of atRA had an increase in the number of UB tips compared to explants grown with minimal media (control); while explants grown in the presence of GC had a reduction in the number of UB tips compared to control explants. (32 X magnification).

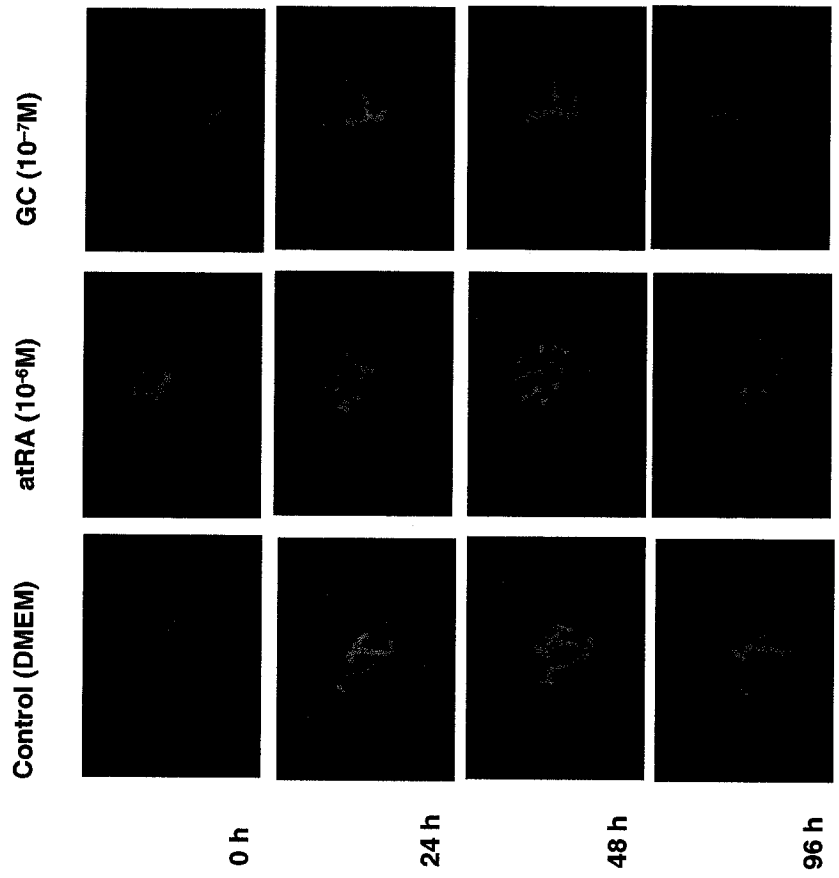
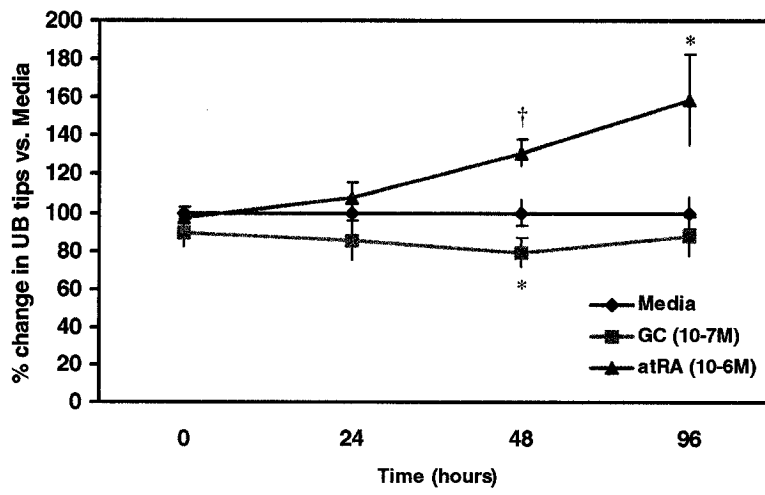


Figure 4.10 E11.5 *Hoxb7/Gfp* Explant Growth

E11.5 *Hoxb7/Gfp* kidney rudiments were dissected and grown in minimal DMEM media with 1% serum (media) +/- all trans retinoic acid (atRA, 10^{-6} M) and +/- cortisol (GC, 10^{-7} M). The number of ureteric bud (UB) tips was counted after 0, 24, 48, and 96 hours in culture at 37°C in humidified 5% CO₂ in air chamber. The mean % difference in UB tips for each explant was calculated as a percent difference of the media control group. When explants were treated with atRA, an increase in the number of UB tips is observed compared to control explants, while GC decreases the number of UB tips compared to control explants.



† $p \leq 0.05$ vs Ctl
* $p \leq 0.001$ vs Ctl

Figure 4.11 *Lgl1* mRNA expression in E11.5 *Hoxb7/Gfp* explants treated for 96h +/- atRA (10^{-6} uM).

Explants treated with atRA (10^{-6} M) have 1.77 higher *Lgl1* mRNA levels compared to nontreated explants after standardization with β 2-microglobulin (housekeeping gene) shown by real-time RT-PCR ($p= 0.06$).

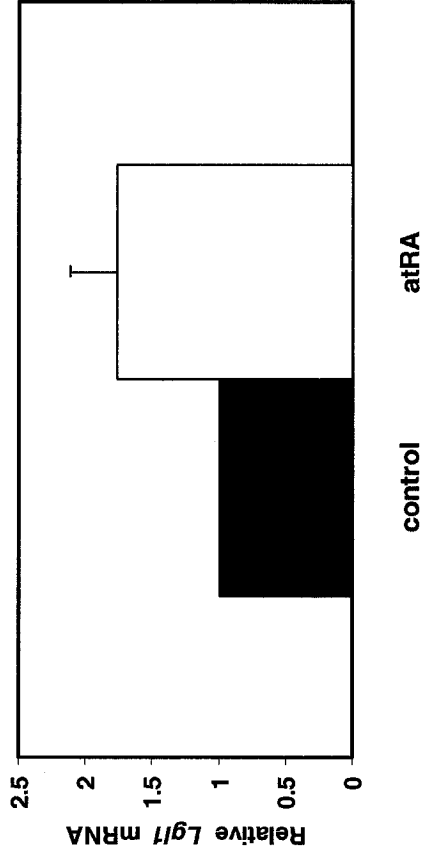
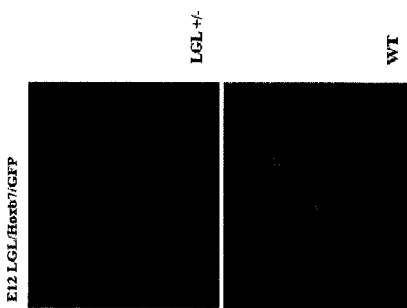


Figure 4.12 E12.5 *Lgl1/ Hoxb7/Gfp* kidneys

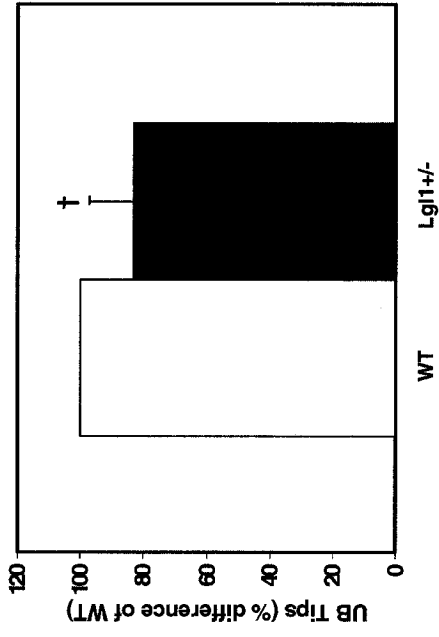
A) E12.5 *Lgl1/ Hoxb7/Gfp* kidneys were dissected and images were captured under fluorescent light at 32X magnification.

B) Ureteric bud (UB) tips were counted in *Lgl1*^{+/-} */Hoxb7/Gfp* mice and wildtype (WT) littermates. The *Lgl1*^{+/-} mice have 80% the number of UB tips compared to WT littermates (p=0.028).

A)



B)

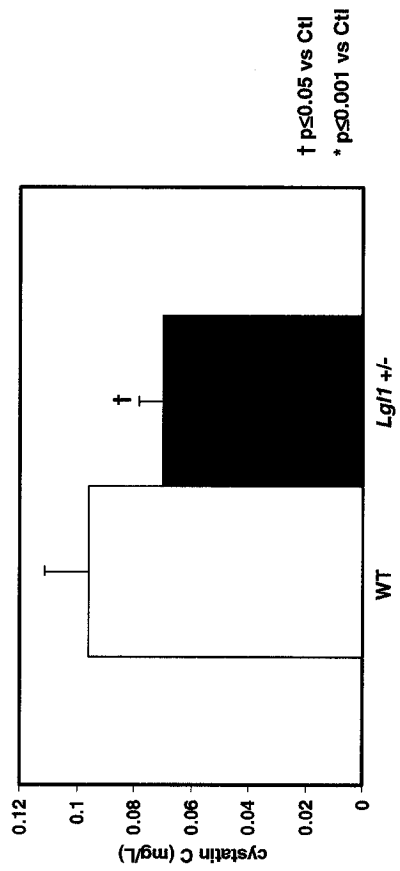


† p<0.05 vs Ctl

* p<0.001 vs Ctl

Figure 4.13 *Lgl1*^{+/-} aged mice do not have increased levels of serum cystatin C

Aged *Lgl1*^{+/-} mice (N=4) have a mean of 0.07 mg/L of serum cystatin C compared to age and sex matched wildtype controls (N=5) (0.096mg/L) p=0.015.



4.4 DISCUSSION

In the kidney, vitamin A deficiency has severe repercussions (Ross, McCaffery et al. 2000) causing renal agenesis in pups born from vitamin A deficient (VAD) rodents (Lelievre-Pegorier, Vilar et al. 1998) and renal hypoplasia from mild VA deficiency (Lelievre-Pegorier, Vilar et al. 1998). The physiological form of vitamin A is all-trans retinoic acid (atRA) (Zile and Deluca 1965; Zile 2001), which is known to accelerate new nephron formation 2-3 fold in embryonic fetal kidneys (Vilar, Gilbert et al. 1996). Although the importance of RA in renal branching has been accepted for some time, the mechanism by which it induces this process still remains poorly understood. One model proposes that RA indirectly increases UB branching by stimulating an as yet identified secreted mesenchymal molecule (Batourina, Choi et al. 2002).

In 1999, the Kaplan laboratory identified a novel gene, late gestation lung protein 1 (*Lgl1*), which was stimulated by glucocorticoids (GC) in the lung mesenchyme (Kaplan, Ledoux et al. 1999). Antisense oligonucleotide experiments to inhibit *Lgl1* expression identified an affect on pulmonary airway branching morphogenesis (Oyewumi, Kaplan et al. 2003). Furthermore, LGL1 was found to be a secreted glycoprotein imported by lung epithelial cells (Oyewumi, Kaplan et al. 2003).

Epithelial branching is a common feature of mammalian organogenesis (Hu and Rosenblum 2003) with many developmental pathways shared between the lung and the kidney (<http://www.ana.ed.ac.uk/anatomy/database/orghome.html>). We investigated *Lgl1*'s role in renal branching morphogenesis.

Consistent with the expression pattern of *Lgl1* in the lung (Kaplan, Ledoux et al. 1999), we show that *Lgl1* is expressed in mesenchymal cells of the fetal kidney. Similarly, we observed *Lgl1* mRNA in mesenchymal cells around the mid gut epithelial lining (Figure 4.3). Based on these observations, we speculate that LGL1 may be a branching morphogen secreted by mesenchyme in several developing organs, including the kidney and the gastrointestinal tract.

To examine the effects of LGL1 mutations on kidney development, we studied the renal phenotype of *Lgl1* knockout mice, kindly provided by Drs. F. Kaplan and N. Swezey. Homozygous knockout *Lgl1*^{-/-} mice are embryonic lethal prior to renal

development (unpublished data). The *Lgll*^{+/-} heterozygous mice have a 20% reduction in UB tips compared to wild type littermates (Figure 4.12). This subtle reduction in branching may account for reduced renal function in adult mice (which remains to be tested), although at 8 months of age, we did not detect an increase in serum cystatin C levels (Figure 4.13). Presumably, at this stage, glomerular hypertrophy compensates for this modest reduction in nephron number. Thus, serum collected from older *Lgll*^{+/-} mice, when nephron “burnout” presumably would occur, may reveal an increase in cystatin C levels.

Lgll was originally observed as a glucocorticoid (GC) induced gene in late embryonic stages of lung development (Kaplan, Ledoux et al. 1999) for which we show similar GC stimulation in renal cells (Figure 4.7, 4.8). These observations are puzzling since inhibition of *Lgll* has been shown to decrease branching in young pulmonary explants (Oyewumi, Kaplan et al. 2003) and decreases the number of UB tips in embryonic kidneys (Figure 4.12). How can *Lgll* be a branching molecule induced by GC when in the lung, GC stimulates maturation (Garbrecht, Klein et al. 2006), and inhibits branching in both the lung (Garbrecht, Klein et al. 2006) and the kidney (Figure 4.9, 4.10)? This apparent contradiction may be explained by our observations that *Lgll* expression is also induced by retinoic acid (RA). RA is known to stimulate branching of both fetal lung and kidney (Ross, McCaffery et al. 2000). Thus we postulate that *Lgll* may have two separate roles in development. In early organogenesis, it is induced by RA to drive branching. In later stages, GC induced *Lgll* may enhance terminal differentiation of the branched structure.

Retinoic acid receptor (*RAR*) α ^{-/-}; *RAR* β ²^{-/-} embryos were observed to have arrested development of the stromal compartments, renal hypoplasia and downregulation of *c-Ret* expression (Batourina, Gim et al. 2001). Based on these observation, Batourina *et al.* hypothesized that RA was stimulating an unknown molecule in the stromal mesenchyme (where *RAR* α and *RAR* β are located) to drive ureteric branching (Batourina, Gim et al. 2001). We found that *Lgll* is stimulated by RA in renal mesenchymal cells (Fig 4.7, 4.8) and that an increase in branching in kidney explants treated with RA correlated with an increase in *Lgll* mRNA (Figure 4.9, 4.10, 4.11). Our

data suggests that *Lgll* could be the unknown molecule that is stimulated by RA to affect UB branching in the model proposed by Batourina et al (2001).

Interestingly, in the retinoic acid receptor (*RAR*) $\alpha^{-/-}$; *RAR* $\beta 2^{-/-}$ embryos, both the kidney and the lung are affected. These embryos have renal hypoplasia and arrested development of the stromal compartments of their kidney (Mendelsohn, Lohnes et al. 1994) and also present with pulmonary agenesis, tracheoesophageal fistula and lobular agenesis (Mendelsohn, Lohnes et al. 1994). Other work has shown that early lung development and branching is dependent on RA. If RA is absent or reduced, it affects lung bud outgrowth (Wilson, Roth et al. 1953; Mollard, Ghyselinck et al. 2000), which results in lung agenesis or hypoplasia (Shenefelt RE et al. 1972; Wilson JG et al. 1953). Furthermore, when premature low birth weight infants were given vitamin A supplementation, they had a decreased chance of developing bronchopulmonary dysplasia (Tyson, Wright et al. 1999). These findings suggest that vitamin A and its derivative, RA, are critical for lung development, as they are in kidney development. We hypothesize that *Lgll* may be a target for RA induced branching in both of these organs in early development.

Prenatal GC treatment is known to reduce nephron numbers in animal models (Wintour, Moritz et al. 2003); Woods LL, et al. 2005) and cause the adults to be hypertensive (Wintour, Moritz et al. 2003) Furthermore, GC treatment altered renal expression of several key regulatory molecules (Massmann GA, et al. 2006). Concurrent with these observations, we show that GC suppresses branching in renal explant cultures (Figure 4.9, 4.10). Addition of GC on early lung explants inhibits branching and causes premature maturation (Oshika, Liu et al. 1998). Near the end of gestation, fetal GC levels rise sharply, which coincides with final maturation of the fetal lung and stimulates surfactant synthesis (Bolt RJ, et al. 2001; Garbrecht MT, et al. 2006; Gonzales LW et al. 2002; Smith et al. 1973). Thus, we propose that *Lgll* must have a second function that would explain the induction by GC in late lung and kidney. This secondary role would coincide with the sustained LGL1 expression we observed in adult kidneys (Figure 4.5).

Taking all of this into account, we propose a model for the effects of *Lgll*. We hypothesize that retinoic acid stimulates *Lgll* in early development in both the lung and the kidney to induce branching of these organs. During terminal differentiation at late

stages of gestation, when fetal levels of GC normally rise, we hypothesize that *Lgl1* has a second function, coinciding with the known maturation effects of GC (Figure 4.14). In our model, *Lgl1*'s expression would be temporally regulated by different factors; however, we recognise that *Lgl1*'s function would also need to change in order to account for the different effects it has on the epithelium. Presumably, during development, *Lgl1* is altered (by alternative spicing or some other mechanism) or the cellular environment changes (differentiation of new cell types, expression of different receptors or partners) to account for this change in function.

In conclusion, we have shown that *Lgl1* is induced by RA and affects renal branching morphogenesis. We hypothesize that GC stimulates *Lgl1* in both the lung and the kidney, resulting in a second function for *Lgl1* that remains to be elucidated.

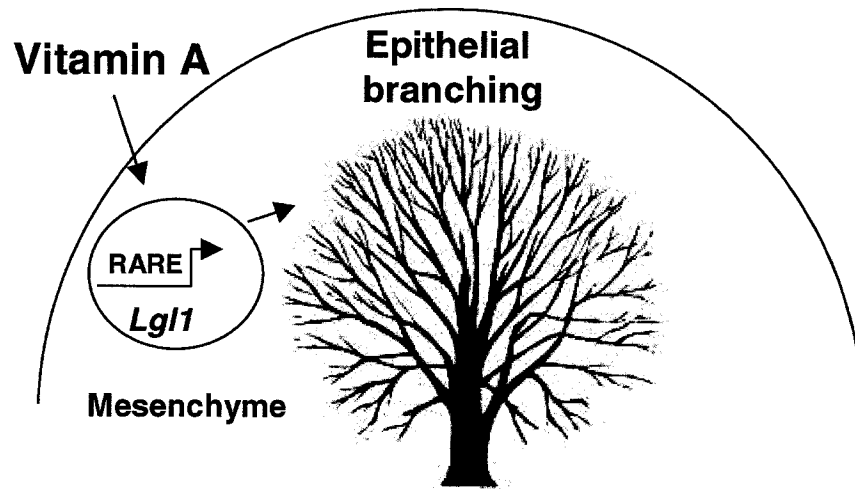
Figure 4.14 Model of the dual function of *Lgll* in development

In the both the lung and the kidney, *Lgll* is expressed in the mesenchyme, where it is believed to induce the epithelium. In the following model, we propose *Lgll* has two different effects in A) early and B) late development.

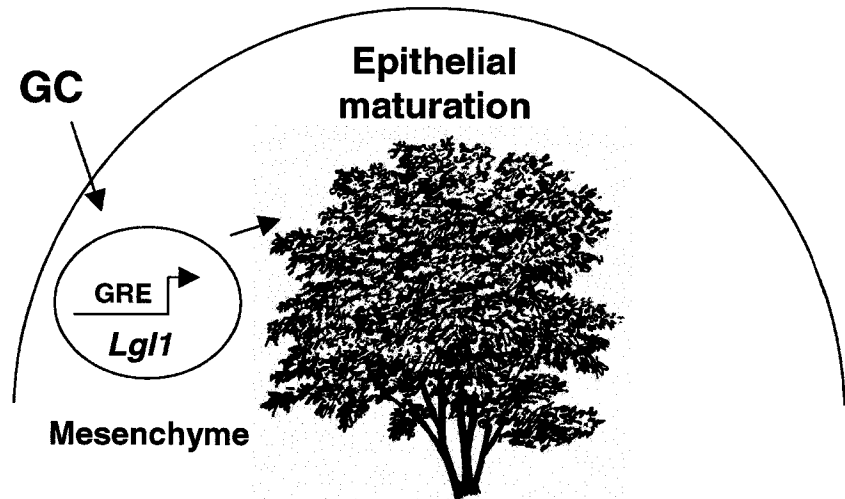
A) In early development, *Lgll* is involved in branching, which we hypothesize is driven by retinoic acid (RA), the physiological metabolite of vitamin A. RA binds to RA response elements (RARE) in the promoter region to drive expression of *Lgll*. LGL1 is secreted and induces branching of both pulmonary and renal epithelium.

B) In late development, we hypothesize that glucocorticoids (GC) induces *Lgll* to cause a second function, which may include maturation of the epithelium. GC binds to glucocorticoid response elements (GRE) in promoter region of *Lgll* to drive expression of target genes. The effect of GC induced *Lgll* in both the kidney and the lung remains unknown.

A) EARLY DEVELOPMENT



B) LATE DEVELOPMENT



ACKNOWLEDGEMENTS

This study was supported by an operating grant from the Canadian Institutes of Health Research (MOP 12954). Dr. Paul Goodyer is the recipient of a James McGill (CIHR) Research Chair.

CHAPTER 5
CONCLUSIONS

5.1 CONCLUSIONS AND FUTURE DIRECTIONS

Work performed in the present thesis has advanced the knowledge of two important genetic determinants of nephron formation: *PAX2* and *Lgll*.

We linked a *PAX2* haplotype with a 10% reduction in renal volume that is in linkage disequilibrium with an allele that decreases *PAX2* expression. The 10% reduction in volume accounts for part of the nephron deficit observed in patients that developed essential hypertension (Keller et al 2003). Thus, other genes must be implicated in subtle renal hypoplasia. Potential candidates include downstream targets of *PAX2*, *GDNF* and *RALDH2*. *Gdnf*^{+/-} mice develop hypertension as adults, making it a good candidate. The rate-determining enzyme for the conversion of vitamin A to RA is *RALDH2*. Thus, subtle variations in this gene may account for decreased availability of RA required for nephron formation.

The allele specific reduction in *PAX2* expression is most likely the mechanism by which kidney volume is reduced. In order to confirm this hypothesis, we will genotype the exonic SNP (rs18008998) in our patient cohort to examine the possible association between mean kidney volume and the C allele of SNP rs1800898, which decreases *PAX2* expression. Furthermore, it is interesting to speculate how reduced levels of *PAX2* transcription affect downstream targets that ultimately influence nephron formation.

We also determined that *Lgll* is a target of RA and affects renal branching morphogenesis. However, the mechanism by which RA induces *Lgll* is unknown. It would be interesting to confirm that *Lgll* is a secreted glycoprotein taken up by the UB, as it is in lung epithelium.

Lgll may be the unknown molecule in the MM that is stimulated by RA to induce branching. In order to confirm this, one could characterize *Lgll* expression in the *RARα*^{-/-} / *RARβ*^{-/-} embryos to determine if they have decreased *Lgll* expression. Conversely, it would be interesting to know if c-*Ret* expression is reduced in the *Lgll*^{+/-} mice.

In order to further understand the role of *Lgll* in the kidney, creation of a conditional knock mouse that would target *Lgll* deletion specifically in the kidney, or target *Lgll* deletion at the onset of renal organogenesis would be interesting to develop.

Our model for the dual function of *Lgl1* needs to be confirmed. Experiments should examine *Lgl1* in late organogenesis when we hypothesize that GC effects *Lgl1*. Although we show that GC inhibits renal branching, the effects of GC during kidney development remain poorly understood. It is presumed that some maturational event involving GC induction of *Lgl1* during late renal organogenesis occurs, although this remains to be confirmed.

Finally, the role of *Lgl1* in the development of other branching organs, such as in mid gut, should be studied. We hypothesize its role will be similar to what it is in the lung and kidney.

5.2 SUMMARY

In normal human populations, nephron number varies widely from 300,000 to over one million nephrons per kidney. This large range was once dismissed as sub-clinical variation, but recently it has been found that individuals at the lower end of the nephron spectrum are at increased risk of developing essential hypertension as adults. Final nephron number is a reflection of fetal kidney branching events, which is completed prior to birth. Thus, mechanisms that influence fetal kidney branching will in turn influence an individual's functional kidney reserve for life. While the mechanisms that influence branching are important, they remain unknown.

The work presented in this thesis has examined two important pathways that influence renal branching morphogenesis and final nephron number: the *PAX2* pathway and the retinoic acid (RA) pathway.

Homozygous *PAX2* mutations cause renal agenesis and heterozygous mutations cause a hereditary syndrome of renal hypoplasia (RCS). *PAX2* has been reported to have many functions in the kidney, including determination of nephric duct cell fate (Bouchard et al. 2002), activation of *Gdnf* (Brohpy et al. 2001), a trophic factor for the UB, stimulation of mesenchymal differentiation into epithelium of emerging nephrons (Dressler et al. 1990); and influencing the rate of branching morphogenesis through its anti-apoptotic effect on UB cells (Dziarmaga et al). Thus, *PAX2* is an excellent candidate for influencing sub-optimal branching events observed in normal individuals born in the lower nephron endowment spectrum. We hypothesized that common variations in *PAX2* would be responsible for a subtle reduction in functional nephron mass of normal newborns. In order to address this hypothesis, we chose haplotype tagging single nucleotide polymorphisms (htSNPs) in the *PAX2* gene region to demonstrate an association between a common haplotype and a 10% reduction in kidney volume. Thus, we presume that an ancestral polymorphism lying on the associated haplotype has been conserved and has expanded to occur commonly (18%) in the population. Using an exonic SNP in linkage disequilibrium with this haplotype, we were able to show that the level of *PAX2* expression is altered by an allele. The reduction in *PAX2* expression may account for smaller kidney volume, which is associated with the haplotype.

RA has been demonstrated to influence nephron formation (Villar et al); however, the mechanisms involved remain a mystery. A model in which RA has an indirect effect on UB branching through stimulation of a mesenchymal molecule has been proposed (Batourina et al). We hypothesized *Lgll* as a candidate gene for the indirect effects of RA on UB branching based on studies of the lung. We characterized *Lgll*, in the developing kidney and showed that it is expressed in mesenchymal cells and that it is responsive to RA. Experiments involving the *Lgll*^{+/-} mouse showed a reduction in UB tips. Based on these observations, we have implicated *Lgll* in nephron formation as a downstream target of RA.

REFERENCES

- (2003). "The International HapMap Project." Nature **426**(6968): 789-96.
- Ardissino, G., V. Dacco, et al. (2003). "Epidemiology of chronic renal failure in children: data from the ItalKid project." Pediatrics **111**(4 Pt 1): e382-7.
- Armstrong, J. F., K. Pritchard-Jones, et al. (1993). "The expression of the Wilms' tumour gene, WT1, in the developing mammalian embryo." Mech Dev **40**(1-2): 85-97.
- Austin, M. A., P. J. Talmud, et al. (2004). "Association of apolipoprotein A5 variants with LDL particle size and triglyceride in Japanese Americans." Biochim Biophys Acta **1688**(1): 1-9.
- Batourina, E., C. Choi, et al. (2002). "Distal ureter morphogenesis depends on epithelial cell remodeling mediated by vitamin A and Ret." Nat Genet **32**(1): 109-15.
- Batourina, E., S. Gim, et al. (2001). "Vitamin A controls epithelial/mesenchymal interactions through Ret expression." Nat Genet **27**(1): 74-8.
- Beyer, W.H. Standard Mathematical Tables. 28th Ed. CRC Press. Boca Raton, Fl. 1987, page 131
- Bhat, P. V., M. Marcinkiewicz, et al. (1998). "Changing patterns of renal retinal dehydrogenase expression parallel nephron development in the rat." J Histochem Cytochem **46**(9): 1025-32.
- Bouchard, M. (2003). "[Pax genes and cell specification]." Med Sci (Paris) **19**(5): 535-7.
- Bouchard, M., A. Souabni, et al. (2002). "Nephric lineage specification by Pax2 and Pax8." Genes Dev **16**(22): 2958-70.
- Brenner, B. M., D. L. Garcia, et al. (1988). "Glomeruli and blood pressure. Less of one, more the other?" Am J Hypertens **1**(4 Pt 1): 335-47.
- Brenner, B. M. and E. L. Milford (1993). "Nephron underdosing: a programmed cause of chronic renal allograft failure." Am J Kidney Dis **21**(5 Suppl 2): 66-72.
- Brophy, P. D., L. Ostrom, et al. (2001). "Regulation of ureteric bud outgrowth by Pax2-dependent activation of the glial derived neurotrophic factor gene." Development **128**(23): 4747-56.

- Cacalano, G., I. Farinas, et al. (1998). "GFRalpha1 is an essential receptor component for GDNF in the developing nervous system and kidney." Neuron **21**(1): 53-62.
- Carlson, C. S., M. A. Eberle, et al. (2004). "Selecting a maximally informative set of single-nucleotide polymorphisms for association analyses using linkage disequilibrium." Am J Hum Genet **74**(1): 106-20.
- Cass, A., J. Cunningham, et al. (2001). "Regional variation in the incidence of end-stage renal disease in Indigenous Australians." Med J Aust **175**(1): 24-7.
- Cavalli-Sforza, L. L. and A. Piazza (1993). "Human genomic diversity in Europe: a summary of recent research and prospects for the future." Eur J Hum Genet **1**(1): 3-18.
- Clark, A. T. and J. F. Bertram (1999). "Molecular regulation of nephron endowment." Am J Physiol **276**(4 Pt 2): F485-97.
- Clark, P., A. Dziarmaga, et al. (2004). "Rescue of defective branching nephrogenesis in renal-coloboma syndrome by the caspase inhibitor, Z-VAD-fmk." J Am Soc Nephrol **15**(2): 299-305.
- Cullen-McEwen, L. A., J. Drago, et al. (2001). "Nephron endowment in glial cell line-derived neurotrophic factor (GDNF) heterozygous mice." Kidney Int **60**(1): 31-6.
- Cullen-McEwen, L. A., M. M. Kett, et al. (2003). "Nephron number, renal function, and arterial pressure in aged GDNF heterozygous mice." Hypertension **41**(2): 335-40.
- Daly, M. J., J. D. Rioux, et al. (2001). "High-resolution haplotype structure in the human genome." Nat Genet **29**(2): 229-32.
- Dehbi, M., M. Ghahremani, et al. (1996). "The paired-box transcription factor, PAX2, positively modulates expression of the Wilms' tumor suppressor gene (WT1)." Oncogene **13**(3): 447-53.
- Devriendt, K., G. Matthijs, et al. (1998). "Missense mutation and hexanucleotide duplication in the PAX2 gene in two unrelated families with renal-coloboma syndrome (MIM 120330)." Hum Genet **103**(2): 149-53.
- Dorfler, P. and M. Busslinger (1996). "C-terminal activating and inhibitory domains determine the transactivation potential of BSAP (Pax-5), Pax-2 and Pax-8." Embo J **15**(8): 1971-82.

- Dressler, G. R. (1996). "Pax-2, kidney development, and oncogenesis." Med Pediatr Oncol **27**(5): 440-4.
- Dressler, G. R., U. Deutsch, et al. (1990). "Pax2, a new murine paired-box-containing gene and its expression in the developing excretory system." Development **109**(4): 787-95.
- Dziarmaga, A., P. Clark, et al. (2003). "Ureteric bud apoptosis and renal hypoplasia in transgenic PAX2-Bax fetal mice mimics the renal-coloboma syndrome." J Am Soc Nephrol **14**(11): 2767-74.
- Dziarmaga, A., M. Eccles, et al. (2006). "Suppression of Ureteric Bud Apoptosis Rescues Nephron Endowment and Adult Renal Function in Pax2 Mutant Mice." J Am Soc Nephrol **17**(6): 1568-1575.
- Dziarmaga, A., P. A. Hueber, et al. (2006). "Neuronal apoptosis inhibitory protein (NAIP) is expressed in developing kidney and is regulated by PAX2." Am J Physiol Renal Physiol.
- Dziarmaga, A., Julien, J-P., Eccles, M. and Goodyer, P. (2003). Targeted Bcl-2 Expression in Ureteric Bud Cells Rescues the Hypoplastic Kidney Phenotype of Pax2^{1Neu} Mutant Mice. The American Society of Nephrology, San Diego, CA, The Journal of the American Society of Nephrology.
- Dziarmaga, A., J. Quinlan, et al. (2006). "Renal hypoplasia: lessons from Pax2." Pediatr Nephrol **21**(1): 26-31.
- Eccles, M. R. (1998). "The role of PAX2 in normal and abnormal development of the urinary tract." Pediatr Nephrol **12**(9): 712-20.
- Eccles, M. R., S. He, et al. (2002). "PAX genes in development and disease: the role of PAX2 in urogenital tract development." Int J Dev Biol **46**(4): 535-44.
- Eccles, M. R. and L. A. Schimmenti (1999). "Renal-coloboma syndrome: a multi-system developmental disorder caused by PAX2 mutations." Clin Genet **56**(1): 1-9.
- Eccles, M. R., L. J. Wallis, et al. (1992). "Expression of the PAX2 gene in human fetal kidney and Wilms' tumor." Cell Growth Differ **3**(5): 279-89.
- Enomoto, H., T. Araki, et al. (1998). "GFR alpha1-deficient mice have deficits in the enteric nervous system and kidneys." Neuron **21**(2): 317-24.

- Fassi, A., F. Sangalli, et al. (1998). "Progressive glomerular injury in the MWF rat is predicted by inborn nephron deficit." J Am Soc Nephrol **9**(8): 1399-406.
- Favor, J., R. Sandulache, et al. (1996). "The mouse Pax2(1Neu) mutation is identical to a human PAX2 mutation in a family with renal-coloboma syndrome and results in developmental defects of the brain, ear, eye, and kidney." Proc Natl Acad Sci U S A **93**(24): 13870-5.
- Filler G, Priem F, Vollmer I, Gellermann J, Jung K. :Pediatr Nephrol. 1999 Aug;13(6):501-5
- Gabriel, S. B., S. F. Schaffner, et al. (2002). "The structure of haplotype blocks in the human genome." Science **296**(5576): 2225-9.
- Garbrecht, M. R., J. M. Klein, et al. (2006). "Glucocorticoid metabolism in the human fetal lung: implications for lung development and the pulmonary surfactant system." Biol Neonate **89**(2): 109-19.
- Gelb, A., G. Manligas, et al. (2001). "Identification of two novel polymorphisms (g.903C>T and g.1544C>T) in the PAX2 gene." Hum Mutat **17**(2): 155.
- Gilbert, T. (2002). "Vitamin A and kidney development." Nephrol Dial Transplant **17 Suppl 9**: 78-80.
- Gilbert, T. and C. Merlet-Benichou (2000). "Retinoids and nephron mass control." Pediatr Nephrol **14**(12): 1137-44.
- Gnarra, J. R. and G. R. Dressler (1995). "Expression of Pax-2 in human renal cell carcinoma and growth inhibition by antisense oligonucleotides." Cancer Res **55**(18): 4092-8.
- Gragnoli, C., E. Milord, et al. (2005). "Linkage study of the glucagon receptor gene with type 2 diabetes mellitus in Italians." Metabolism **54**(6): 786-7.
- Hinchliffe, S. A., P. H. Sargent, et al. (1991). "Human intrauterine renal growth expressed in absolute number of glomeruli assessed by the disector method and Cavalieri principle." Lab Invest **64**(6): 777-84.
- Hoy, W. E., M. D. Hughson, et al. (2005). "Nephron number, hypertension, renal disease, and renal failure." J Am Soc Nephrol **16**(9): 2557-64.

- Hoy, W. E., M. D. Hughson, et al. (2006). "Reduced nephron number and glomerulomegaly in Australian Aborigines: a group at high risk for renal disease and hypertension." Kidney Int **70**(1): 104-10.
- Hu, M. C. and N. D. Rosenblum (2003). "Genetic regulation of branching morphogenesis: lessons learned from loss-of-function phenotypes." Pediatr Res **54**(4): 433-8.
- Hughson, M., A. B. Farris, 3rd, et al. (2003). "Glomerular number and size in autopsy kidneys: the relationship to birth weight." Kidney Int **63**(6): 2113-22.
- Hughson, M. D., R. Douglas-Denton, et al. (2006). "Hypertension, glomerular number, and birth weight in African Americans and white subjects in the southeastern United States." Kidney Int **69**(4): 671-8.
- Kaplan, F., P. Ledoux, et al. (1999). "A novel developmentally regulated gene in lung mesenchyme: homology to a tumor-derived trypsin inhibitor." Am J Physiol **276**(6 Pt 1): L1027-36.
- Keller, G., G. Zimmer, et al. (2003). "Nephron number in patients with primary hypertension." N Engl J Med **348**(2): 101-8.
- Keller, S. A., J. M. Jones, et al. (1994). "Kidney and retinal defects (Krd), a transgene-induced mutation with a deletion of mouse chromosome 19 that includes the Pax2 locus." Genomics **23**(2): 309-20.
- Kispert, A., S. Vainio, et al. (1996). "Proteoglycans are required for maintenance of Wnt-11 expression in the ureter tips." Development **122**(11): 3627-37.
- Kitamura, Y., K. Okumura, et al. (2004). "Association of plasminogen activator inhibitor-1 4G/5G gene polymorphism with variations in the LDL particle size in healthy Japanese men." Clin Chim Acta **347**(1-2): 209-16.
- Kreidberg, J. A., H. Sariola, et al. (1993). "WT-1 is required for early kidney development." Cell **74**(4): 679-91.
- Lechner, M. S. and G. R. Dressler (1996). "Mapping of Pax-2 transcription activation domains." J Biol Chem **271**(35): 21088-93.
- Lee, H. Y., D. F. Dohi, et al. (1998). "All-trans retinoic acid converts E2F into a transcriptional suppressor and inhibits the growth of normal human bronchial

- epithelial cells through a retinoic acid receptor- dependent signaling pathway." J Clin Invest **101**(5): 1012-9.
- Lee, M. O., C. L. Manthey, et al. (1991). "Identification of mouse liver aldehyde dehydrogenases that catalyze the oxidation of retinaldehyde to retinoic acid." Biochem Pharmacol **42**(6): 1279-85.
- Leid, M. (1994). "Ligand-induced alteration of the protease sensitivity of retinoid X receptor alpha." J Biol Chem **269**(19): 14175-81.
- Leid, M., P. Kastner, et al. (1992). "Multiplicity generates diversity in the retinoic acid signalling pathways." Trends Biochem Sci **17**(10): 427-33.
- Leid, M., P. Kastner, et al. (1993). "Retinoic acid signal transduction pathways." Ann N Y Acad Sci **684**: 19-34.
- Lelievre-Pegorier, M., J. Vilar, et al. (1998). "Mild vitamin A deficiency leads to inborn nephron deficit in the rat." Kidney Int **54**(5): 1455-62.
- Lelievre-Pegorier, M., J. Vilar, et al. (1998). "Mild vitamin A deficiency leads to inborn nephron deficit in the rat." Kidney Int **54**: 1455-62.
- Lin, Y., A. Liu, et al. (2001). "Induction of ureter branching as a response to Wnt-2b signaling during early kidney organogenesis." Dev Dyn **222**(1): 26-39.
- Livak, K. J. and T. D. Schmittgen (2001). "Analysis of relative gene expression data using real-time quantitative PCR and the 2(-Delta Delta C(T)) Method." Methods **25**(4): 402-8.
- Mansouri, A., K. Chowdhury, et al. (1998). "Follicular cells of the thyroid gland require Pax8 gene function." Nat Genet **19**(1): 87-90.
- McConnell, L. M., G. D. Sanders, et al. (1999). "Evaluation of genetic tests: APOE genotyping for the diagnosis of Alzheimer disease." Genet Test **3**(1): 47-53.
- Mendelsohn, C., D. Lohnes, et al. (1994). "Function of the retinoic acid receptors (RARs) during development (II). Multiple abnormalities at various stages of organogenesis in RAR double mutants." Development **120**(10): 2749-71.
- Mendelsohn, C., M. Mark, et al. (1994). "Retinoic acid receptor beta 2 (RAR beta 2) null mutant mice appear normal." Dev Biol **166**(1): 246-58.
- Metzger, R. J. and M. A. Krasnow (1999). "Genetic control of branching morphogenesis." Science **284**(5420): 1635-9.

- Mollard, R., N. B. Ghyselinck, et al. (2000). "Stage-dependent responses of the developing lung to retinoic acid signaling." *Int J Dev Biol* **44**(5): 457-62.
- Moore, M. W., R. D. Klein, et al. (1996). "Renal and neuronal abnormalities in mice lacking GDNF." *Nature* **382**(6586): 76-9.
- Mosteller RD: Simplified Calculation of Body Surface Area. *N Engl J Med* 1987 Oct 22;317(17):1098)
- Narahara, K., E. Baker, et al. (1997). "Localisation of a 10q breakpoint within the PAX2 gene in a patient with a de novo t(10;13) translocation and optic nerve coloboma-renal disease." *J Med Genet* **34**(3): 213-6.
- Nyengaard, J. R. and T. F. Bendtsen (1992). "Glomerular number and size in relation to age, kidney weight, and body surface in normal man." *Anat Rec* **232**(2): 194-201.
- Oshika, E., S. Liu, et al. (1998). "Glucocorticoid-induced effects on pattern formation and epithelial cell differentiation in early embryonic rat lungs." *Pediatr Res* **43**(3): 305-14.
- Oyewumi, L., F. Kaplan, et al. (2003). "Antisense oligodeoxynucleotides decrease LGL1 mRNA and protein levels and inhibit branching morphogenesis in fetal rat lung." *Am J Respir Cell Mol Biol* **28**(2): 232-40.
- Oyewumi, L., F. Kaplan, et al. (2003). "Lgl1, a mesenchymal modulator of early lung branching morphogenesis, is a secreted glycoprotein imported by late gestation lung epithelial cells." *Biochem J* **376**(Pt 1): 61-9.
- Pastinen, T., B. Ge, et al. (2006). "Influence of human genome polymorphism on gene expression." *Hum Mol Genet* **15 Spec No 1**: R9-16.
- Perelman, R. H., M. J. Engle, et al. (1981). "Perspectives on fetal lung development." *Lung* **159**(2): 53-80.
- Pichel, J. G., L. Shen, et al. (1996). "Defects in enteric innervation and kidney development in mice lacking GDNF." *Nature* **382**(6586): 73-6.
- Pierik, M., H. Yang, et al. (2005). "The IBD international genetics consortium provides further evidence for linkage to IBD4 and shows gene-environment interaction." *Inflamm Bowel Dis* **11**(1): 1-7.

- Plachov, D., K. Chowdhury, et al. (1990). "Pax8, a murine paired box gene expressed in the developing excretory system and thyroid gland." Development **110**(2): 643-51.
- Pohl, M., R. O. Stuart, et al. (2000). "Branching morphogenesis during kidney development." Annu Rev Physiol **62**: 595-620.
- Porteous, S., E. Torban, et al. (2000). "Primary renal hypoplasia in humans and mice with PAX2 mutations: evidence of increased apoptosis in fetal kidneys of Pax2(1Neu) +/- mutant mice." Hum Mol Genet **9**(1): 1-11.
- Rauchman, M. I., S. K. Nigam, et al. (1993). "An osmotically tolerant inner medullary collecting duct cell line from an SV40 transgenic mouse." Am J Physiol **265**(3 Pt 2): F416-24.
- Ross, S. A., P. J. McCaffery, et al. (2000). "Retinoids in embryonal development." Physiol Rev **80**(3): 1021-54.
- Roth-Kleiner, M. and M. Post (2003). "Genetic control of lung development." Biol Neonate **84**(1): 83-8.
- Roth-Kleiner, M. and M. Post (2005). "Similarities and dissimilarities of branching and septation during lung development." Pediatr Pulmonol **40**(2): 113-34.
- Royer, P., R. Habib, et al. (1967). "[Bilateral renal hypoplasia with oligonephronia. (Study of 21 cases)]." Arch Fr Pediatr **24**(3): 249-68.
- Salomon, R., A. L. Tellier, et al. (2001). "PAX2 mutations in oligomeganephronia." Kidney Int **59**(2): 457-62.
- Samuel, T., W. E. Hoy, et al. (2005). "Determinants of glomerular volume in different cortical zones of the human kidney." J Am Soc Nephrol **16**(10): 3102-9.
- Sanchez, M. P., I. Silos-Santiago, et al. (1996). "Renal agenesis and the absence of enteric neurons in mice lacking GDNF." Nature **382**(6586): 70-3.
- Sanyanusin, P., L. A. McNoe, et al. (1995). "Mutation of PAX2 in two siblings with renal-coloboma syndrome." Hum Mol Genet **4**(11): 2183-4.
- Sanyanusin, P., J. H. Norrish, et al. (1996). "Genomic structure of the human PAX2 gene." Genomics **35**(1): 258-61.

- Sanyanusin, P., L. A. Schimmenti, et al. (1995). "Mutation of the PAX2 gene in a family with optic nerve colobomas, renal anomalies and vesicoureteral reflux." Nat Genet **9**(4): 358-64.
- Sanyanusin, P., L. A. Schimmenti, et al. (1996). "Mutation of the gene in a family with optic nerve colobomas, renal anomalies and vesicoureteral reflux." Nat Genet **13**(1): 129.
- Sariola, H. and M. Saarma (2003). "Novel functions and signalling pathways for GDNF." J Cell Sci **116**(Pt 19): 3855-62.
- Schimmenti, L. A., H. E. Cunliffe, et al. (1997). "Further delineation of renal-coloboma syndrome in patients with extreme variability of phenotype and identical PAX2 mutations." Am J Hum Genet **60**(4): 869-78.
- Schmidt, I. M., K. M. Main, et al. (2004). "Kidney growth in 717 healthy children aged 0-18 months: a longitudinal cohort study." Pediatr Nephrol **19**(9): 992-1003.
- Schuchardt, A., V. D'Agati, et al. (1994). "Defects in the kidney and enteric nervous system of mice lacking the tyrosine kinase receptor Ret." Nature **367**(6461): 380-3.
- Schuchardt, A., V. D'Agati, et al. (1996). "Renal agenesis and hypodysplasia in ret-k-mutant mice result from defects in ureteric bud development." Development **122**(6): 1919-29.
- Shah, M. M., R. V. Sampogna, et al. (2004). "Branching morphogenesis and kidney disease." Development **131**(7): 1449-62.
- Shim, H. H., B. N. Nakamura, et al. (1999). "Identification of two single nucleotide polymorphisms in exon 8 of PAX2." Mol Genet Metab **68**(4): 507-10.
- Simons, J. L., A. P. Provoost, et al. (1994). "Modulation of glomerular hypertension defines susceptibility to progressive glomerular injury." Kidney Int **46**(2): 396-404.
- Slifer, M. A., E. R. Martin, et al. (2006). "Lack of association between UBQLN1 and Alzheimer disease." Am J Med Genet B Neuropsychiatr Genet **141**(3): 208-13.
- Srinivas, S., M. R. Goldberg, et al. (1999). "Expression of green fluorescent protein in the ureteric bud of transgenic mice: a new tool for the analysis of ureteric bud morphogenesis." Dev Genet **24**(3-4): 241-51.

- Srinivas, S., Z. Wu, et al. (1999). "Dominant effects of RET receptor misexpression and ligand-independent RET signaling on ureteric bud development." Development **126**(7): 1375-86.
- Stark, K., S. Vainio, et al. (1994). "Epithelial transformation of metanephric mesenchyme in the developing kidney regulated by Wnt-4." Nature **372**(6507): 679-83.
- Taimi, M., C. Helvig, et al. (2004). "A novel human cytochrome P450, CYP26C1, involved in metabolism of 9-cis and all-trans isomers of retinoic acid." J Biol Chem **279**(1): 77-85.
- Tavassoli, K., W. Ruger, et al. (1997). "Alternative splicing in PAX2 generates a new reading frame and an extended conserved coding region at the carboxy terminus." Hum Genet **101**(3): 371-5.
- Tejani, A. H., E. K. Sullivan, et al. (1997). "Pediatric renal transplantation--the NAPRTCS experience." Clin Transpl: 87-100.
- Torban, E., A. Dziarmaga, et al. (2006). "PAX2 activates WNT4 expression during mammalian kidney development." J Biol Chem **281**(18): 12705-12.
- Torday, J. S., H. M. Zinman, et al. (1986). "Glucocorticoid regulation of DNA, protein and surfactant phospholipid in developing lung. Temporal relationship between growth and differentiation." Dev Pharmacol Ther **9**(2): 125-31.
- Torres, M., E. Gomez-Pardo, et al. (1995). "Pax-2 controls multiple steps of urogenital development." Development **121**(12): 4057-65.
- Torres, M., E. Gomez-Pardo, et al. (1996). "Pax2 contributes to inner ear patterning and optic nerve trajectory." Development **122**(11): 3381-91.
- Tulassay, T. and B. Vasarhelyi (2002). "Birth weight and renal function." Curr Opin Nephrol Hypertens **11**(3): 347-52.
- Tyson, J. E., L. L. Wright, et al. (1999). "Vitamin A supplementation for extremely-low-birth-weight infants. National Institute of Child Health and Human Development Neonatal Research Network." N Engl J Med **340**(25): 1962-8.
- Undlien, D. E., B. A. Lie, et al. (2001). "HLA complex genes in type 1 diabetes and other autoimmune diseases. Which genes are involved?" Trends Genet **17**(2): 93-100.

- Valerius, M. T., L. T. Patterson, et al. (2002). "Microarray analysis of novel cell lines representing two stages of metanephric mesenchyme differentiation." Mech Dev **112**(1-2): 219-32.
- Vehaskari, V. M., D. H. Aviles, et al. (2001). "Prenatal programming of adult hypertension in the rat." Kidney Int **59**(1): 238-45.
- Vilar, J., T. Gilbert, et al. (1996). "Metanephros organogenesis is highly stimulated by vitamin A derivatives in organ culture." Kidney Int **49**(5): 1478-87.
- Ward, T. A., A. Nebel, et al. (1994). "Alternative messenger RNA forms and open reading frames within an additional conserved region of the human PAX-2 gene." Cell Growth Differ **5**(9): 1015-21.
- Weaver, R. G., L. F. Cashwell, et al. (1988). "Optic nerve coloboma associated with renal disease." Am J Med Genet **29**(3): 597-605.
- Wilson, J. G., C. B. Roth, et al. (1953). "An analysis of the syndrome of malformations induced by maternal vitamin A deficiency. Effects of restoration of vitamin A at various times during gestation." Am J Anat **92**(2): 189-217.
- Wintour, E. M., K. M. Moritz, et al. (2003). "Reduced nephron number in adult sheep, hypertensive as a result of prenatal glucocorticoid treatment." J Physiol **549**(Pt 3): 929-35.
- Zile, M. and H. F. Deluca (1965). "A biologically active metabolite of retinoic acid from rat liver." Biochem J **97**(1): 180-6.
- Zile, M. H. (2001). "Function of vitamin A in vertebrate embryonic development." J Nutr **131**(3): 705-8.
- Zile, M. H., R. C. Inhorn, et al. (1982). "Metabolism in vivo of all-trans-retinoic acid. Biosynthesis of 13-cis-retinoic acid and all-trans- and 13-cis-retinoyl glucuronides in the intestinal mucosa of the rat." J Biol Chem **257**(7): 3544-50.

APPENDIX I

PRESENTATIONS and PUBLICATIONS

- 2006 Dziarmega, A., Quinlan, J. and Goodyer, P. **Renal Hypoplasia: Lessons from Pax2.** *Pediatric Nephrology*. In Press.
- 2006 Quinlan, J., Goodyer, P. **Lgl-1, a retinoic acid stimulated branching morphogen in the kidney.** *Society of Pediatric Research*, San Francisco, USA.
- 2005 Quinlan, J., Goodyer, P. **Lgl-1, a retinoic acid stimulated gene in the kidney.** *American Society of Nephrology*, Philadelphia, USA.
- 2005 Quinlan, J., Kaplan, F., Goodyer, P. **Lgl-1, a novel gene in kidney development.** *Reproduction and Developmental Axis Conference*, McGill University, Montreal, QC
- 2005 Quinlan, J., Kaplan, F., Goodyer, P. **Lgl-1, a novel gene in the kidney.** *Annual Biomedical Research Seminar*, McGill University, Montreal, QC
- 2005 Quinlan, J., Hudson, T., Benjamin, A., Roy, A., Goodyer, P. **Genetic Determinants of Subtle Renal Hypoplasia.** *Annual Biomedical Research Seminar*, McGill University, Montreal, QC
- 2004 Quinlan, J., Goodyer, P. **Genes involved in small kidneys.** *Montreal Children's Hospital Research Day*, Montreal, QC
- 2004 Iglesias, D. Quinlan, J. Mohamed, Goodyer, P. **Canonical Wnt Signalling.** *American Society of Nephrology*, St.Louis, USA.

APPENDIX II

Compliance forms